

**SHEAR WAVE ULTRASOUND ELASTOGRAPHY OF THE
SHOULDER JOINT TENDONS.**

BY

HARASHALATA RAMDEV

A dissertation submitted to the Faculty of Health Sciences in full compliance for
the requirement for the Master's Degree in Technology: Radiography at Durban
University of Technology

I, Harashalata Ramdev, do hereby declare that this dissertation represents my
own work, both in concept and execution.

JUNE 2019

Harashalata Ramdev

Date

Approved for final submission

Dr Nalini Govender
Supervisor

Date

Ms Zombuso Dlodla
Co- Supervisor

Date

DEDICATION

This dissertation is dedicated to my lovely mum who always stood by me, providing me with mental support and patience throughout my study.

To my loving sister Usha, for encouraging me to go one step further to accomplish my goal.

To my loving family and friends, for their ongoing support throughout my study.

To my dear departed dad and brother Vickram who always believed that education was a stepping stone to success.

Above all, thanks to God Almighty for providing me with the strength to persevere and complete this project.

ACKNOWLEDGEMENTS

I thank the Almighty God and the following people for their kind assistance and support in composing this dissertation:

I am grateful to my mum for always being there for me.

To Dr Nalini Govender, thank you for your excellent supervision, time and continued guidance. I truly appreciate your support and constant motivation.

To Ms Zombuso (Cynthia) Dlodla, thank you for your excellent supervision, time and continued guidance. I truly appreciate your support and motivation.

To Professor Glenda Matthews, thank you for all your time and assistance with my statistical analysis.

To Dr M. Naidoo, thank you for your radiology input and supervision.

To Dr Jackpersad and Partners Inc, thank you for allowing me to conduct the research in the private radiology practice.

To my family and friends, thank you for your unwavering support.

To the staff of Mount Edgecombe X-ray department, thank you for your kind support.

To all the people who participated in this study, thank you for your time and incredible support.

To DUT radiology department and DUT staff, thank you for your kind assistance in permitting me to undertake this study.

To Derna Fynn, thank you so much for your kind assistance in the final editing of my dissertation.

TABLE OF CONTENTS

LIST OF ABBREVIATIONS	i
LIST OF FIGURES	ii
LIST OF TABLES	iii
LIST OF APPENDICES	iv
ABSTRACT	v
DEFINITIONS USED IN DISSERTATION	vii
CHAPTER 1: INTRODUCTION	1
1.1 BACKGROUND AND CLINICAL SIGNIFICANCE	2
1.2 RATIONALE	3
1.3 AIMS AND OBJECTIVES OF THE STUDY	6
1.3.1 Aim	6
1.3.2 Objectives	6
CHAPTER 2: LITERATURE REVIEW	7
2.1 INTRODUCTION	8
2.2 ANATOMY OF SHOULDER JOINT AND ASSOCIATED TENDONS	8
2.2.1 Structural and physiological features of rotator cuff tendon	9
2.2.2 Structural and physiological features of the biceps tendon	11
2.3 PATHOLOGY ASSOCIATED WITH THE SHOULDER JOINT	11
2.3.1 Rotator cuff pathology	12
2.3.2 Biceps tendon pathology	14
2.3.3 Prevalence and clinical features of rotator cuff and biceps tendon pathology	14
2.3.4 Common causes of shoulder pathologies	16
2.4 TREATMENT OF SHOULDER JOINT PATHOLOGIES	17
2.5 DIAGNOSTIC TOOLS USED IN THE DETERMINATION OF SHOULDER PATHOLOGY	18
2.5.1 Plain film radiography	19

2.5.2	Magnetic Resonance Imaging (MRI) and Magnetic Resonance Elastography (MRE)	19
2.5.3	Ultrasound	20
2.5.3.1	Brightness Modulation ultrasound (B-Mode ultrasound)	21
2.5.3.2	Doppler ultrasound	23
2.6	ELASTOGRAPHY	24
2.6.1.	Theoretical framework of ultrasound elastography based on the Young's modulus theory of elasticity	25
2.6.2	Types of Elastographic techniques	27
2.6.2.1	Strain ultrasound Elastography (SUE)	28
2.6.2.2	Shear wave Ultrasound Elastography (SWUE)	31
2.7	PRECAUTIONARY MEASURES WHEN USING ULTRASOUND ELASTOGRAPHY	34
2.8	APPLICATIONS OF ULTRASOUND ELASTOGRAPHY	34
2.8.1	Clinical use in organs	34
2.8.2	Clinical use in the Musculoskeletal System	36
2.8.2.1	Clinical use in Rotator Cuff tendons	37
2.8.2.2	Cinical use in Biceps Tendons	40
2.9	CONCLUSION	40
	CHAPTER 3: METHODOLOGY	41
3.1	STUDY DESIGN AND POPULATION	42
3.2	ETHICAL APPROVAL AND STUDY SAMPLING	42
3.2.1	Ethical approval	42
3.2.2	Target population and recruitment	42
3.2.3	Inclusion Criteria	43
3.2.4	Exclusion Criteria	43
3.3	DATA COLLECTION	43
3.3.1	Research procedure of collection of B-Mode ultrasound data	44

3.3.2 Research procedure of collection of shear wave ultrasound	
Elastography data	46
3.4 DATA ANALYSIS	48
CHAPTER 4: RESULTS	49
4.1 INTRODUCTION	50
4.2 DEMOGRAPHIC CHARACTERISTICS	50
4.3 B-MODE AND SHEAR WAVE ULTRASOUND ANALYSIS	51
4.3.1 B-Mode Ultrasound Analysis	51
4.3.2 Elastography Colour Map and Shear Wave Analysis	51
4.4 BIVARIATE ANALYSIS OF TENDONS	56
4.4.1 Analyses of all evaluated tendons based on gender variation	56
4.4.2 Analyses of all evaluated tendons based on age categorisation	58
4.4.3 Analyses of all evaluated tendons based on race	58
4.4.4 Analyses of all evaluated tendons based on Body Mass Index (BMI)	61
4.4.5 Analyses of all evaluated tendons based on 'Level of Activity'	62
4.4.6 Tendon characteristics at humeral insertion	62
4.5 REFERENCE VALUES OF ALL TENDONS BASED ON THE 95% CONFIDENCE INTERVALS	67
4.6 CONCLUSION	69
CHAPTER 5: DISCUSSION	70
5.1 INTRODUCTION	71
5.2 B-MODE ULTRASOUND AND ELASTOGRAPHY ANALYSIS	72
5.2.1 B-Mode Ultrasound Analysis	72
5.2.2 Elastography Analysis	74
5.2.2.1 Colour Map analysis	75
5.2.2.2 Shear Wave analysis	75
5.3 GENDER ANALYSIS	78

5.4	AGE ANALYSIS	80
5.5	RACE ANALYSIS	81
5.6	BODY MASS INDEX AND LEVEL OF ACTIVITY	82
5.7	CONCLUSION	84
CHAPTER 6: CONCLUSION		84
REFERENCES		89
APPENDICES		106

LIST OF ABBREVIATIONS

ALARA	As Low As Reasonably Achievable
ARFI	Acoustic Radiation Force Impulse
B-Mode	Brightness Modulation
BMI	Body Mass Index
CI	Confidence Interval
kPa	kilopascal
m/sec	metres per second
E	Youngs Modulus Theory
MHz	MegaHertz
MI	Mechanical Index
MRI	Magnetic Resonance Imaging
MRE	Magnetic Resonance Elastography
<i>p</i> -value	probability value or level of significance
ROI	Region of Interest
RCI	Rotator Cuff Interval
Sag	Sagittal
Std	Standard
SUE	Strain Ultrasound Elastography
SWUE	Shear Wave Ultrasound Elastography
TI	Thermal Index

LIST OF FIGURES

Figure 2.1	Tendons of the rotator cuff around the humeral head	9
Figure 2.2	B- Mode ultrasound of the sagittal scan of supraspinatus tendon	23
Figure 2. 3	(a) Strain ultrasound tissue compression by transducer	30
	(b) Measure of resultant tissue displacement	30
Figure 2.4	Strain ultrasound elastography of supraspinatus tendon	30
Figure 2.5	Principles of shear wave ultrasound elastography	31
Figure 2.6	(a) B-Mode normal supraspinatus tendon	33
Figure 2.7	(b) Shear wave color map	33
Figure 2.8	(c) Sample volumes in Region of interest (ROI)	33
Figure 3.1	GE Logiq E9 Ultrasound Equipment	45
Figure 3.2	Transducer position on Shoulder	45
Figure 4.1	B-Mode images of left biceps tendon (a-b), left subscapularis tendon (c-d), right supraspinatus tendon (e-f), left infraspinatus tendon (g-h) and right teres minor tendon (i-j)	52
Figure 4.2	Shear wave colour mapping and kPa values of left biceps tendon (a-b), left subscapularis tendon (c-d), right supraspinatus tendon (e-f), left infraspinatus tendon (g-h) and right teres minor tendon (i-j)	53

LIST OF TABLES

Table 4.1	Demographic frequencies of study population	50
Table 4.2	Colour maps (dark blue, dark to light blue and a mixture of colours) of rotator cuff and biceps tendons at humeral head insertion	54
Table 4.3	Shear wave elastography (kPa) of all evaluated tendons (n=260)	55
Table 4.4	Gender differences in Shear wave elastography, measured in kPa	57
Table 4.5	Mean kPa values based on age categorisation	59
Table 4.6	Mean kPa values for the four race groups using ANOVA	60
Table 4.7	Mean kPa values based on Body Mass Index	61
Table 4.8	Mean kPa values based on Level of Activity	63
Table 4.9	Tendon characteristics at humeral insertion of study population (n=260)	64
Table 4.10	Tendon characteristics at humeral insertion based on age categorisation	64
Table 4.11	Tendon characteristics at humeral insertion based on race	65
Table 4.12	Tendon characteristics at humeral insertion based on Body Mass Index	66
Table 4.13	Tendon characteristics at humeral insertion based on “Level of Activity”	67
Table 4.14	Reference ranges of the rotator cuff and biceps tendons based on the Confidence interval	68

LIST OF APPENDICES

Appendix 1A	Permission requested from Director of Radiology	106
Appendix 1 B	Permission granted from Director of Radiology	107
Appendix 1 C	Permission granted from director of Radiology at commencement of research	108
Appendix 2	Permission granted from Institutional research Ethics Committee (IREC)	109
Appendix 3A	Request for permission from Hospital Manager	110
Appendix 3B	Permission granted from Hospital Manager	111
Appendix 4 A	Letter of information in English	112
Appendix 4 B	Letter of information in isiZulu	113
Appendix 5 A	Consent form in English	115
Appendix 5B	Consent form in isiZulu	117
Appendix 6A	Advertisement in English	119
Appendix 6B	Advertisement in IsiZulu	120
Appendix 7	Consult with biostatistician	121
Appendix 8	Data collection tool	124

ABSTRACT

Background: The assessment of tissue elasticity in clinical practice has not been well established. Shear wave ultrasound elastography is a recent technique which quantitatively estimates tissue elasticity. This study, therefore, aimed to assess the biomechanics of the rotator cuff and biceps tendons of the shoulder joint in asymptomatic participants, in order to establish a reference range for use in clinical practice. The objectives of this study were to measure the elasticity of the rotator cuff and biceps tendons (in kilopascals), using shear wave ultrasound elastography and to establish a shear wave ultrasound elastographic reference range of the rotator cuff and biceps tendons for use in clinical practice.

Methods: This quantitative study included 260 asymptomatic participants aged between 21 and 45 years (mean age 34.52 ± 7.75 years). The demographic data incorporated participants' age, gender, race, weight, height, daily lifestyle activities, body mass index and medical history. Data was collected using a demographic questionnaire, B-Mode ultrasound and shear wave ultrasound elastography, using the GE Logiq E 9 equipment. The proximal, middle and distal sites of the biceps, subscapularis, and supraspinatus and infraspinatus tendons were imaged in both longitudinal and axial planes. The teres minor tendon was imaged in a single sagittal and axial plane.

Results: The reference ranges of the rotator cuff and biceps tendons have been evaluated by finding 95% confidence intervals for the mean elasticity for each of the tendons. A 95% confidence interval provides a lower and upper limit into which 95% of tendon measurements would be expected to fall. The reference ranges for the mean tendon elasticity for the tendons were as follows:

For the biceps tendon in sagittal and axial planes, the reference ranges are 102.52-108.34 kPa and 96.44-101.08 kPa respectively. For the subscapularis tendon in sagittal and axial planes, the reference ranges are 102.84-110.60 kPa and 110.60 kPa-108.02 kPa respectively. The supraspinatus tendon in sagittal and axial planes have reference ranges 106.83-114.54 kPa and 102.29-109.59 kPa, respectively. The infraspinatus tendon in sagittal and axial planes

have reference ranges 102.39-111.87 kPa and 99.61-107.77 kPa respectively. The reference ranges for teres minor tendon in sagittal and axial planes are 96.90-101.20 kPa and 96.68-101.09 kPa respectively.

There was a statistically significant difference in the reference values observed between males and females for the proximal, middle and distal sites of the biceps tendon in the sagittal plane ($p<0.05$). The reference values ranged from 101.93 ± 18.84 kPa- 104.09 ± 16.86 kPa (in females) and 109.40 ± 18.15 kPa- 109.41 ± 19.07 kPa (in males). A statistically significant difference was also noted in the teres minor tendon in the sagittal and axial planes ($p<0.05$). The reference values ranged from 96.71 ± 16.49 kPa (in females)- 102.74 ± 18.76 kPa (in males) in the sagittal plane and 97.03 ± 18.29 kPa (in females)- 101.79 ± 17.39 kPa (in males) in the axial plane.

Conclusion: This study provided a non-invasive estimate of the elasticity of the rotator cuff and biceps tendons in kPa, using shear wave ultrasound elastography (SWUE). The results of our study have the potential to complement B-Mode ultrasound in the diagnosis, treatment and follow up of rotator cuff and biceps tendon pathology.

DEFINITIONS USED IN DISSERTATION

Acoustic impedance: The amount of echoes reflected back to the transducer after encountering a tissue interface (Kaur 2013: 3890).

Anterior: Anterior refers to the front of the body or anatomical structure (Sheng 2013: 29).

Artefact: Artefact is a distortion of ultrasound tissue by shadowing artefact – when an ultrasound wave encounters a highly reflective surface such as soft tissue / bone interface, the displayed image of the interface will be bright. Tissues distal to the reflective surface will be displayed as a black shadow (Nader, John and Kendall 2016: 34 and Nordenfur 2013: 2).

Axial: Axial or transverse planes or level are at right angles to the sagittal or median plane (Sheng 2013: 29).

Anechoic: Anechoic is defined as a black B- Mode ultrasound display that features tissues such as blood and fluid as uniform internal acoustic impedance and does not reflect any waves (Nader, John and Kendall 2016:27).

Anisotropy: Anisotropy occurs when the ultrasound beam is angled relative to the long axis of the structure. To correct for anisotropy, the target structure should be positioned perpendicular to the ultrasound beam, so that the transducer probe will capture the reflected sound waves (Gupta and Robinson 2015: 206 and Guo *et al* 2016: 362).

Acoustic Radiation Force Impulse: Acoustic radiation force impulse is a type of strain ultrasound whereby tissue is excited internally by a focussed ultrasound pulse instead of external compression such as manual or physiological compression (Rahman *et al.* 2013:77).

Attenuation: This term applies to the time required for a wave to move from the transducer and back closely, indicating the displayed depth of the structure. Attenuation is measured in decibels per centimetre of tissue per MHz (Nader, John and Kendall 2016:28).

B-Mode ultrasound: The standard brightness mode (B-Mode) or sonogram represents the degree of the reflected wave as an intensity level between 0 (black) and 255 (white) (Frisch 2011: 27). B-Mode ultrasound images are derived from longitudinal waves. (Kaur 2013: 388).

Calcific tendinopathy: Calcific tendinopathy of rotator cuff refers to the intratendinous deposition of calcium, largely carbonate apatite. It is typically associated with a non-degenerative rotator cuff (Messina *et al.* 2015:1).

Doppler: Doppler ultrasound is a special ultrasound technique that evaluates blood flow through a blood vessel, including the body's major arteries and veins in the abdomen, arms, legs and neck. Doppler ultrasound measures the direction and speed of blood cells as they move through vessels (Kaur 2013: 390)

Dynamic ultrasonography: Dynamic ultrasonography is performed with varying degrees of patient arm rotation and joint stress manoeuvres (Oliviera *et al.* 2017: 2).

Elasticity: The elasticity of a material represents its tendency to resume its original size and shape after being subjected to a deforming force or stress (Corazza 2015: 1).

Elastogram: Elastogram is a colour coded or greyscale map which displays strain information, superimposed over a B-Mode image. It is widely accepted that red colour signifies soft tissues, blue indicates hard tissues and yellow/green corresponds to tissues of moderate stiffness (Drakonaki, Allen and Wilson 2012: 1436).

Elastography: This is an imaging technique which measures the elasticity of tissues through the use of B- mode ultrasound. The colour mapping over B- mode images can be visualised in grey scale or colour on an ultrasound monitor. Hard or stiff tissues may be colour - coded as blue and soft tissues may be colour - coded as red (Ohuegbe 2014: 13).

Entheses: Entheses is defined as the focal tissue insertion of the tendon, ligament, fascia or muscles to bone (Kehl, Corr and Weisman 2016: 313).

Enthesitis: Enthesitis is the inflammatory condition of the enthesis, as a result of repeated biomechanical stress (Kehl, Corr and Weisman 2016: 313).

Footprint: The mean maximum mediolateral width of the supraspinatus insertion onto the humerus in the coronal plane (Ohuegbe 2014: 13) is referred to as the footprint.

Hyperechoic: Bright B-Mode ultrasound image displays characteristics of tissue interface with different acoustic impedance such as soft tissue to bone or air (Nader, John and Kendall 2016: 27).

Hypoechoic: Hypoechoic is the term given to a mixed display of echogenic tissue which is heterogeneous. The display has similar acoustic impedance such as muscle, fat and neural tissue (Nader, John and Kendall 2016: 27).

Modulus of elasticity: For a homogeneous isotropic solid, the ratio of stress/strain is a constant called the 'modulus of elasticity.' A modulus (usually expressed in units of Pa) measures the amount of force per unit area (stress) needed to achieve a given amount of deformation (Corazzo 2015: 3).

Mechanical Index (MI): Mechanical index-MI is the ratio of the adjusted peak negative pressure on the ultrasound wave to the square root of the frequency (Nader, John and Kendall 2016: 35).

Posterior: Posterior refers to the back of the body or anatomical structure (Sheng 2013: 29).

Rotator cuff tendon: Rotator cuff tendons are a group of tendons in the shoulder responsible for movement and rotation, and comprise the supraspinatus, infraspinatus, and subscapularis and teres minor tendons. (Ohuegbe 2014: 13).

Rotator cuff interval: This term refers to the gap between the supraspinatus and subscapularis tendons and consists of the long head of biceps tendon, the coracohumeral ligament forming the roof lying superficial to the longhead of the biceps tendon, and the anterior glenohumeral ligament (Gupta and Robinson 2015:204).

Refraction: Refraction occurs when the direction of ultrasound waves change after coming into contact with two tissues with different speeds of sound transmission (Kaur 2013:390).

Sagittal: The sagittal or median plane passes through the body from front to back and divides it into two symmetrical right and left halves. Any plane parallel to this is also known as a sagittal or paramedian plane (Sheng 2013: 29).

Stress: Force per unit area (Corazzo 2015: 33).

Strain ultrasound elastography (SUE): Also described as compression elastography, SUE is an ultrasound technique based on low - frequency compression, usually applied manually, using a held ultrasound transducer. The main principle of strain ultrasound elastography is that a compressive force (stress) is applied to tissue, causing axial tissue displacement (strain) (Rahman *et al.* 2013: 77).

Shear wave ultrasound elastography (SWUE): Shear waves are generated within tissue when the conventional ultrasound waves, produced by the transducer, interact with tissue. Shear waves propagate perpendicular to the axial displacement caused by the ultrasound pulse and attenuate 10000 times more rapidly than conventional ultrasound. The velocity of shear waves can be measured by calculating Young's modulus. This technique yields both quantitative study as in colour-coded elastograms and quantitative measurement of shear wave velocity in kPa or cm per sec (Rahman *et al.* 2013:78).

Shoulder Impingement: This can be defined as compression of the rotator cuff and the subacromial bursa against the anteroinferior aspect of the acromion and the coracoacromial ligament that leads to pain and/or weakness around the shoulder joint (Van Zuydam *et al.* 2014: 34 and Oliveira *et al.* 2017: 10).

Stiffness: Stiffness is defined as force over displacement and has units of force per distance. It is a measure of the rigidity of an object, and is influenced by the elastic modulus of the object itself, its shape, and size (Ryu and Jeong 2017: 5).

Thermal Index (TI): TI is the ratio of the system power to the power required to cause 1° (one degree) Celsius increase in tissue temperature. This output display standard was developed to quantify the energy output in relation to the thermal and cavitation formation defects (Nader, John and Kendall 2016:35).

Tendinopathy: Tendinopathy is defined as the painful condition occurring from mechanical, degenerative, and overuse diseases, and is associated with degeneration and disorganization of the collagenous structure, changes in the proteoglycan and water contents, increased cellularity, fatty infiltration, and neovascularization (Ryu and Jeong 2017: 6 and Ohuegbe 2014: 21).

Tendinosis: Tendinosis is used to describe a histopathological state of degenerative tendon without any inflammatory signs or correlation with clinical symptoms (Ohuegbe 2014:14).

Transducer: The transducer, also called an ultrasound probe, emits pulses of sound waves. Medical Ultrasound imaging is done using ultrasonic waves in a 3 to 20 MHz range. (Kaur 2013: 389).

Transient ultrasound elastography: This is a variation of the shear wave whereby tissue is excited by a burst of vibration (mechanical excitation) from the ultrasound transducer, to estimate the speed of shear waves in tissues. However, the vibration is transient (momentary), consequently separating the forward waves from the reflected waves (Sarvazyan, Urban and Greenleaf 2013: 1138).

Young's modulus theory: The Young's modulus E , is a physical specification that can define the biomechanical changes in tissue, thereby characterizing soft and hard tissue (Genisson *et al.* 2013:488 and Sayvazyan, Urban and Greenleaf 2013: 1141). The formula for shear wave has been determined as $\mu = c_s^2 \rho$ where μ is shear modulus and c_s is the speed of shear wave propagation velocity and ρ is density assumed to be 1000 Kg/m^3 for all soft tissues (Eby *et al.* 2013: 2381 and Shiina *et al.* 2015:1134).

Transverse: Transverse or axial planes or level are at right angles to the sagittal or median plane (Sheng 2013: 29)

CHAPTER 1: INTRODUCTION

1.1 BACKGROUND AND CLINICAL SIGNIFICANCE

Rotator cuff tendinopathy and tears are frequent causes of shoulder pain and dysfunction, thus, implementing an early treatment plan is crucial (Chepeha, Bouliane and Sheps 2015: 240; Trent 2013: 15). Tendon quality and function is an important prognostic factor to clinicians when determining a treatment protocol (Naidoo, Lazarus and Sathypal 2016: 975). An accurate diagnosis based on the biomechanical features of this musculoskeletal abnormality, is therefore essential (Qiu *et al.* 2015: 89; Klauser *et al.* 2014: 622; Cowling, Gamble and Rangan 2011:13). Although the tendon is distinguished by hard tissue in its normal state, it is predisposed to tissue alteration as a result of degeneration or injuries (Ryu and Jeong 2017: 5). Subsequently, tendons are susceptible to tears initiated by weakened collagen fibres, as well as reduced elasticity of tendons (Ooi *et al.* 2014: 1). Therefore, predisposing factors strongly linked to rotator cuff tears may be intrinsic, such as degeneration due to an ageing process, or extrinsic, such as trauma (Hou *et al.* 2017: 95; Trent 2013: 14; Hodgson, O'Connor and Grainger 2012: 1160; Frisch 2011: 20). Hence, detection and treatment of tendinopathies are of paramount importance in the prevention of chronic pains or tendon tears (Dirrichs *et al.* 2016: 1205; DeWall 2013: 13; Song 2014: 498).

Ultrasound imaging, such as B-Mode ultrasound, is currently used in the assessment of rotator cuff and biceps tendons (Oliveira *et al.* 2017: 2). Notwithstanding the established technique of B-Mode ultrasound, few attempts have been made to quantify tendon pathology (Chernak and Thelen 2012: 2618). Therefore, the advent of new imaging modalities advances have made it possible to provide new critical insight into musculoskeletal function by direct measurements of tendons and muscles *in vivo* (Sikdar, Wei and Cortes 2014: 126). It is perceived that characterization and objective assessments of the shoulder joint may confer added clinical diagnostic value (Gennisson *et al.* 2013: 48). Recent studies report that virtual palpations such as elastography, employ the use of ultrasound to estimate the strain and elasticity of soft tissue (Qiu *et al.* 2015: 89; Takenaga *et al.* 2015: 2939; Song 2014: 30; DeWall 2013: 2) thus allowing these features to be displayed in real time (Tudisco *et al.* 2015:393).

Elastography is based on the principle that when stress (mechanical or physical) is applied to tissue, changes (strain) occur in the tissue, depending on the elastic properties of the tissue (Corazza 2015: 2). Thus, measurements of elasticity of hard or soft tissue reflecting the quality of tissue (healthy and diseased) may contribute to clinical diagnosis (Li and Cao

2017: 3; Tudisco *et al.* 2015: 393; Ophir *et al.* 1991: 111). As stated by Garra (2015: 683), the two most frequently used techniques for tissue elasticity assessment are strain ultrasound elastography (SUE) and shear wave ultrasound elastography (SWUE).

Early musculoskeletal studies have been evaluated by compression or strain ultrasound elastography (SUE) (Hou *et al.* 2017: 95) with limited shear wave ultrasound elastography (SWUE) investigations. Whilst a qualitative or semi quantitative study is rendered by SUE (Ooi *et al.* 2014: 1) the use of SWUE is perceived to enhance technology in terms of reproducibility and quantification (Hou *et al.* 2017: 96; Qiu *et al.* 2015: 90; Shiina *et al.* 2015: 1127). It has been postulated that this form of tissue assessment may identify pathology before it can be detected on B-Mode ultrasound (Winn, Lalam and Cassar-Pullicino 2016: 869). Therefore, this technique is envisaged to clinically improve the diagnosis of shoulder injuries, pathologies and/or treatment (Winn, Lalam and Cassar-Pullicino 2016: 876; Corazza 2015: 2).

1.2 RATIONALE

Palpation and physical tests are dependent on direct contact to superficial organs only, whereas elastographic techniques can be applied to deep organs (Gennisson 2016: 1). Conventional imaging modalities such as plain film radiography and B-Mode ultrasound imaging are limited to subjective analyses (Klauser *et al.* 2014: 1; Peltz *et al.* 2013: 1151). Furthermore, inflammation or early soft tissue changes may not be demonstrated with plain film radiography (Kehl, Corr and Weisman 2016: 7). Moreover, rotator cuff disorders and enthesitis may be completely missed on normal radiographs (Riente *et al.* 2013: 332). Although Magnetic Resonance Imaging (MRI) and Magnetic Resonance Arthrography (MRA) may demonstrate a high accuracy of rotator cuff tears, they are expensive and intra-articular injections used during these procedures are invasive (Trent 2013: 17). Taking into consideration the inadequate provision of real time data, the ability of these investigations to quantify musculo skeletal dynamics remains limited (Sikdar, Wei and Cortes 2014: 10; Trent 2013: 17).

B-Mode ultrasound has been recognised as a viable alternative for soft tissue imaging owing to its affordability, real time imaging and lack of ionizing radiation (Li and Cao 2017: 3; Kaur 2013: 393). However, it is deficient in the provision of tendon morphology (Wu *et al.* 2012: 85) including rotator cuff pathology (Gennisson 2016: 1; Hatta *et al.* 2015: 3854; Ooi *et al.*

2014: 1). Concomitantly, clinical distinction between tendinopathy and tendon tears pose numerous challenges as normal and diseased tissue may share similar ultrasound echogenicity (Lee *et al.* 2016b: 724; Ooi *et al.* 2014: 1), consequently delaying early diagnosis (Dirrichs *et al.* 2016: 1211). In addition, highly reflecting interfaces of tissues are prone to shadowing artefacts (Nordenfur 2013: 2).

The challenge to delineate the specific site, size and extent of tissue injury for patient treatment outcome has been the focus of considerable concern (Trent 2013: 41). Under these circumstances, additional methods are required to detect the potential for underlying tendon pathology for mucoid degeneration or small interstitial tears before they become apparent on conventional B-Mode imaging (Nwawka 2016: 433; Winn, Lalam and Cassar-Pullicino 2016: 871). It is envisaged in these cases that ultrasound elastography, an additional imaging technique, could detect irregularities not evident on B-Mode ultrasound imaging (Galletti *et al.* 2015: 325).

Strain ultrasound elastography has also been widely employed in the ultrasound examination of the pancreas, breast, thyroid, cervix and lymph nodes (Paluch *et al.* 2016: 241; Drakonaki, Allen and Wilson 2012: 1436). According to Roskopf *et al.* (2015: 486) ultrasound elastographic studies for musculoskeletal applications have been scarce. The Achilles tendon was the first tendon to be investigated using SUE (De Zordo *et al.* 2010: 394). Prior ultrasound elastography studies of rotator cuff tendons have mostly focussed on the supraspinatus tendon. A semi quantitative strain ultrasound study of the supraspinatus tendon highlighted the lack of quantitative values (Muraki *et al.* 2015: 12).

In view of shear waves travelling at a faster rate through stiff tissues, the measurement of the propagated shear wave speed contributes to valuable information on tissue (Wu *et al.* 2012: 81). Thus by using Young's modulus (numerical constant), numerical calculations of tissue stiffness or elasticity index (EI) in kilopascals (Simic 2012: 2; Ooi *et al.* 2014: 5; Shiina *et al.* 2015: 1139), or in metres per sec (m/s) can be achieved (Corazzo 2015: 5). Gennisson *et al.* (2013: 494) affirms that the accessibility of numerical data accessed with SWUE permits modification of the dynamic range for optimum visualization of structures, thus initiating new applications of this mode of imaging (Wu *et al.* 2012)

Although shear wave ultrasound elastography of supraspinatus tendons in asymptomatic participants were conducted by (Arda *et al.* 2011: 535), it failed to compare normal and pathological rotator cuff tendons (Tudisco *et al.* 2015:394). Marcy, Thariat and Lacout (2012: 2) criticized the above study for the omission of the number of image acquisition, size of region of interest, as well as the omission of formal reference scanning planes. In addition, the lack of characterization of tendon quality in different age groups has been highlighted (Winn, Lalam and Cassar-Pullicino 2016: 872; Tudisco *et al.* 2015: 396). Paluch *et al.* (2016: 245), however, were concerned that the focus has been more on case studies and small population studies without control groups, as opposed to focus on both symptomatic and asymptomatic tendon studies.

South African studies using elastography are limited. The breakthrough study of the SWUE of liver was conducted by Dr Rajabally in 2016 (Rajabally 2017:1). A Fibroscan ultrasound machine was utilised whereby shear wave speed of the liver could be measured using vibration- controlled transient elastography to assess liver fibrosis. Dr Rajabally stated that early treatment obviated the need for liver biopsy, especially for conditions such as viral hepatitis, non-alcoholic fatty liver disease, alcoholic liver disease and cholestatic liver disease (Rajabally 2017:1).

Ultrasound elastography has been proven to be fast, convenient and easily available (Hatta *et al.* 2015:3850) as well as being non-invasive, safe, inexpensive and reproducible (Tudisco *et al.* 2015: 293; Wu *et al.* 2012: 80; Arda *et al.* 2011: 532). The advantage of SWUE procedure over SUE, is the manual decrease in compression, merely by maintaining transducer contact with skin, therefore maintaining imaging consistency (Inami and Kawakami 2016: 314; Qiu *et al.* 2015: 90; Rahman *et al.* 2013: 78). A further benefit of ultrasound elastography has been its ability to precisely indicate the place of a possible biopsy in regions of pathological tissue (Zaleska-Dorobisza *et al.* 2013: 646). Taking this into consideration, the provisions for better diagnosis can be ascertained (Gennisson *et al.* 2013: 488). In addition, the assessment of hardness of calcifications in tendons using shear wave ultrasound elastography may be used in clinical practice to select a specific type of treatment (Saltykova 2013: 15). The establishment of a wide range of normal and pathological shear wave ultrasound elastography reference values has been proposed (Marcy, Thariat and Lacout 2012: 5). It has been suggested that the quantitative characteristic of SWUE may provide an objective tool for monitoring the progression of disease or as a follow up post treatment measure (Dirrichs *et al.*

2016:1205 and Greenleaf and Urban 2016:1202). Therefore, it's potential in the prediction of recovery time following treatment may guide in the timely return to an active lifestyle after normal findings of tendon elastograms (Winn, Lalam and Cassar-Pullicino 2016: 876).

Although various studies have explored the use of SWUE (Ooi *et al* 2014: 11), concerns were recently raised by Baumer *et al* (2018: 287); Hatta *et al* (2015: 3854); Muraki *et al* (2015: 120); Tudisco *et al* (2015: 397); Rahman *et al* (2013: 8); Botar Jid *et al* (2012: 239) regarding the lack of quantification of musculoskeletal tissues including standardization of musculoskeletal investigation. To date, however, SWUE quantification for asymptomatic and symptomatic rotator cuff tendons has not been well established (Hou *et al.* 2017:105). The paucity of data on shear wave studies on the rotator cuff and biceps tendons warranted the undertaking of the current study. Therefore, reference ranges for the subscapularis, infraspinatus, teres minor and biceps tendons were key to this study.

1.3 AIMS AND OBJECTIVES OF THE STUDY

1.3.1 Aim

The aim of this study was to assess the biomechanics of the rotator cuff and biceps tendons of the shoulder joint in asymptomatic participants, in order to establish a reference range for use in clinical practice.

1.3.2 Objectives

The objectives of this study were:

- To measure the elasticity of the rotator cuff and biceps tendons and report in kilopascals, using shear wave ultrasound elastography.
- To establish a shear wave ultrasound elastographic reference range of the rotator cuff and biceps tendons for use in clinical practice.

CHAPTER 2: LITERATURE REVIEW

2.1 INTRODUCTION

Shoulder pain is one of the most prevalent musculoskeletal complaints encountered at health care facilities (Lee *et al.* 2016b: 1607). This could be due to a variety of reasons, one major cause, attributed to rotator cuff tendinopathy or tears (Chepeha, Bouliane and Sheps 2015; 240). As reported by Park *et al.* (2013: 1359) the shoulder joint is subject to damage due to its large range of movement. Although there are 26 groups of muscle controlling the shoulder girdle, the rotator cuff, tasked as the main stabilizer of the glenohumeral joint, is therefore integral to upper limb function (Sheng 2013: 27).

Clinical practice employs various imaging modalities prior to treatment of shoulder pathology such as plain film radiography, B- Mode ultrasound and Magnetic Resonance Imaging (MRI) (Trent 2013: 6). Although the high incidence of rotator cuff disorders has led to the growth of musculoskeletal ultrasound, this imaging method may be restricted to some degree in the assessment of rotator cuff pathology (Gupta and Robinson 2015: 203). Studies demonstrate that non-invasive, real time ultrasound elastography technique, also known as virtual palpation, uses ultrasound to estimate the strain and elastic modulus of soft tissue (Sahan *et al.* 2018: 192; Ooi *et al.* 2014: 2; Song 2014: 30; DeWall 2013: 2). It is envisaged that ultrasound elastography may provide additional and clinically relevant information pertaining to tissue quality and quantification (Tudisco *et al.* 2015: 393; Gennisson *et al.* 2013: 287). Since tendons respond to load bearing of tissues, a comprehension of the mechanisms of tendon biomechanics is imperative (Lavagnino *et al.* 2015: 813), as accurate and early diagnosis remains pivotal in the management of tendon pathology (Ooi *et al.* 2014: 1).

2.2 ANATOMY OF SHOULDER JOINT AND ASSOCIATED TENDONS

The shoulder joint is a ball and socket joint formed by the synovial articulation of the glenoid cavity and humeral head (Sheng 2013: 23). It is made up of joints, muscles, ligaments, bursa, capsules and bones. The articular surfaces of the shoulder joint are lined by articular cartilage, whilst the glenoid rim is strengthened by a fibrocartilaginous labrum (Sheng 2013: 23; Gupta and Robinson 2015: 204). The highly complex and dynamic design of this joint contributes significantly to a large range of motion, thus predisposing it to instability. Three main bones associated with the shoulder joint include: the humerus, clavicle and scapula, with the flat impressions or facets of the greater tuberosity of the humerus serving as insertion for the rotator cuff tendons (Gupta and Robinson 2015: 204; Sheng 2013: 23).

Moreover, an integral feature of the shoulder complex is the acromio clavicular joint (AC joint), as well as the subacromial subdeltoid bursa, a sac situated below the acromion process and coraco acromial ligament, extending over the rotator cuff tendons (Gupta and Robinson 2015: 210).

2.2.1 Structural and physiological features of rotator cuff tendons

The rotator cuff tendons that surround the shoulder joint include: the supraspinatus, subscapularis, infraspinatus, teres minor and biceps tendons (Gupta and Robinson 2015: 204) (Figure 2.1). Healthy rotator cuff tendons are made up primarily of Type 1 collagen fibres in contrast to Type 111 collagen found in degenerative and torn tendons (Screen *et al.* 2015: 793; Trent 2013: 13; Frisch 2011: 22).

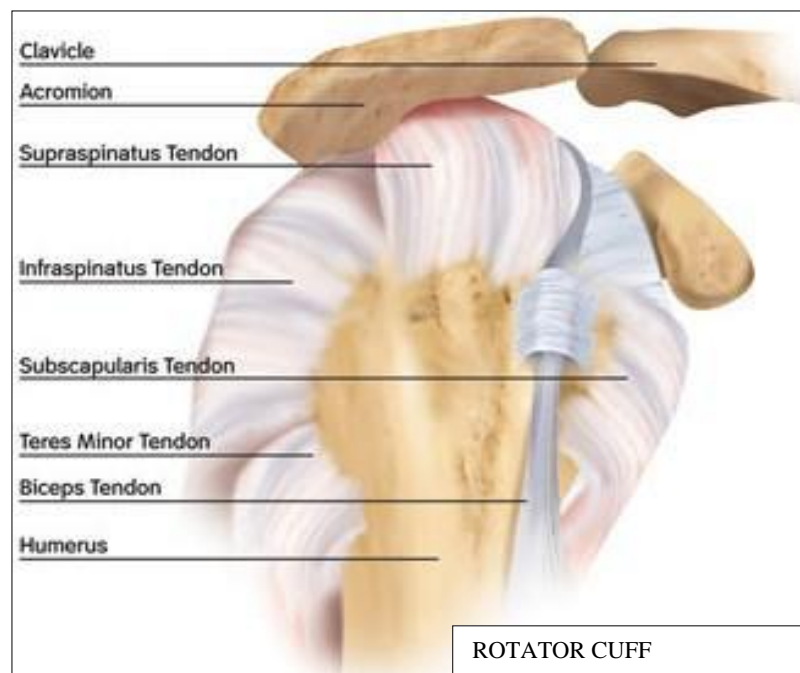


Figure 2.1: Tendons of the rotator cuff around the humeral head: Adapted from Trent (2013: 13)

Tendons connect muscles to the bones, thereby providing skeletal stability and movement by the transmission of contractile force from muscle to bone (Lavagnino *et al.* 2015: 813). Collagen fibres are grouped into fascicles and sub fascicles, which are enclosed by an endotendon sheaths, thus allowing tendons to modify their level of stiffness during movement. It is therefore plausible that the tensile properties of tendons depend on the rate at which the tendon is loaded (Maganaris *et al.* 2017: 2; Lavagnino *et al.* 2015: 813; Weinreb *et al.* 2014: 66; Trent 2013: 13). Tendon fibres are also distinguished by hard tissue in its

normal state and also differ from tendon to tendon (Weinreb *et al.* 2014: 66), and thus can be predisposed to tissue alteration due to degeneration or injuries (Ryu and Jeong 2017: 189).

Stability of the humeral head within the glenoid fossa is provided by the rotator cuff tendons (Escamilla, Hooks and Wilk 2014: 15). Movement of this joint is supported by four muscles working in tandem with their associated multiple layered rotator cuff tendons attached to the proximal humerus (Matthewson *et al.* 2015: 1; Jacobsen 2011: 7; Frisch 2011: 19). The rotator cuff tendons are known to merge with each other and the fibrous capsule of the shoulder joint to create the distinguishing feature of the cuff (Naidoo, Lazarus and Satyapal. 2016: 975). The subscapularis muscle located anterior to the scapula, provides muscular support, including dynamic anterior stability of the gleno humeral joint (Gupta and Robinson 2015: 204; Singh 2012: 285; Beggs 2011: 101). The subscapularis tendon inserts into the lesser tuberosity of the humerus (Singh 2012: 285). Both the subscapularis muscle and its associated tendon enable internal arm rotation, whereas the supraspinatus tendon, located in the suprascapular fossa of the scapula, enables elevation and abduction of the arm (Sheng 2013: 30).

The superior aspect of the supraspinatus muscle and associated tendon is convex and in contact with the sub acromial bursa, whilst the inferior surface is in close contact with the articular cartilage (Guerini *et al.* 2012: 1). Insertion of the supraspinatus tendon on the superior and part middle facet of the greater tuberosity makes up the tendons “footprint” which is 12 mm in width in the medial to lateral plane (Gupta and Robinson 2015: 204). In contrast, the infraspinatus muscle, located posterior and below the spine of the scapula, inserts in the middle facet of the greater tuberosity (Oliveira *et al.* 2017: 11). The tendon linked to it enables external rotation of the humerus, whilst the teres minor muscle and tendon, located inferior to infraspinatus, enables outward turning of the arm (Trent 2013: 13 and Drakonaki, Allen and Wilson 2012: 1435). However, the trapezoid shape defines the teres minor tendon from the infraspinatus tendon (Jacobsen 2011: 7). In addition, the teres minor tendon inserts into the inferior facet of the greater tuberosity and is identified as the most posterior part of the rotator cuff tendon (Lee *et al.* 2016a: 1623; Takenaga *et al.* 2015: 2940). Thus, the teres minor tendon plays an important role in the external rotation of the humerus, together with the infraspinatus tendon (Lee *et al.* 2016a: 1623).

2.2.2 Structural and physiological features of the biceps tendon

The shoulder is also stabilized by the biceps tendon by providing support of the arm during abduction (Lee *et al.* 2016a: 1608; Redondo-Alonso *et al.* 2014: 7). The longhead of the biceps originates from the superior aspect of the glenoid labrum and courses through the shoulder joint and rotator cuff interval before entering the bicipital groove. The extent of the longhead of the biceps tendon is ascertained from its entrance into the bicipital groove to the myotendinous junction (Gupta and Robinson 2015: 206; Drakonaki, Allen and Wilson 2012: 1435; Beggs 2011: 101). The longhead of the biceps tendon, defined as a noncontractile traction tendon, permits smooth movement of the humeral head (Lee *et al.* 2016a: 1607). This tendon, found in the bicipital groove on the anterolateral aspect of the head of humerus, is also surrounded by minimal fluid, characteristic of asymptomatic findings (Messina *et al.* 2015: 6; Singh 2012: 285). Moreover, the rotator cuff interval reinforces the shoulder joint, thereby enabling movement and position of the longhead of the biceps tendon in the bicipital groove (Tamborrini *et al.* 2017: 107; Lee *et al.* 2016a: 1608). The rotator cuff interval is a triangular region between the anterior leading edge of the supraspinatus tendon and the superior edge of the subscapularis tendon (Oliveira *et al.* 2017: 8; Drakonaki, Allen and Wilson 2012: 1435).

2.3 PATHOLOGY ASSOCIATED WITH THE SHOULDER JOINT

The shoulder joint is predisposed to various pathologies, including rotator cuff tendinopathy and shoulder impingement complications (Van Zuydam *et al.* 2015: 34). Shoulder impingements are used as clinical evidence to establish the degree of tissue damage in the shoulder joint (Escamilla, Hooks and Wilk 2014: 13). The sub acromial impingement and the posterior shoulder impingement are examples of shoulder impingement (Escamilla, Hooks and Wilk 2014: 13). Sub acromial impingement is a clinical syndrome which occurs as a result of friction between the rotator cuff tendons and the greater tuberosity of the humerus. It is associated with a spectrum of pathology including sub acromial bursitis, partial rotator cuff tears and biceps tendinitis (Escamilla, Hooks and Wilk 2014: 13; Singh 2012: 287). In contrast, internal impingement is triggered by exertion of the posterior labrum and inferior section of the supraspinatus and infraspinatus tendons during movement and is related to stiff posterior shoulder joint capsule (Van Zuydam *et al.* 2015: 34; Escamilla, Hooks and Wilk 2014: 13; Tagg *et al.* 2013: 3; Singh 2012: 287). Non-rotator cuff pathologies, in contrast, may also include glenohumeral joint effusion, calcifying bursitis, dislocation and synovitis (Gaitini 2012: 9). Likewise, the enthesis, which refers to the insertion of ligaments, fascia,

muscles and tendons into bone, can also lead to inflammations such as enthesitis, due to repeated biomechanical stress (Kehl, Corr and Weisman 2016: 313).

2.3.1 Rotator cuff pathology

Rotator cuff disease is defined as a progressive disorder of the rotator cuff tendons that is multifactorial in nature (Naidoo *et al.* 2016: 975; Seo, Yoo and Ryu. 2014: 143). Biochemical alterations in tissue result in weakened collagen fibres and reduced tendon elasticity, thereby predisposing the tendon to tears (Ooi *et al.* 2014: 1; Nodenfur 2013: 3). The importance of early diagnosis of rotator cuff tears is therefore crucial, as untreated tears may ultimately enlarge, eventually resulting in fatty degeneration and deterioration of the shoulder muscle (Nazarian *et al.* 2013: 590; Sheng 2013: 38). Tendinosis or tendinopathy occurs as a result of degenerative or overused tendons, which subsequently lead to gradual softening of the diseased tendons (Ohuegbe 2014: 21; Hodgson, O'Connor and Grainger 2012: 1160).

The supraspinatus tendon was demonstrated as the most frequently affected tendon in the impingement process (Escamilla, Hooks and Wilk 2014: 15), with reduced blood supply and old age cited as major causes. Chronic tendinopathy usually occurs due to repetitive micro trauma and vascular changes, which causes a breakdown in collagen fibres (Tudisco *et al.* 2015: 393), whereas calcific tendonitis is linked with disorders of thyroid gland and oestrogen metabolism, as well as alcohol abuse and obesity (Henning *et al.* 2015: 44). As stated by Messina *et al.* (2015: 2), calcific tendinopathy of rotator cuff tendons occur as a result of calcium deposits (mainly carbonate apatite) within the tendons. However, calcific tendonitis must be clearly differentiated from the degenerative calcification that presents within a torn tendon (Henning *et al.* 2015: 45).

Pathologic conditions cause alterations in mechanical properties of tissues, thus classification of rotator cuff tears is essential (Trent 2013: 15). These tears are classified according to the degree of change in the fibre structure (Gaitini 2012: 6). In addition, tendon tear sizes are categorised as either small (<1cm), medium (1-3 cm); large (3 -5 cm) or > 5 cm tears (Tagg *et al.* 2013: 6). Furthermore, rotator cuff tears can be classified as full thickness tears located on the articular surface, extending across to the bursal surface of the tendon (Weinreb *et al.* 2014: 66; Hodgson, O'Connor and Grainger 2012: 1164). On the contrary, partial thickness tears are located either on the articular, bursal or intratendinous surface of rotator cuff tendons (Matthewson *et al.* 2015:4) and may coexist with tendinosis (Singh 2012: 288).

Studies have shown that most full thickness tears occur at the footprint of the greater tuberosity at the insertion of the supraspinatus tendon (Riente *et al.* 2013: 331), and is often confirmed using B-Mode ultrasound (Singh 2012: 288). Full thickness tears are depicted as hypoechoic or anechoic tendon defects that extend from the articular to the bursal surface (Lee *et al.* 2016a: 1616). The use of B- Mode ultrasound in the identification of full thickness tears can thus be limiting as a result of the presence of echogenic debris, tissue scarring, or herniation of the deltoid muscle in the region of the tear (Beggs 2011: 3). Studies have confirmed that these tears often affect the supraspinatus tendon in the hypo vascular region at its insertion and are frequently noted at the anterior attachment to the greater tuberosity of the humerus (Tagg *et al.* 2013: 6; Hodgson, O'Connor and Grainger 2012: 1163).

Complete tears of the rotator cuff tendon may lead to a medial tendon retraction as a full-thickness tear, as it affects the full width of the tendon (Gaitini 2012: 6). Consequently, tendon retraction under the acromion often results in nonappearance of the rotator cuff with fluid or herniation of the deltoid muscle in the region of the defect (Beggs 2011: 104). Moreover, such tears may involve the infraspinatus tendon, subscapularis tendon and longhead of the biceps tendon (Singh 2012: 286), whilst a secondary indicator of rotator cuff tears include fluid presence in the subdeltoid bursa and biceps tendon sheath (Beggs 2011: 104).

In contrast, partial thickness tears are classified based on their location, with the tear communicating to either the articular or bursal surface of the tendon, whilst intrasubstance tears occur within the tendon (Matthewson *et al.* 2014: 4; Sheng 2013: 42; Trent. 2013:15). The width of rotator cuff tears also vary with small tears. A few millimetres in width can affect a single tear in comparison to large tears which exceed 5mm in width and may involve more than one tendon (Frisch 2011: 21). Tendon tears thus weaken tendon structure and are primarily located in areas of degenerative change (Frisch 2011: 21). Therefore, healing tendons with scar tissue, located especially around the edges of torn rotator cuff tendons, are biomechanically inferior to intact tendons, thereby reducing its ability to withstand strain or tensile strength (Chaudhury *et al.* 2011: 945).

Although tears of the infraspinatus tendons are uncommon, such tears are common in athletes participating in over-arm throwing activities (Singh 2012: 290). These individuals usually present with internal (postero-superior) impingement. Sheng (2013: 49) maintained that

overhead throwing athletes are predisposed to partial thickness tears as the rotator cuff tendons often undergo repetitive strain and extreme force during deceleration. In addition, joint effusion in the gleno humeral joint space may be present. (Singh 2012: 290). An earlier study on the infraspinatus tendon of sheep cadavers suggested that tendon rupture may be a consequence of excessive load-bearing of the tendon (Frisch 2014: 3818). This acousto elastic ultrasound study indicated that the bursal side of the tendon was less stiff (in contrast to the bursal side of the human infraspinatus tendon) than the articular side. However, a significant limitation of this study was the inadequacy of the experimental set up for transducer fibre alignment and thus, further quantitative assessments were advocated (Frisch 2014: 3818). Of note, isolated subscapularis tears occur less frequently than supraspinatus or infraspinatus tendon tears and generally occur in combination with the latter tendon tears, as a result of a traumatic event (Dong *et al.* 2015: 1485). Nevertheless, Singh (2012: 288) reported that tears of the teres minor tendon remain uncommon.

2.3.2 Biceps tendon pathology

It has been reported that biceps tendon tears may result from a supraspinatus tear extending across the rotator cuff interval to the subscapularis tendon (Beggs 2011: 110). The indicated condition consequently leads to biceps instability when the tendon is displaced medially from the bicipital groove (Beggs 2011: 110). This may be attributed to the position of the fibres of the subscapularis tendons which form the floor of the sheath of the biceps tendon (Sheng 2013:38). Several researchers have postulated that biceps tendinitis and tendinosis are frequently associated with rotator cuff tears (Seo, Yoo and Ryu 2014: 272; Yoon *et al.* 2014: 107; Cowling, Gamble and Rangan 2011: 15). These investigators ascertained that biceps tendinopathy encompasses a range of pathologies, including inflammatory tenosynovitis (effusion of the synovial sheath around tendon) to tendinosis, caused by degeneration. Although minimal fluid around the biceps tendon is frequently observed and asymptomatic, discernible effusion is evident in symptomatic patients (Messina *et al.* 2015:6).

2.3.3 Prevalence and clinical features of rotator cuff and biceps tendon pathology

Rotator cuff pathology, a common cause of shoulder pain, precipitates limited range of arm movement (Chepeha, Bouliane and Sheps 2015: 240; Trent 2013: 15). Approximately 20% of the entire adult population is affected, especially those above 50 years of age (Park *et al.* 2013: 1360). It is estimated that more than 50 % of the American population will present with

rotator cuff tears by the age of 70 years, even though asymptomatic (Nazarian *et al.* 2013: 590). Consequently 250,000 rotator cuff surgeries are performed in the United States annually (Baumer *et al.* 2018: 282). Likewise, the annual prevalence of shoulder complaint in South Africa is approximately 46.7% with a lifetime prevalence of 66, 7% (Van Zuydam *et al.* 2015: 34). Thus, any anomaly that occurs in the shoulder region can lead to debilitation of the arm and therefore a loss in functional status (Muraki *et al.* 2015: 120; Escamilla, Hooks and Wilk 2014: 13; Dranonaki, Allen and Wilson 2012: 1435).

An ultrasound B- Mode study, conducted in a Japanese village, concluded that asymptomatic tears of the rotator were more common in participants over 50 years than symptomatic tears (Minagawa *et al.* 2013: 8). These investigators highlighted the prevalence of tear in each decade, namely, 0% in the 20s to 40s, 10.7% in the 50s, 15.2% in the 60s, 26.5% in the 70s, and 36.6% in the 80s respectively. However, their studies were conducted on a largely ageing population where the average age of a participant was 70 years. A limitation to the study of asymptomatic rotator cuff tears was the exclusion of the urban population. Although it was acknowledged that the use of MRI may have strengthened the outcomes of the study, this method of imaging was considered expensive for the purpose of mass screening (Minagawa *et al.* 2103: 11).

Localised tenderness, swelling of tendon and impaired arm movements are characteristic clinical features which with patients present at health care facilities (Maganaris *et al.* 2017: 4; Ooi *et al.* 2014: 1). The management protocol necessitates clinical assessment of the shoulder to rule out compression of the rotator cuff and the subacromial bursa against the anteroinferior aspect of the acromion and the coracoacromial ligament (Van Zuydam *et al.* 2015: 34). Most patients suffering from biceps tendinitis or tendinosis usually present with a deep, throbbing pain in the anterior shoulder (Yoon *et al.* 2014: 107). Furthermore, rupture of the long head of the biceps tendon may be characterized by a lump in the anterior arm known as the ‘Popeye’ sign (Gaitini: 2012: 9). Tendon disruption occurs at the intraarticular level, consequently leading to an empty bicipital groove. In conjunction with acute tears, the tendon stump appears surrounded by fluid (Gaitini: 2012: 9). Other clinical indications may include tenosynovitis or dislocation or subscapularis tear (Lee *et al.* 2016a: 1610).

The number of supraspinatus tendon tears has increased from approximately 64% (Iagnocco *et al.* 2003:356) to 80% (Messina *et al.* 2015: 2). Also, recent reports have demonstrated tears

of the infraspinatus approximate (15%) followed by subscapularis tendon (5%) (Messina *et al.* 2015:2). In addition, calcifications of the rotator cuff tendons are frequently identified, affecting almost 7% of patients who present with shoulder pain (Henning *et al.* 2015: 43), with the most recurring impaction of the supraspinatus tendon, followed by the infraspinatus and the subscapularis tendons (Henning *et al.* 2015: 440; Riente *et al.* 2013: 331).

2.3.4 Common causes of shoulder pathologies

Shoulder pathology encompasses a wide range, from rotator cuff pathologies to calcifying tendinosis, synovitis and acromioclavicular arthritis, including acromial spurs and hyperostosis at the greater tuberosity of the humerus (Gaitini 2012: 9 and Beggs 2011: 108). Age related factors, medical conditions and genetics are some of the factors which contribute to calcific tendinosis caused by deposition of calcium hydroxyapatite crystals (Lee *et al.* 2016a: 1612). Factors affecting the acromioclavicular joint include osteoarthritis, trauma or synovial cysts crystals (Lee *et al.* 2016a: 1612). According to Lee *et al.* (2016a: 1612) bursitis of the sub acromial sub deltoid bursa may occur as a result of rotator cuff tears or an inflammatory process. Primary causes may include rheumatoid arthritis, gout and tuberculosis, including other inflammatory conditions, whilst secondary causes may be related to rotator cuff tendinopathy, tears or anterior shoulder impingement (Messina *et al.* 2015: 2).

Rotator cuff pathology appears to occur in response to a combination of both intrinsic and extrinsic factors (Naidoo, Lazarus and Satyapal 2016: 975; Trent. 2013:15). Intrinsic factors are attributable to the ageing process, microscopic changes and decreased vascularity of tendons. (Matthewson *et al.* 2015: 3). Microscopic changes are precipitated by the decrease in the water content and breakdown of collagen fibres (Tudisco *et al.* 2015: 393; Matthewson *et al.* 2015: 3; Hodgson, O'Connor and Grainger 2012: 1160). Asymptomatic tears of the rotator cuff tendons in older individuals above 50 years of age are common, ranging from 6% to 40 % (Beggs 2011: 108). Notwithstanding, older individuals are prone to rotator cuff tears due to the decrease in strength of tendons (Sheng 2031: 44). This has been reaffirmed by Weinreb *et al.* (2014: 67), who highlighted intrinsic degeneration to be a primary cause of most rotator cuff tears. In contrast, extrinsic factors have been linked to trauma or anatomical factors such as hooked, curved, and laterally sloping acromion and narrowing of the coracoacromial arch (Van Zuydam *et al.* 2015: 35; Trent 2013: 14). Extrinsic factors are strongly correlated to rotator cuff tears which increase contact pressure between the rotator cuff tendons and the

coracoacromial ligament (Kijima *et al.* 2013: 1). In addition, subacromial impingement, glenohumeral instability and internal impingement are further extrinsic factors that can contribute to rotator cuff pathology (Matthewson *et al.* 2015: 3). Thus, taking into consideration the varying degrees of rotator cuff disease, a variety of management procedures are generally proposed (Messina *et al.* 2015: 6).

2.4 TREATMENT OF SHOULDER JOINT PATHOLOGY

Clinical management of rotator cuff pathologies poses a challenge to health care professionals (Roskopf *et al.* 2016: 466). Current modes of shoulder pathology treatments include physical therapy, surgery or a combination of both (Trent 2013: 16; Frisch 2011: 30). Non-surgical treatment often includes the use of anti-inflammatory drugs, steroid injections, reduction of activities and physio therapy (Mesina *et al.* 2015: 6; Trent 2013: 16). Asymptomatic calcific tendinopathy may be treated conservatively, whereas lithotripsy or ultrasound guided irrigation of calcifications may be effective in selected cases (Messina *et al.* 2015: 2). Also, subacromial subdeltoid bursitis may be treated with corticosteroids in order to reduce inflammation and pain (Messina *et al.* 2015; 2). Rehabilitation approaches are aimed at changing the mechanical properties of tissues (Brandenburg *et al.* 2014: 2208). The most appropriate course of treatment is generally based on the presence of either a partial or full-thickness rotator cuff tear, depending on whether the tear is acute or chronic (Edwards *et al.* 2016: 284).

Surgery is usually recommended for patients who have responded poorly to conservative treatment within three to six months, or patients with full thickness tears (Trent 2013: 16). This may involve the reattachment of the torn rotator cuff tendon insertion into the humeral head or decompression whereby the size of the sub acromial space is increased (Edwards *et al.* 2016: 283). Furthermore, younger patients who present with acute tears greater than 1cm often benefit from surgical procedures, in contrast to older patients (> 65 years), due to muscle atrophy and fatty infiltration (Edwards *et al.* 2016: 295). However, much conflict prevails regarding clinical assessments surrounding surgical versus non-surgical interventions (Edwards *et al.* 2016: 280). Contrary to the previous researchers, another group advocated surgical treatment for older patients (50-75 years) presenting with small to medium supraspinatus tears of less than 3cm, as this yielded a better recovery. (De Carli *et al.* 2017: 40. Prolonged exercise rehabilitation was advised by other investigators for tendinopathies, including small full thickness and partial thickness tears (Edwards *et al.* 2016: 295). Edwards

et al. (2016: 295), however, observed that conservative treatment yielded a 73-80 % effective recovery. Alternatively, De Carli *et al* (2017: 40) advocated physiotherapy in patients not undergoing surgery, in order to reduce the rate of the tendon re-tear.

Other forms of therapies for tendon pathologies include the injection of platelet-rich-plasma (PRP) in athletes to precipitate healing and tissue regeneration (Nwawka 2016: 4; Messina *et al.* 2015: 3; Ehrenfest *et al.* 2014: 4), as well as the ablation of diseased tendon tissue via the use of an ultrasound guided needle to the hypoechoic region of tendon tissue, for debridement, emulsification and fluid aspiration (Escamilla, Hooks and Wilk 2014:15). However, Nourissat *et al.* (2015 cited in Messina *et al.* 2015: 3) contended that current data did not support the use of PRP as a first line treatment for tendinopathy but may be considered in specific cases of tendinopathies following the failure of corticosteroid injections. Therefore, it is also essential to consider the quantification of local stress properties within the diseased tendon, when deliberating the choice of management (Maganaris *et al.* 2017: 5).

2.5 DIAGNOSTIC TOOLS USED IN THE DETERMINATION OF SHOULDER PATHOLOGY

To date there are several techniques utilised in defining pathology associated with rotator cuff and biceps tendon such as palpation, plain film radiography, Magnetic Resonance Imaging (MRI), ultrasound and elastography (Trent 2013: 17; Nowicki and Dobruch-Sobczak 2016: 114). Palpation has been used to identify tumours as being harder tissues when compared to surrounding tissues (Nowicki and Dobruch-Sobczak 2016: 114). Whilst organ palpation is instrumental in assessing the characteristic tissue consistency within the shoulder (Brandenburg *et al.* 2014: 2207), access to deeper tissues are limited by this method (Bhargava *et al.* 2013: 25). Thus, its use in early detection of the disease pathology, its diagnosis and prognosis is restricted and offers low sensitivity (Garra 2015: 680; Song 2014: 30). Beggs (2011: 101) reported that the Neers and Hawkins test yielded moderate sensitivity (59-76%) and specificity (47%-625) for full thickness tears. Ilhanli *et al.* (2015: 31) ascertained that these tests are clinically useful in diagnosis of rotator cuff tears when incorporated with other physical tests. It is therefore imperative for health care professions to identify and test new imaging modalities.

Imaging methods have improved over time, thereby making it possible to assess *in vivo* musculoskeletal function by direct measurements of tendons and muscles (Sikdar, Wei and Cortes 2014: 126; Ooi *et al.* 2014: 2). The advancement in ultrasound technology has led to the implementation of new imaging techniques such as elastography to quantitatively assess tissue changes (Guerini *et al.* 2012: 1; Chernak and Thelen 2012: 1). Several studies demonstrate that the commercially available elastography or virtual palpation technique (Shiina *et al.* 2015: 1127) use standard ultrasound equipment to estimate the strain and elasticity of soft tissue (Ilhanli *et al.* 2015: 31; Song 2014: 30; DeWall 2013: 2). This is a non-invasive method that has the potential to qualitatively and quantitatively evaluate tissue stiffness (Shin *et al.* 2016: 3362; Winn, Lalam and Cassar-Pullicino 2016: 868; Tudisco *et al.* 2015: 394).

2.5.1 Plain film radiography

Plain film radiography is routinely used to demonstrate signs of rotator cuff pathologies by viewing images of the bony outlines of the shoulder joint, including the humerus (Nazarian *et al.* 2013: 590). A rotator cuff tear in particular, may be indirectly identified by the presence of cortical irregularities of the greater tuberosity (Nazarian *et al.* 2013: 590). In addition, acromioclavicular osteoarthritis with inferior osteophyte formation, acromial enthesophytes or sclerosis, and cystic changes of the humeral head, are verified with plain film radiography (Van Zuydam *et al.* 2015: 36). Although plain film radiography is able to identify sub acromial spurs, it is impossible to exclude the presence of rotator cuff partial thickness tears (Trent 2013: 17). This form of imaging is therefore limited in the demonstration of inflammation or early soft tissue changes (Kehl *et al.* 2016: 7).

2.5.2 Magnetic Resonance Imaging (MRI) and Magnetic Resonance Elastography (MRE)

Magnetic Resonance Imaging (MRI) is referred to as the gold standard in the diagnosis of shoulder pathologies (Tudisco *et al.* 2015: 394). This diagnostic tool provides evaluation of all shoulder structures, in addition to cartilage and bone marrow imaging (Nazarian *et al.* 2013: 591). Although MRI and Magnetic Resonance Arthrography demonstrates a high accuracy of rotator cuff tears, there is limited availability of the equipment, as the machinery is expensive (Ooi *et al.* 2013: 2). Besides, MRI lacks the potential to provide real time data and intraarticular injections used during the procedure are invasive (Trent 2013: 17). Furthermore, this method is inadequate for use on individuals with metallic implants and

electronic devices (Nazarian *et al.* 2013: 591). Whilst it has the potential to diagnose full thickness tears with a 92.1% sensitivity and 92.9% specificity, it is limited in the diagnosis of partial thickness tears due to its 63.6% sensitivity and 91.7% specificity (Nazarian *et al.* 2013: 591).

Magnetic resonance elastography (MRE) is used for quantitative assessment of shear waves in tissues (Sarvazyan, Urban and Greenleaf 2013: 1138). The resulting shear wave measured with MRI uses harmonic waves at a specific frequency typically ranging from 20 to 200 Hz (Sarvazyan, Urban and Greenleaf 2013: 1138). MRE is a technique that can provide mechanical properties of tissues such as shear modulus (Dresner *et al.* 2001: 269). This method of imaging adopts a phase contrast MRI method to measure the stiffness of tissues by observing the generation of shear wave in material, thereby measuring its speed in metres/sec (Dresner *et al.* 2001: 269). MRE is beneficial in evaluating liver fibrosis, breast lesions, cardiac and brain tumours (Bhargava *et al.* 2013: 29). Further applications include muscular imaging, in particular, cardiac muscles (Dresner *et al.* 2001: 276). However, measurement is often affected by space, and thus positioning of the subject may be restricted (Muraki *et al.* 2015: 121), thereby limiting its potential in quantifying musculo skeletal dynamics (Sikdar, Cortes and Wei 2014: 10). Ultrasound elastography has been advocated as a more suitable option, due to the advantage of dynamic assessment manoeuvres of joint positions in real time (Muraki *et al.* 2014: 21).

2.5.3 Ultrasound

Ultrasound evaluation of shoulder pathologies in particular rotator cuff imaging, commenced in 1977 and has subsequently become a popular diagnostic modality, developing with constant evolving technology (Nazarian *et al.* 2013: 591 and Gennisson *et al.* 2013: 487). A remarkable feature of ultrasound is that it is a rapid examination performed in real time, is cost effective, radiation free and usually the first-line imaging technique for the assessment of shoulder pathology (Messina *et al.* 2015: 1; Gaitini 2012: 2; Singh 2012: 284). This diagnostic technique enables the visualisation and interpretation of human body structures including tendons, muscles, joints, vessels and internal organs by the display of their echo pattern (Lee *et al.* 2016a: 1606; Shiina *et al.* 2015: 1126). Pertinent images of fascicles in muscle and collagen strands in tendons can be clearly envisaged as a result of the different acoustic properties at various tissue boundaries. Consequently, unique speckled pattern of

tissues emerge following the propagation of ultrasound waves into tissue (Sikdar, Cortes and Wei 2015: 3).

2.5.3.1 Brightness Modulation ultrasound (B-Mode ultrasound)

B-Mode (standard brightness mode) or sonogram pertains to the degree of the reflected wave with an intensity level between 0 (black) and 255 (white) (Frisch 2011: 27). Images of conventional B-Mode ultrasound are derived from longitudinal waves, by use of a transducer placed directly on and moved over the patient's body (Greenleaf and Urban 2016: 1201; Kaur 2013: 388). Through the activation of electrical charge, the transmitted sound waves travel at high speeds through the tissue (1450–1550 m/s) with the aid of piezoelectric material lined inside the transducer (Nordenfur 2013: 1 and Garra 2015: 689). The frequency of the B-Mode transducers (with range between 1-20 MHz) (Gennisson *et al.* 2015: 1), subsequently allows for the reflected waves from the observed tissue to be visualised on a television monitor (Nordenfur 2013: 1; Kaur 2013: 388). Current transducers are equipped with a wide range of frequencies, designed to improve image quality (Bamidele *et al.* 2015:21).

Normal tendon images on longitudinal sagittal B-Mode ultrasound images are described as closely spaced echogenic parallel lines on a B- Mode ultrasound imaging scanner whilst on transverse orientation of the transducer, images are depicted as multiple echogenic dots (Hodgson, O'Connor and Grainger 2012: 1158). The supraspinatus tendon is identified by its convex surface and is depicted as having a bird's beak appearance (Lee *et al.* 2016a: 1614). It has a homogenous echo pattern, tapering distally at its insertion into the greater tuberosity, where the footprint is seen as a shallow depression of the cortex of the humerus (Beggs 2011: 102). The hyaline cartilage is seen as an anechoic area that covers the articular surface of the cortex, whilst the subacromial subdeltoid bursa is identified on the concave side, between the supraspinatus tendon and the deltoid muscle (Beggs 2011: 103) (Figure 2.2).

Of note, B-Mode ultrasound, as opposed to Magnetic Resonance Imaging (MRI) is a dynamic examination, for it enables the examiner to repeat and rescan the region of interest. It has been indicated that dynamic studies provide added benefit in visualization of tendons in motion, observed during internal and external arm manipulation (Oliveira *et al.* 2017: 2; Guo *et al.* 2016: 362; Van Zuydam *et al.* 2015: 360). However, a drawback encountered during the ultrasound examination of tendons may well be anisotropy. Anisotropy, in B-Mode imaging, has been described as the deflection of the ultrasound beam, especially in the

imaging of tendons and ligaments, attributable to the arrangement of tissue fibres. Consequently, normal hyperechoic tendon may appear hypoechoic instead of hyperechoic, attributable to the region of interest not being positioned perpendicular to the ultrasound beam (Guo *et al.* 2016: 362; Nader, John and Kendall 2016: 35). Thus it is critical that the transducer be placed parallel to the tendons in order to avoid anisotropy which can simulate a disease process (Oliveria *et al.* 2016:5; Hodgson, O'Connor and Grainger 2012: 1158).

B-Mode ultrasound scans have improved the diagnosis, prognosis and monitoring of disease outcomes (Kang *et al.* 2013: 497). The detection of tendinosis generally presents as a heterogeneous, hypoechoic poorly defined thickened tendon (Dong *et al.* 2015: 1485; Sahan *et al.* 2018: 196). This diagnostic tool enables the visualization of partial thickness tendon tears as a hypoechoic defect in the tendon, with resultant tendon thickness alteration (Gaitini 2012: 6), whilst full thickness tears appear anechoic or as low level echoes as a result of the presence of fluid (Beggs 2011: 113). In addition, massive tears of the rotator cuff resulting in the exposure of the humeral head, precipitated by the supraspinatus tendon retraction, is called the 'naked' head sign on B-Mode ultrasound (Gaitini 2012: 6). B-Mode ultrasound is also beneficial in the detection of muscle injuries such as myofascial tears and intramuscular haematoma (Nwawka 2016: 430). Thus, the capability of recognizing the specific site and extent of rotator cuff tendon injury is significant for patient treatment outcome (Trent 2013: 41).

Although tendinopathy may demonstrate a loss of the normal fibrillary structure with reduced echogenicity on B-Mode ultrasound investigations, (Kang *et al.* 2013: 497; Hodgson, O'Connor and Grainger 2012: 1160), it is also possible for tendon pathologies to show similar isoechoic patterns in pathologies such as oedema, haemorrhage, mucoid degeneration, or tears (Bamidele *et al.* 2015: 21). Moreover, tendon thickening may occur with tendinopathy with the possibility of calcification within the tendon (Hodgson, O'Connor and Grainger 2012:1160). A potential pitfall in B-Mode scan, however, is the inability to distinguish between intrasubstance and partial-thickness tears from focal tendinopathy (Gaitini 2012: 2). Hodgson, O'Connor and Grainger (2012: 1160) have indicated that tendon tears may demonstrate anechoic fluid in an acute condition, with an increase in echogenicity as it becomes organised thus making it indistinguishable from surrounding tendon tissue , whilst shadowing artefacts may arise from highly reflecting interfaces of tissues (Nordenfur 2013: 2).

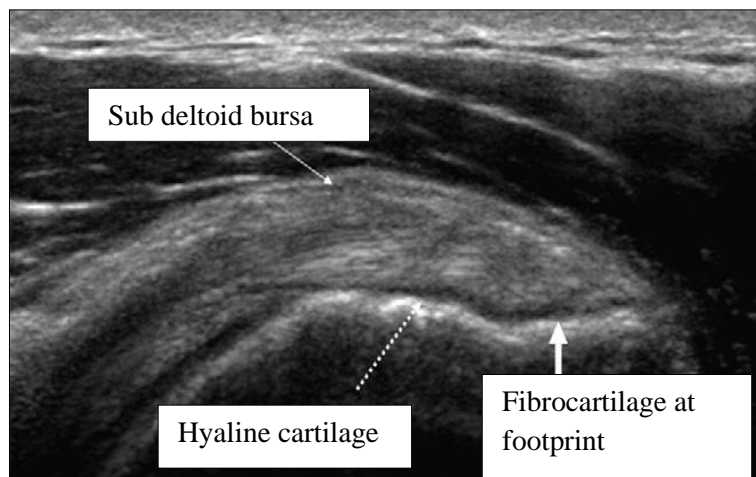


Figure 2.2: B-Mode ultrasound of the sagittal scan of supraspinatus tendon. The tendon has a convex bursal surface as it narrows to insert on the greater tuberosity. The hypoechoic subdeltoid bursa (thin arrow) is noted between tendon and deltoid muscle. The anechoic hyaline cartilage (broken arrow) that covers the articular cortex is continuous with the fibrocartilage (thick arrow) at the footprint. The footprint is seen as a shallow depression in the humeral cortex. Adapted from Beggs (2011: 103).

2.5.3.2 Doppler ultrasound

Doppler ultrasound has the potential to measure the direction and speed of blood cells as they move through vessels. Its use in evaluating tissue vascularity to exclude inflammatory conditions is quite significant (Nwawka 2016: 429 and Kang *et al.* 2013: 497). This technique is based on the Doppler Effect which describes a change in frequency of ultrasound waves reflected from moving objects such as red blood cells. Spectral Doppler exhibits the systolic and diastolic velocity in the blood vessels in each cardiac cycle by calculation of the resistive index to assess tissue inflammation (Filippucci *et al.* 2013: 85). Power Doppler ultrasound has also been used to detect and monitor the progression of pathological tendons (Dirrichs *et al.* 2016: 1204). Although Doppler ultrasound imaging is used in the assessment of blood flow abnormalities in shoulder pathology, rheumatologists are interested in new modalities which can provide additional information (Filippucci *et al.* 2013: 83).

2.6 ELASTOGRAPHY

Although B- Mode ultrasound provides images of structure and form of organs, it is deficient in the provision of quantitative information of tissue elastic properties (Ryu and Jeong 2017: 185; Shiina *et al.* 2015:1126). The elasticity of tissue refers to its potential to return to its original state after undergoing compression or stress (Nowicki and Dobruch- Sobczak 2016: 114). Therefore, the sole objective of elastography is to focus on the imaging of tissue stiffness in order to provide a relevant diagnostic tool for diagnosis of organ pathology (Gennisson *et al.* 2013: 287). Elastography is based on the principle that suggests changes (strain) in the tissue exposed to either mechanical or physical stress, and is dependent on the elastic properties of the tissue (Corazza 2015: 2).

Strain or compression elastography, which was initially described by Dr Jonathan Ophir (Ophir *et al.* 1991: 111), maps elastic properties of tissue by compression through the application of pressure from a hand held transducer (Ilhanli *et al.* 2015: 31 and Shiina *et al.* 2015:1129). These investigators compressed areas of tissue and tracked speckles of change in ultrasound echoes on pre and post compression ultrasound images, concluding that harder tissues deformed less under compression than softer tissues (Ophir *et al.* 1991: 111). Elastography data reported tissue stiffness as a grey or colour-coded map displayed on an ultrasound monitor (Nowicki and Dobruch-Sobczak 2016: 117). Various factors determine stiffness of biological tissue, and are related to the composition of tissue such as fat and fibre (Shiina *et al.* 2015: 1127). Thus, measurements of elasticity of hard or soft tissue which reflect the quality of tissue can be evaluated (Tudisco *et al.* 2015: 393). An added benefit of ultrasound elastography is that it is non-invasive, safe and inexpensive (Tudisco *et al.* 2015: 393). This method is independent from grey scale B-Mode ultrasound and Doppler imaging (Rahman *et al.* 2013: 76).

One of the first areas of the body to be widely investigated in the diagnosis of cancer using strain elastography was the breast (Shiina *et al.* 2015: 1130). The use of ultrasound elastography is predominant in some areas of medicine, especially in the field of oncology where it is utilised for imaging of lesions in the liver, breast or prostate in order to differentiate between benign and malignant lesions (Paluch *et al.* 2016: 241; Drakonaki, Allen and Wilson 2012: 1437). Elastography has also been widely employed in the ultrasound examination of the pancreas, thyroid, cervix and lymph nodes as well as in musculoskeletal studies (Ohuegbe 2014: 34; Drakonaki, Allen and Wilson 2012: 1436).

Further studies of elastography include the assessment of liver fibrosis, skin and subcutaneous tissues, vascular and cardiac pathologies (Bhargava *et al.* 2013: 26).

2.6.1 Theoretical framework of ultrasound elastography based on the Young's modulus theory of elasticity

Ultrasound elastography has emerged as a valuable ancillary tool for the evaluation of biomechanical properties of skeletal muscle and tendons (Eby *et al.* 2013: 2382). Therefore, a theoretical model is required to non-invasively calculate the elastic modulus from the measured local deformation generated by the shear wave transmission (Wang *et al.* 2013: 1). The distribution of stress in tissue is unknown with strain ultrasound elastography; therefore, Young's modulus of elasticity cannot be directly estimated (Sikdar, Cortes and Wei 2014: 130). Alternatively, shear wave ultrasound elastography (on which this study is based) is related to the local shear elastic modulus or Young's modulus and has been approved by the US Food and Drug Administration (Hou *et al.* 2017: 96). Young's modulus has been identified as a numerical constant, named after the 18th century English physician and physicist Thomas Young (Encyclopaedia Britannica: Young's modulus 2016: 1). Thomas Young measured the stiffness of a metal rod by applying strain to the solid material. The stiffness defines the relationship between stress (force per unit area) and strain (deformation) (Encyclopaedia Britannica: Young's modulus 2016: 1).

Numerical calculations of tissue stiffness or elasticity index (EI) thereby allow for measurement to be captured as kilopascals (Shiina *et al.* 2015: 1139; Ooi *et al.* 2014: 5; Simic *et al.* 2012: 2) or metres per sec (m/s) (Corazzo 2015: 5). The Young's modulus theory, denoted as E , is reported as a physical specification which was documented by Professor Sarvazyan (Gennisson 2016: 1). The aim of this theory is to determine tissue deformability and its purpose in elastography, by applying stress to tissue in order to distinguish between soft and hard (stiff) tissues (Sarvazyan, Urban and Greenleaf 2013: 1141; Gennisson *et al.* 2013: 488). The formula employed for use in shear wave elastography is $\mu = c_s^2 \rho$ where μ is shear modulus, c_s is speed of shear wave propagation velocity and ρ is density assumed to be 1000 Kg/m^3 for all soft tissues (Shiina *et al.* 2015: 1134; Eby *et al.* 2013: 2381). Therefore, a low speed is associated with a soft medium whilst a high speed corresponds to a stiff medium (Eby *et al.* 2013: 2381). However, the speed of shear waves is dependent on the direction of tissue fibres, as musculoskeletal tendons are anisotropic (Li and Cao 2017: 27; Sarvazyan, Urban and Greenleaf 2013: 1142).

Moreover, Young's modulus theory is based on the supposition that the material under examination is linear, isotropic, incompressible or homogenous in nature (Shiina *et al.* 2015: 1129; Inami and Kawakami 2016: 314). This theory works well with the breast, liver or thyroid tissue, when compared to muscle tissue which is anisotropic in nature (Inami and Kawakami 2016: 314). Although this assumption is employed, soft tissues exhibit nonlinear, viscoelastic and heterogenous properties capable of affecting measurements (Shiina *et al.* 2015: 1138). Since most tissues lack these tissue characteristics, tissue stiffness can be reported as shear wave velocity (meters/second), or as a modulus (Pascal) (Greenleaf and Urban 2016: 1201; Shiina *et al.* 2015: 1139). It has been ascertained that viscosity and nonlinear materials are dependent on the initial excitation of frequency of strain imaging or shear waves (Shiina *et al.* 2015:1138). Thus if the medium is elastic the tissue under examination has the potential to resume its original shape after shear wave propagation (Simic *et al.* 2012: 20; Palmeri and Nightingale 2011: 433).

It is reported that shear waves have the ability to characterise factors such as tissue anisotropy, viscosity and nonlinearity (Sarvazyan, Urban and Greenleaf. 2013: 1142), as well as the ability to travel faster in harder materials (Klauser *et al.* 2014: 2). This characterisation of tissue elasticity contributed to diagnostic significance, similar to qualitative palpation used by clinicians in conditions such as breast tumors and liver fibrosis (Eby *et al.* 2013: 2386; Greenleaf and Urban 2016: 1201; Shiina *et al.* 2015: 1139). However, variations in shear wave recordings of tendons have been identified (Ryu and Jeong 2017: 6 Taljanovic *et al.* 2017: 864; Chen *et al.* 2013: 449). The Young's modulus of a normal tendon as reported by Ryu and Jeong (2017: 6), is approximately 400-1,300 kPa whilst shear wave quantification in the Achilles tendon is recorded as 98.8 kPa \pm 47.1 kPa Arda *et al.* (2011 cited in Taljanovic *et al.* 2017: 864) and in a study by Chen *et al.* (2013: 449) as 291.91 \pm 4.38 kPa respectively.

Limitations to the Young's Modulus theory include measurement conditions where the intensity of the force to a region of interest may result in artefact, due to poor contact between the transducer and surface of body. In addition, the acoustic difference between tissues can lead to a greater refraction (change of direction) with shear waves. (Shiina *et al.* 2015: 10). Considering that the application of stress to fluids yield equivalent pressure in all directions, shear waves do not exist in pure fluids (Winn, Lalam and Cassar-Pullicino 2016: 869), hence cystic structures cannot be adequately investigated (Winn, Lalam and Cassar-Pullicino 2016:870 and Bamber *et al.* 2013: 171). Concerns have been raised regarding very superficial

structures, as a particular depth is required for the propagation of shear waves (Paluch *et al.* 2016: 242; Drakonaki, Allen and Wilson 2012: 1437). Since shear waves are attenuated in tissues at a depth, very deep tissues (> 9 cm from the skin) cannot be assessed (Winn, Lalam and Cassar-Pullicino 2016: 869).

The orientation of the ultrasound transducer has been pivotal in obtaining significant results in the investigation of cadavers of brachialis muscles (Eby *et al.* 2013: 2386). This study established that shear waves did not propagate well for transducer orientations in 45° and 90° to the long axis of muscle fibre (Eby *et al.* 2013: 2386). It was suggested by the aforementioned investigators that the transducer be positioned perpendicular to the tissue to avoid anisotropy. Greenleaf and Urban (2016: 1201) expounded on the fact that waves travel faster along tendon fibres than across the fibres and therefore advised SWUE measurement be done under controlled conditions for the detection of tendinopathy. Interestingly, Young's modulus theory held well for cadavers of beef muscle fibres that were parallel, as shear waves propagated readily along the fibres rather than perpendicular to the muscle fibres (Gennisson *et al.* 2013: 536). Cosgrove *et al.* (2013: 247) also highlighted transducer orientation in order to avoid factors of anisotropy (tissue refraction of the ultrasound beam due to orientation of tendon fibres) (Nader, John and Kendall 2016: 35), as the B-Mode appearance influenced elastogram images.

2.6.2 Types of Elastographic techniques

Several ultrasound elastographic techniques are currently in use in clinical practice (Drakonaki, Allen and Wilson 2012: 1436). The basic difference between these techniques depends on the source of applied pressure and therefore tissue displacement (Paluch *et al.* 2016: 241). Basic techniques include strain ultrasound elastography (SUE), shear wave ultrasound elastography (SWUE), transient ultrasound elastography and acoustic radiation force impulse (ARFI) ultrasound elastography (Drakonaki, Allen and Wilson 2012: 1436). Strain ultrasound elastography (SUE) is the most commonly used method where tissue is compressed manually (stress) by a hand held transducer with resultant axial displacement of tissue (strain) (Drakonaki, Allen and Wilson 2012: 1435). ARFI is a type of strain ultrasound whereby tissue is excited internally rather than externally by a focussed ultrasound pulse (Paluch *et al.* 2016: 242). This technique allows for the imaging of deep structures that are not accessible by strain ultrasound (Paluch *et al.* 2016: 242).

In contrast to SUE, transient elastography is distinguished as a variation of shear waveultrasound elastography (Sarvazyan, Urban and Greenleaf 2013: 1138). This method has been described as the generation of tissue excitement by a burst of vibration (mechanical excitation) from the ultrasound transducer, to estimate the speed of shear waves in tissues. However, the vibration is transient (momentary), consequently separating the forward waves from the reflected waves. Transient elastography is used mainly for examination of liver disease (Paluch *et al.* 2016: 242; Shiina *et al.* 2015: 1135; Drakonaki, Allen and Wilson 2012: 1437). Increased velocities of transient waves have been reported in higher degrees of liver fibrosis (Li and Cao 2017: 10). In addition, supersonic shear wave utilises multiple push beams, focussed at varying depths within tissue, consequently permitting examination of a larger field with an ultrafast plane-wave imaging technique in combination with a high frame rate (Brandenburg *et al.* 2014: 2211). Applications in breast lesions, thyroid nodules and liver fibrosis have been explored with this technique (Li and Cao 2017: 13).

2.6.2.1 Strain Ultrasound Elastography (SUE)

Strain ultrasound elastography and shear wave ultrasound elastography are frequently used in clinical practice (Garra 2015: 683; Ooi *et al.* 2014:11). Strain ultrasound elastography (SUE) was the first method developed (Ilhanli *et al.* 2015: 30) and involves the placement of a transducer, perpendicular over an examined structure (Paluch *et al.* 2016: 241). This technique was described by Dr Jonathan Ophir, and is reported to map elastic properties of tissue through compression, from a hand held ultrasound transducer (Ophir *et al.* 1991 cited in Ilhanli *et al.* 2015: 31). Furthermore, this technique involves the use of some degree of force, externally applied to tissue surface (Qiu *et al.* 2015: 89) (Figure 2.3). Strain ultrasound elastography records the change in size or shape of tissue elasticity produced by a force, applied on a unit area called stress (Rahman *et al.* 2013:77).

The resultant image superimposes on a conventional B-Mode image. It is displayed next to a B-Mode ultrasound image in a grey or colour coded strain distribution map called an elastogram (Figure 2.4). Soft tissue identification may be encoded as red for soft tissue, blue for hard tissue and yellow/green for intermediate stiffness (Ooi *et al.* 2014: 20; Drakonaki, Allen and Wilson 2012: 1436). This coding, however, is dependent on the operator or

vendor's preference (Ooi *et al.* 2014: 20; Drakonaki, Allen and Wilson 2012: 1436). This method of assessing tissue stiffness is restricted to a qualitative evaluation (Carlsen *et al.* 2015: 236). Major limitations experienced with this method include the lack of consistency in tissue compression over an examined region (Qiu *et al.* 2015:90:42; Ohuegbe 2014: 42; Rahman *et al.* 2013:78).

The value of ultrasound elastographic technique in characterising tissue stiffness in rotator cuff tendons has been acknowledged by many (Muraki *et al.* 2015: 121 and Galletti *et al.* 2015: 325). The Achilles tendon was the first and the most studied structure to be investigated using SUE (De Zordo *et al.* 2010:1; Cosgrove *et al.* 2013: 247). SUE of the supraspinatus tendon established that soft tissues deformed more and hard tissues less with application of pressure (Lalitha, Reddy and Reddy. 2011: 366). Botar Jid *et al.* (2012: 243) maintained that tendons displayed reduced elasticity during contraction and patient position. Yoon *et al.* (2014: 111) verified images of tissue softening with SUE in the investigation of an intratendinous focal lesion or peritendinous involvement in patients with biceps tendinitis or tendinosis. However, fluid around the biceps tendons posed a challenge, underestimating the grade of SUE.

Strain ultrasound elastography of the Achilles tendons demonstrated asymptomatic tendons as hard and pathologic areas, soft (Drakonaki, Allen and Wilson 2012: 1435; Drakonaki, Allen and Wilson 2009: 1197). A similar study by Sconfienza, Silvestri and Cimmino (2010: 377) yielded contradictory results. Nevertheless, the results of this study could have been attributed to technical factors, poor study designs or small population groups (Ooi *et al.* 2014: 5). An essential contribution of SUE is the semi quantitative ratio calculation of the area between affected area and healthy tissue of interest (Carlsen *et al.* 2015: 236; Garra 2015: 686; (Franchi-Abella, Elie and Correias 2013: 498). One such example of a strain ratio study conducted by Kijima *et al* (2013: 2) established that the coracoacromial ligament stiffened with age but softened in the presence of a rotator cuff tear. Drakonaki, Allen and Wilson (2009: 1196) reported good reproducibility with strain index measurements of the Achilles tendon but conceded that this was not an absolute measurement of tendon stiffness.

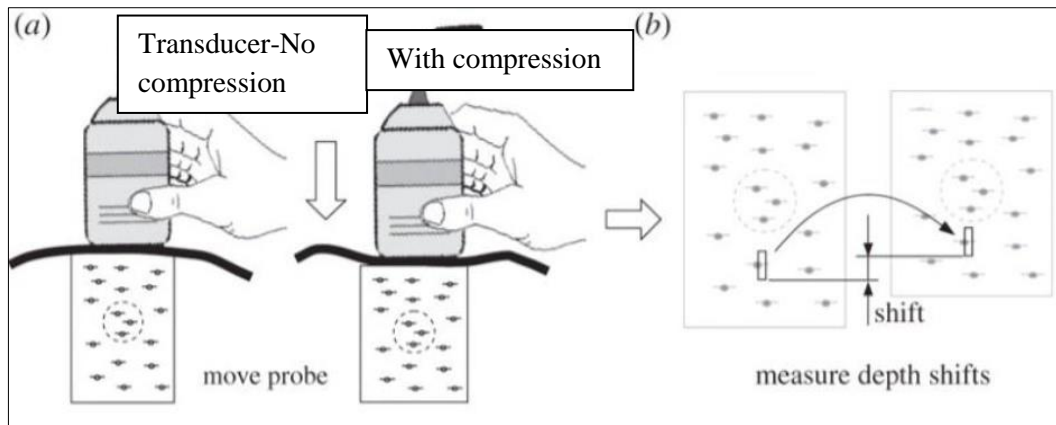


Figure 2. 3: (a) Strain ultrasound tissue compression by transducer (b) Measurement of resultant tissue displacement. Adapted from Trent (2013:10).

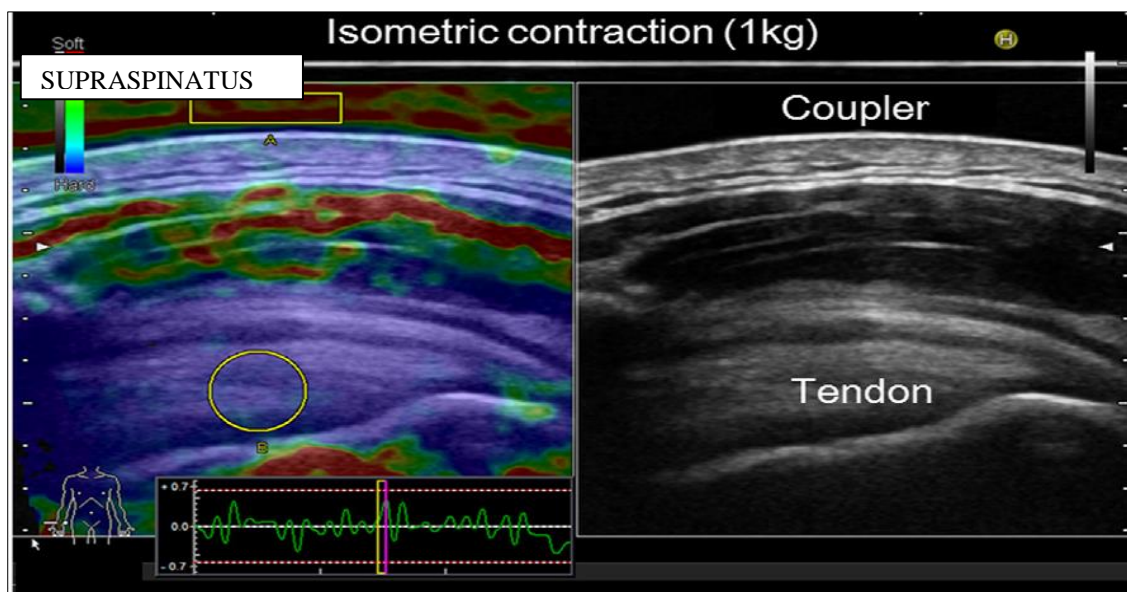


Figure 2.4: Strain ultrasound elastography of supraspinatus tendon. Region of interest (ROI) of supraspinatus is indicated by a yellow circle and ROI on acoustic gel is indicated by yellow rectangles. Blue represents hard elasticity. Adapted from Muraki *et al.* (2015: 125).

2.6.2.2 Shear Wave Ultrasound Elastography (SWUE)

Shear wave ultrasound elastography is a contemporary ultrasound technique that can quantitatively measure the biomechanical properties of tissue (Hou *et al.* 2017: 96; Qiu *et al.* 2015: 90). Unlike strain ultrasound elastography, SWUE does not require manual compression to evaluate tissue stiffness (Qiu *et al.* 2015:90; Rahman *et al.* 2013: 78). SWUE (first described by Hoyt, Parker and Reubens *et al.* 2007: 1086), is based on the principle where uniform ultrasound push beams are sent into the region of interest within the tissue, resulting in the generation and detection of shear waves or transverse waves within the tissue by the same ultrasound transducer (Winn, Lalam and Cassar-Pullicino 2016:869; Hatta *et al.* 2015: 3853) (Figure 2.5).

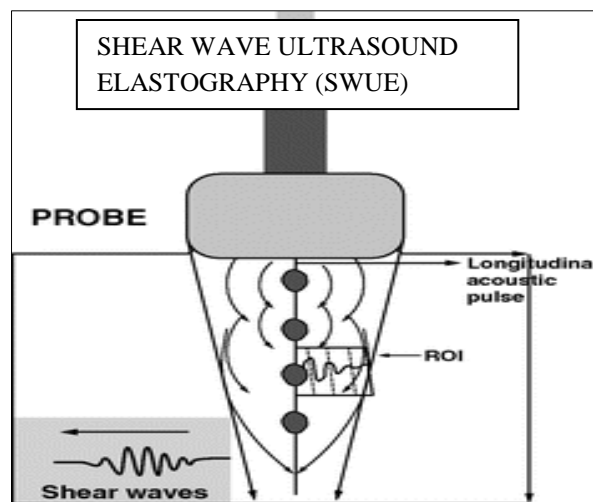


Figure 2.5: Principles of shear wave ultrasound elastography. Transmitted acoustic longitudinal pulse displaces tissue, resulting in shear wave propagation. Shear-wave elasticity value is measured within defined region of interest (ROI) with ultrasound tracking beams lateral to single push beam. Adapted from Arda *et al.* (2011: 533).

It has been reported that this process occurs as a result of the low attenuation of ultrasound, inclusive of a high-frequency thus, high resolution ultrasound imaging (Bamber *et al.* 2013: 171).

The physical properties of shear waves were introduced in 1997 by Professor Sarvazyan, (1997 cited in Song, 2014: 32) to quantitatively measure tissue property. Shear waves are defined as transverse waves that propagate much more slowly (usually 1–10 m/s) in tissue than B- mode ultrasound (Greenleaf and Urban 2016: 1201; Garra, 2015: 689; Drakonaki, Allen and Wilson 2012:1437). Shear waves propagation may be induced by either an external

source such as a vibrating plate or a mechanical punch or acoustic radiation force (Shiina *et al.* 2015:1134 and Palmeri and Nightingale 2011:435). Contrary to B-Mode ultrasound, shear waves diverge transversely in tissue, whilst B Mode longitudinal waves are reflected perpendicular from tissue interfaces (Greenleaf and Urban 2016:1201; Shiina *et al.* 2015: 1134). Hence shear wave particle movement is across the direction of transmission, likened to ripples on the surface of water when disturbed (Cosgrove *et al.* 2013: 239). The resultant shear waves frequency is understood to range from 45-205 Hz within soft materials (Li and Cao 2017: 6). Subsequently, the speed of shear waves are quantified by ultrafast computer systems in the evaluation of tissue composition and elasticity (Roskopf *et al.* 2016: 466). Through the computation of the Young's modulus of elasticity, tissue stiffness can be calculated in kilopascals (Paluch *et al.* 2016: 242; Arda *et al.* 2011: 532).

The resultant shear wave speed image may be displayed as a colour-coded image superimposed over a greyscale B-Mode ultrasound image (Figure 2.6) on a display monitor, with the depiction of softer tissue (depending on the operator and vendor's preference) in blue and stiffer tissue in red (Figure 2.7) (Shin *et al.* 2016: 3366; Hou *et al.* 2017: 98; Ooi *et al.* 2014: 20; Klauser *et al.* 2013: 838; Drakonaki *et al.* 2012: 1436). A cursor placed thereafter over the region of interest is used to calculate the speed of shear waves (Garra 2015:689). As reported by Simic *et al.* (2012: 2), a comparison of multiple areas of interest may be evaluated (Figure 2.8).

Sarvazyan, Urban and Greenleaf (2013: 1140) emphasized that hard tissue such as tendons, cartilage, cancellous and cortical bone, demonstrated very high shear wave speeds ($c_s > 20$ m/s) when applying Young's modulus theory. Chaudury *et al.* (2011: 945) and Klauser *et al.* (2014: 623) verified the application of this theory by observing a higher shear modulus in normal rotator cuff tendons as compared to torn rotator cuff tendons. It stands to reason that the breakdown of collagen fibres in degenerative tendons displayed soft elasticity, whilst tendon repair with fibrotic changes denoted hardening or stiff tissue (Winn, Lalam and Cassar-Pullicino 2016: 871).

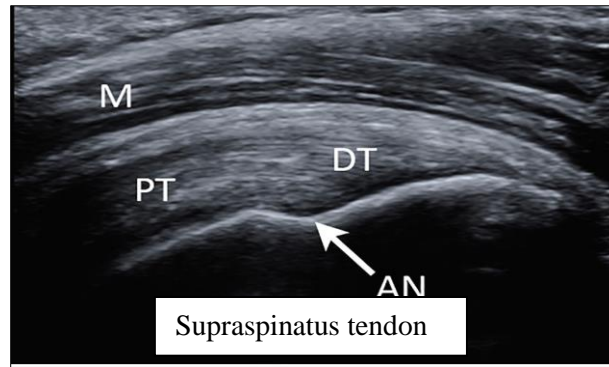


Figure 2.6: (a). B-mode normal supraspinatus tendon. (AN)-Anatomical neck. (PT)- Proximal tendon. (DT)- Distal tendon .M-Deltoid muscle. Adapted from Hou *et al.* (2017: 98)

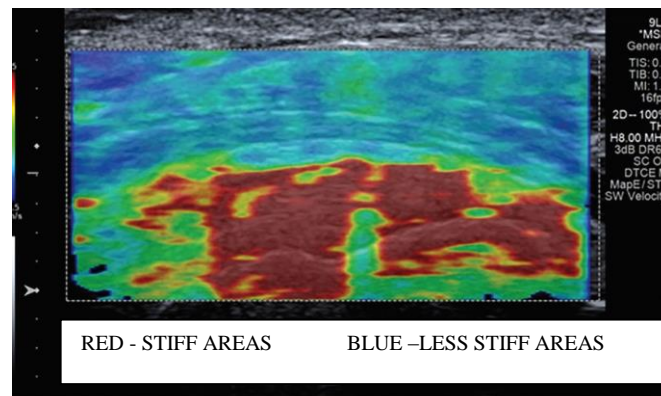


Figure 2.7: (b) Shear wave color map. Red areas – stiffer, less deformable supraspinatus tendon, compared to blue areas - less stiff deltoid muscle. Adapted from Hou *et al.* (2017: 98)

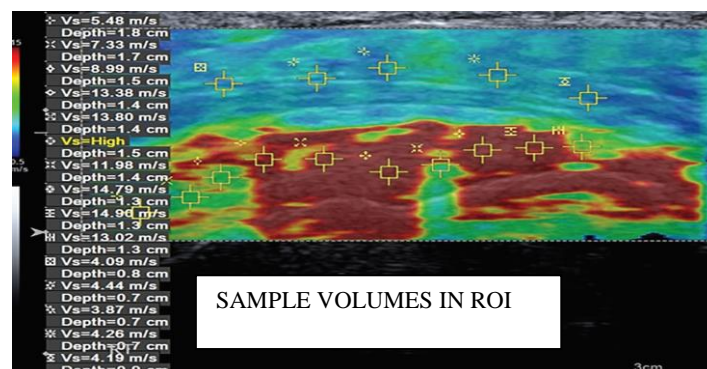


Figure 2.8: (c) Sample volumes in Region of interest ROI). Adapted from Hou *et al.* (2017: 98)

2.7 PRECAUTIONARY MEASURES WHEN USING ULTRASOUND ELASTOGRAPHY

Strain ultrasound elastography (SUE) and shear wave ultrasound elastography (SWUE) techniques follow similar B-Mode ultrasound safety considerations (Bamber *et al.* 2013: 182). Several indices are used to monitor the safety of diagnostic ultrasound imaging. As detailed by Nader, John and Kendall (2016: 36) and Shiina *et al.* (2013: 1137), these include Thermal Index (TI) which can monitor tissue temperature (heating) and Mechanical Index (MI) which can monitor localised tissue damage (acoustic cavitation). More importantly, display of these frequencies is required by the food and drug administration so that the operator is alerted to any possible tissue injury when the indices are high (Nader, John and Kendall 2016: 36). There is no radiation involved as B-Mode ultrasound and shear wave ultrasound elastography are noninvasive. The ALARA (As Low as Reasonably Allowed) principle is generally practiced. Commercially available radiation force elastography ultrasound systems have been manufactured to operate within acceptable limits. To date, no harmful bioeffects have been reported (Shiina *et al.* 2013: 1137).

2.8 APPLICATIONS OF ULTRASOUND ELASTOGRAPHY

2.8.1 Clinical use in organs

The breast has been frequently examined with strain ultrasound elastography since 1997 (Zaleska-Dorobisza *et al.* 2013: 648). SUE studies based on colour-coding were performed on 108 patients (median age: 53.9 years) (Thomas *et al.* 2006:335). Most lesions reported correlated well with cytology, thereby adding additional value to mammograms and B- Mode ultrasound (Thomas *et al.* 2006: 335). Real time elastography results yielded a sensitivity of 91.8% and a specificity of 78 % (Thomas *et al.* 2006: 335). Since then, various other methods have been introduced to assess breast tissue characterisation (Zaleska-Dorobisza *et al.* 2013: 645; Cosgrove *et al.* 2013:242).

Elasticity scores (Tsukuba score) have been developed to classify elastography patterns ranging from benign to malignant lesions. The Tsukuba five point scale (a standardized scale), based largely on a qualitative colour mapping, ranges from score 1 (soft tissue) to score 5 (stiff tissue), with score 5 referring to the extent of malignant tumour invasion beyond the boundary of a lesion into surrounding tissue (Cosgrove *et al.* 2013: 242). Fisher, Sack and Thomas (2013: 820) described a strain ratio which made comparisons between breast tumours and surrounding breast tissue. However, this semi quantitative evaluation yielded

poor results in regions of scar tissue. These investigators advocate the use of shear wave ultrasound elastography on account of its quantifiable characteristic (Fisher, Sack and Thomas 2013: 820). A semi quantitative ultrasound elastography conducted by Nairobiian investigators, to differentiate between benign and malignant breast lesions, showed no difference between SUE and strain ratios of the breast (Mutala, Ndaiga and Aywak. 2016: 1). Zaleska -Dorobisza *et al.* (2013: 645), however, maintained that tumours undergo varying deformation under pressure, when compared to healthy tissue lesions, and therefore elastography was successfully applicable in the diagnosis of malignant lesions. Bamidele *et al* (2015: 21) affirmed that that Young's modulus for breast cancer increased 10-15 times, compared to normal glandular breast tissue.

The use of strain ultrasound elastography on the thyroid nodules was also explored (Hong *et al.* 2009: 861). This three year study conducted between January 2006 to October 2008 on 90 patients who underwent surgical treatment for thyroid nodules, highlighted a tissue stiffness score for SUE from score 1 (low stiffness over nodule) to score 6 (high stiffness over nodule and adjacent tissue) (Hong *et al.* 2009: 861). Results yielded high sensitivity (88%) and specificity (93%) in 68 nodules in the differential diagnosis of thyroid malignancy (Hong *et al.* 2009:861). In contrast, Nyakoe (2015: 1) reported that elastography was not beneficial in determining the presence of malignancy of thyroid nodules. They do, however, suggest the use of fine needle aspiration, cytology and biopsies in order to provide a definitive diagnosis. Nevertheless, elastography has been proven to indicate precisely the place of a possible biopsy in regions of pathological tissue (Zaleska-Dorobisza *et al.* 2013: 646).

Shear wave ultrasound elastography has been extensively applied in examinations of the liver, breast, prostate, rectum and colon including lymph nodes, kidney, brain and carotid artery as well as endoscopic elastography (Carlsen *et al.* 2015:237; Nodenfur 2013: 4; Cosgrove *et al.* 2013: 238). Submitted reports on *invitro* studies on liver diseases demonstrated an increase in the elasticity of tissue (DeWall 2013: 2). Transient elastography, introduced in 2003, was the first method to be used in the assessment of liver disease (Cosgrove *et al.* 2013: 240). African studies on elastography also included transient shear wave elastography of the liver of immunocompromised patients in Nigeria, to exclude liver fibrosis in an attempt to avoid liver biopsy (Hawkins *et al.*2013: 189). Of note, grading and staging of liver fibrosis is pertinent to patient progression or regression with response to treatment (Zaleska-Dorobisza *et al.* 2013: 649).

Although shear wave ultrasound elastography has now become a standard procedure in the assessment of liver fibrosis, it cannot replace the gold standard of biopsy (Winn, Lalam and Cassar-Pullicino 2016: 875). Notwithstanding, it has been affirmed that since biopsies are invasive procedures, complications do occur (Cosgrove *et al.* 2013: 239). South African studies of elastography are scarce. The recent breakthrough study of the SWUE of liver was conducted by Dr Rajabally in Mediclinic, Constantiaberg, 2016 (Rajabally 2017: 1). A Fibroscan ultrasound machine was utilised whereby shear wave speed of the liver could be measured using vibration-controlled transient elastography to assess liver fibrosis. Dr Rajabally (2017: 1) reported that early treatment obviated the need for liver biopsy, especially for conditions such as viral hepatitis, non-alcoholic fatty liver disease, alcoholic liver disease and cholestatic liver disease. In addition, he claimed that early hepatic steatosis could be detected with transient ultrasound elastography prior to conventional B-Mode ultrasound (Rajabally 2017: 1).

The mean elasticity of SWUE of the thyroid, submandibular and parotid glands, masseter and gastrocnemius muscles, supraspinatus and Achilles tendons, renal cortex and pelvis, pancreas, and spleen of 127 healthy volunteers have been evaluated in kilopascals (Arda *et al.* 2011: 532). Unfortunately, this study was lambasted by Marcy, Thariat, and Lacout (2012: 1) for the lack of technical criteria in the assessment of healthy tissue. The aforementioned investigators claimed that the number of image acquisitions, including reference values for the scanning planes (longitudinal and axial), were omitted from the study (Marcy, Thariat and Lacout 2012: 1). Therefore, it was recommended that the utilisation of an adjustable region of interest (ROI) as well as a higher frame rate be applied for SWUE of musculoskeletal assessment of tendons (Wu *et al.* 2012: 83). As determined by Wu *et al.* (2012: 83) shear wave speed travels faster in tendons than in organs such as the liver and thyroid.

2.8.2 Clinical use in the Musculoskeletal System

Ultrasound elastographic application for musculoskeletal applications are limited and remain under investigation (Roskopf *et al.* 2016: 486 and Wu *et al.* 2012: 80). As stated earlier, the Achilles tendon has been the most studied structure with SUE (Cosgrove *et al.* 2013: 247). This tendon was first investigated by (De Zordo *et al.* 2010: 394) using SUE demonstrated perfect correlation with B- mode ultrasound. The advantage of this technique was the use of an easy scanning approach which could identify a relatively large sized tendon predisposed to pathology (Winn, Lalam and Cassar-Pullicino 2016:871). As reported by Drakonaki, Allen

and Wilson (2009: 1197), SUE demonstrated asymptomatic tendons as hard and pathologic areas as soft. Mentioned earlier, a similar study by Sconfienza, Silvestri and Cimmino (2010: 377) yielded contradictory results. Furthermore, a recent cadaveric study of Achilles tendons, histopathology data verified tendon degeneration with SUE (Klauser *et al.* 2013: 842). This study demonstrated loss of tendon fibre integrity, resulting in tendon softening. However, this study was criticized by Chen *et al.* (2013: 450) as experiments performed on animals, or *in vitro* studies, were considered unsuitable as clinical methods. Many *in vitro* studies on muscles established increased stiffness on tension (Eby *et al.* 2013: 2386), as well as repeatability of measurements using SWUE (Peltz *et al.* 2013: 1151).

According to Hou *et al.* (2017: 95) the majority of musculo skeletal studies have been performed with SUE rather than with SWUE investigations. Chen *et al.* (2013: 450) investigated 36 ruptured Achilles tendons and 14 asymptomatic tendons using shear wave ultrasound elastography. The mean elastic score of asymptomatic tendons was reported as higher than symptomatic or pathological Achilles tendons, therefore highlighting the significance of elasticity values of tendons. Taljanovic *et al.* (2017: 865) observed that the mean elasticity values of asymptomatic Achilles tendons yielded a higher shear wave velocity of $291.91 \pm 4, 38$ kPa in contrast to the findings of Arda *et al.* (2011: 535) which yielded a mean elastic value of 98.8 ± 47.1 kPa in asymptomatic men and 62.5 ± 40.1 kPa in women. According to De Zordo *et al.* (2009: 180), SUE has also been used in the assessment of the common extensor tendon of the elbow. The results of this study determined that lateral epicondylitis of common extensor tendons were shown to be softer when compared with healthy volunteers. SWUE has also been used in the investigation of the Achilles tendon. A total of 112 studies by Dirrich and colleagues (2016: 1205) included Achilles, patellar and epicondylar tendons performed (mean age 42 years) yielded higher values in asymptomatic tendons (mean 186 kPa) compared to symptomatic tendons with low kPa (60.3kPa). According to Dirrich *et al.* (2016: 1205) a semi quantitative analysis of the symptomatic tendons, using the SWUE maps were rated as soft (57%), intermediate (38%) and hard (4%).

2.8.2.1 Clinical use in the Rotator Cuff Tendon

A strain ultrasound elastography study performed by Lalitha, Reddy and Reddy *et al.* (2011: 366) established that supraspinatus tendons in young asymptomatic participants exhibited a predominantly blue colour, which represented hardness, whilst blue, green and red were demonstrated in supraspinatus tears, depicted medium and soft elasticity. Srinivasen and

Dubey (2011: 646) challenged the validity of this study with regards to the insufficient application of transducer compression of obliquely positioned supraspinatus tendons. Muraki *et al.* (2015: 125) expressed concern over the lack of reference values after conducting a semi quantitative study of the supraspinatus tendon. Moreover, the above study did not analyse all areas of the tendon (Muraki *et al.* 2015: 6). In addition Trent (2013: 40) and Tudisco *et al.* (2015: 397) suggested that a definite algorithmic program be established in order to determine the extent of rotator cuff disease as well as the necessary treatment protocol.

Prior ultrasound elastography studies of rotator cuff tendons have focussed mainly on the supraspinatus tendon (Muraki *et al.* 2015: 121). There have been conflicting camps on the issue of SUE. The evaluation by Ilhanli *et al.* (2015: 33) of supraspinatus tears using SUE, found no difference in elastic values between males and females supraspinatus tendons in contrast to a SWUE study done by Arda *et al.* (2011: 533). Furthermore, Ilhanli *et al.* (2015: 33) maintained that increased hardness in the supraspinatus tendon was susceptible to partial thickness tears. In addition, there was no difference in the elasticity of the affected shoulder and dominant shoulder. Although a comparison with strain ratio with SUE and B-Mode ultrasound of the supraspinatus tendon improved accuracy, sensitivity and specificity in the diagnosis of tendinopathy (Ohuegbe 2014: 3), this was a semi quantitative study. Also, strain ratio performed with SUE executed on 39 patients with shoulder pain, yielded similar results to MRI grading of rotator cuff tendinopathy (Lee *et al.* 2016b: 723). Nevertheless, the authors acknowledged limitations attributable to amount of force used in transducer application (Lee *et al.* 2016b: 727).

A SWUE study performed on the predominantly used throwing shoulders of healthy baseball players concluded that the posterior and posteroinferior capsules were stiffer and thicker in comparison to non-throwing shoulders (Takenaga *et al.* 2015: 2936). The outcome of this study suggested that prior identification of players at a potential risk of shoulder injuries should be noted, especially pertaining to the glenohumeral internal rotation deficit. Winn, Lalam and Cassar-Pullicino (2016: 868) have advocated the use of elastography of tendons as a screening tool prior to sporting commitments. The integrity of the supraspinatus muscle quality was established in a study by Roskopf *et al.* (2015: 465). This study determined that SWUE decreased with increased fat content (Goutallier stage 0 - 111), but increased in the final stage of fatty infiltration (Goutallier stage 1V).

Although SWUE of supraspinatus tendons of 125 asymptomatic participants (17-63 years) was conducted by (Arda *et al.* 2011: 535), it failed to compare normal and pathological rotator cuff tendons (Tudisco *et al.* 2015: 394). The mean elasticity value for the supraspinatus tendon in males approximated to a value of 36.0 ± 13.0 kPa and for females 29.1 ± 12.4 kPa (Arda *et al.* 2011: 535). In a similar study, Saltykova (2013: 3) recorded mean values of supraspinatus tendons of only 30 asymptomatic participants (20-35 years). The recorded values were as 28.5 kPa in normal supraspinatus tendons as compared to calcific tendinitis stage one of 85.6 kPa and stage four of 266 kPa. Elastography demonstrated the colour blue which represented a hard tendon. SWUE has been proposed for the assessment of the degree of hardness of tendon calcifications in order to select type of treatment (Saltykova 2013: 15). Successful use of fine needle aspirations on calcifications have been performed in the management of rotator cuff tendinitis using ultrasound elastography (Lin *et al.* 2015: 603). These calcifications were categorised into four groups: arc shaped, (echogenic), fragmented (separate echogenic spots), nodular (echogenic nodule without shadowing) and cystic (echogenic wall with anechoic centre) (Lin *et al.* 2015: 608).

Hou *et al.* (2017: 101) maintained that a sample of 32 asymptomatic participants was not large enough for adequate assessment of repeatability for rotator cuff tendon elastographic studies. Moreover, this study failed to demonstrate a strong correlation between SWUE and tendon pathology. However, a relationship between deltoid muscle softening and rotator cuff pathology was established, concomitant with an older population, as the mean age was 42 years in asymptomatic and 56 years in symptomatic population (Hou *et al.* 2017: 101).

Literature on ultrasound elastography of the subscapularis, infraspinatus and teres minor tendons is scarce. Animal cadavars were used in the study of the infraspinatus tendon by Frisch (2011: 38) and deltoid muscle by Hatta *et al.* (2016: 1). Although various studies have explored the use of shear wave ultrasound elastography (Ooi *et al.* 2014: 11), concerns were recently raised by Sahan *et al.* (2018:196); Hatta *et al.* (2015:3854); Muraki *et al.* (2015:120); Rahman *et al.* (2013: 84) regarding the lack of quantification of musculoskeletal tissues including standardisation of ultrasound elastographic examinations. Therefore, as reported by Song (2014: 2), the condition of healthy tissue is indicated by using tissue stiffness as a biomarker and therefore an accurate assessment may add to clinical value by identifying healthy tissue from pathological tissue.

2.8.2.2 Clinical use in the Biceps Tendon

Longitudinal images of the biceps tendon are reported as excellent correlators with B-Mode findings, indicating a mean sensitivity of 94.4% and specificity of 92.1% (Seo, Yoo and Ryu 2014: 271). In contrast, others investigated the biceps tendon in a sample of 20 participants, using both SUE and SWUE in comparison to MRI (Sahan *et al.* 2018: 196). These investigators reported that fluid around biceps tendon noted in MRI studies may generate false positive result as tendinosis, whilst hardness of tendons corresponded to tendinosis (39.42 ± 7.4 kPa for normal tendinosis 20.62 ± 4.6 kPa for control group) (Sahan *et al.* 2018: 196). There was no significant change in the biceps tendon elasticity scores with or without the presence of fluid in the tendon sheath (Sahan *et al.* 2018: 196). In addition, biceps tendon abnormalities were only recorded in 9 participants out of 69 patients who presented with positive rotator cuff pathology during an SUE (Galletti *et al.* 2015: 327).

2.9 CONCLUSION

Early diagnosis of tendinopathy is crucial for monitoring of tendon healing (Baumer *et al.* 2018: 287 and Paluch *et al.* 2016: 245). Various diagnostic tools have been used in the diagnosis of this condition. However, it is perceived that shear wave ultrasound elastography may prove a reliable technique in the provision of consistent quantifiable data (Ooi *et al.* 2014: 1). In addition, Chen *et al.* (2031: 454) postulated that shear wave ultrasound elastography may provide more data on tendon function, compared to B-Mode ultrasound imaging and therefore, will optimize treatment in the rehabilitation process. To date, SWUE quantification for asymptomatic and symptomatic rotator cuff tendons has not been well established (Hou *et al.* 2016: 105). There is limited shear wave data on the rotator cuff and biceps tendons (Muraki *et al.* 2015: 120; Tudisco *et al.* 2015: 397; Ooi *et al.* 2014: 11). Moreover, Winn, Lalam and Cassar-Pullicino (2016: 872) suggest that future considerations ought to be given to characterisation of elastograms of asymptomatic participants of different ages in order to assess tendon alterations. Therefore, reference values are deemed crucial in this quest.

CHAPTER 3: METHODOLOGY

3.1. STUDY DESIGN AND POPULATION

The aim of this study was to assess the biomechanics of the rotator cuff and biceps tendons of the shoulder joint in asymptomatic participants, in order to establish a reference range for use in clinical practice. The objectives of this study were:

- To measure the elasticity of the rotator cuff and biceps tendons and report in kilopascals, using shear wave ultrasound elastography.
- To establish a shear wave ultrasound elastographic reference range of the rotator cuff and biceps tendons for use in clinical practice.

This prospective, quantitative study was conducted in a private radiology practice in Durban, KwaZulu-Natal. The radiology practice provides diagnostic imaging services for the community that resides in the Northwest region of KwaZulu-Natal. Prior permission was sought and granted from this practice in order to confirm study feasibility (Appendix 1A and Appendix1B), and later obtained at the start of the study (Appendix 1C).

3.2 ETHICAL APPROVAL AND STUDY SAMPLING

3.2.1 Ethical approval

Ethical approval to conduct the study was obtained from the Institutional Research Ethics Committee of the Durban University of Technology, KwaZulu-Natal (IREC73/11, Appendix 2). Gatekeeper's permission from the hospital manager was requested and approved (Appendix 3A and 3B). Participation was voluntary and no coercion was used to recruit participants. Prospective participants were verbally informed of the study, as well as provided with the written information letter in English and isiZulu (Appendix 4A and 4B) as required, and assured of confidentiality and anonymity. Confidentiality and anonymity of all participants was maintained by use of participant identification codes. The participant was allowed to participate only if they read and understood the information letter (Appendix 4A and 4B) and signed the consent form (Appendix5A and 5B).

3.2.2 Target population and recruitment

Following receipt of regulatory permission, recruitment of all asymptomatic participants commenced through the use of advertisements in English (Appendix 6A) and isiZulu (Appendix 6B), placed on noticeboards of the radiology practice, hospital, community and shopping centres in the Northwest region of KwaZulu-Natal. A sample number of two hundred and sixty (n=260) was confirmed, in consultation with the institutional biostatistician

(Appendix 7) and previous studies (Hou *et al.* 2017 and Arda *et al.* 2011). This sample number was based on the population of the northwest region of KwaZulu-Natal (Stats. South Africa 2011). Only interested participants who responded to the advertisements were recruited between December 2017 and August 2018 in order to achieve the final sample number of 260 participants. Participants aged between 21-45 years were recruited. Participants aged 45 and older were excluded, because of the increased predisposition to tendinopathy within this age group (Park *et al.* 2013: 1360), whilst those aged 21 years were included to represent the lower age scale of the young adult population as well as being able to independently provide consent to participate in the research (Strode, Slack and Essack 2010: 248).

All interested participants were recruited based on the following inclusion and exclusion criteria.

3.2.3 Inclusion Criteria

- Asymptomatic participants with no history of shoulder pain
- Aged between 21-45 years
- Participants not on any steroids or anti-inflammatory medication for a period of 24 hours (Wright 2016)

3.2.4 Exclusion Criteria

- Participants presenting with shoulder pain
- Participants younger than 21 years and older than 45 years of age
- Participants with a history of carcinoma or systemic inflammatory disorder

3.3 DATA COLLECTION

All recruited participants were required to complete a demographic section of the data collection tool (Appendix 8) which included both a demographic and ultrasound section. The demographic data incorporated participants' age, gender, race, weight, height, daily lifestyle activities, body mass index and medical history. The ultrasound section comprised of ultrasound data of the selected parameters.

Ultrasound data was collected using ultrasound equipment, GE Logiq E 9 (Figure 3.1) which was used to evaluate both B-Mode ultrasound and shear wave ultrasound elastography of the rotator cuff and biceps tendons. Basic ultrasound equipment consists of a transducer or probe,

scanner, computer and television monitor (Kaur 2013: 388). The transducer frequency ranges from 10-14 MHz range.

3.3.1 Research procedure of collection of B-Mode ultrasound data

Each participant was informed of the nature of the ultrasound examination prior to the ultrasound procedure. Those participants who presented with abnormal findings were advised to see a health care professional for further management. All sonographic examinations performed during the research were overseen by a senior radiologist with experience in B-Mode ultrasound. All examinations were performed by the senior sonographer who activated the controls on the GE Logiq E9 ultrasound equipment. The anatomical structures were examined in two planes, ie, the sagittal and axial planes as standard protocol (Gupta and Robinson 2015: 207; Singh 2012: 285; Beggs 2011: 2; Cowling, Gamble and Rangan 2011: 14). The size of the shear wave ultrasound elastography window was selected in relationship to the size of the tendon to be examined. The proximal, middle and distal sites of the tendons were scanned in both planes by a hand held transducer (Figure 3.2).

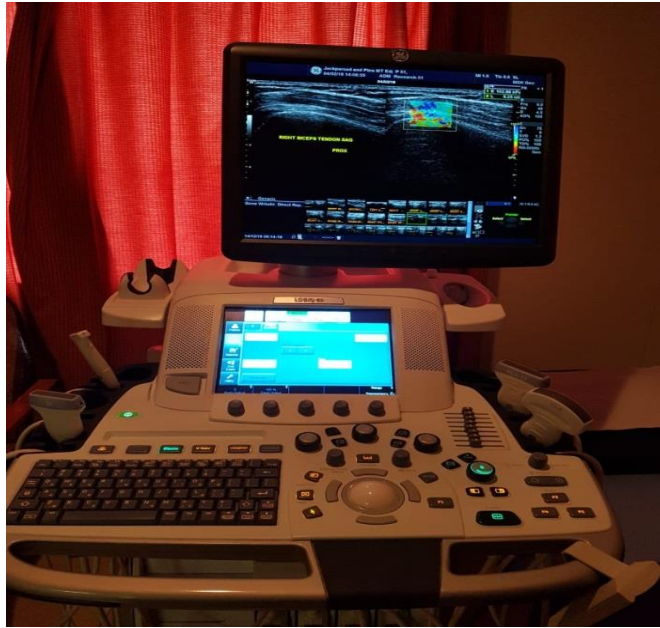


Figure 3. 1: GE Logiq E9 Ultrasound Equipment used to obtain B-Mode and Shear wave ultrasound images.

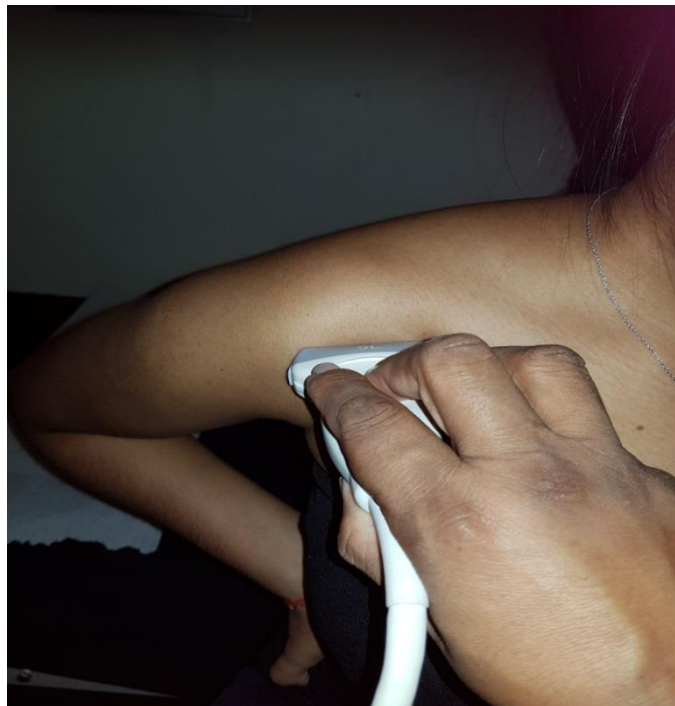


Figure 3.2 Transducer position over participant's anterior shoulder region

The participant was asked to be seated on a chair in an upright and relaxed position, facing the sonographer. A multi frequency linear transducer (10MHz to 14 MHz) onto which a small amount of gel (coupling medium) was applied, was gently placed on the participants

shoulder. A routine protocol thereafter was followed to conduct an initial B- Mode scan of the shoulder joint:

- The participant was seated on a stool, facing the sonographer. Imaging of the biceps tendon was performed with his/her hand placed on the lap, palms facing up and elbows flexed at 90 degrees. After identifying the biceps tendon in the bicipital groove, in the anterior shoulder, the participant was asked to externally rotate the arm to assess for subluxation of the tendon from its groove.
- Following this, the subscapularis tendon was then surveyed from its insertion in the lesser tuberosity of the humerus in the anterior shoulder, with abduction of the forearm, thus in external rotation, fixing the elbow on the iliac crest.
- The acromio-clavicular joint and coracoacromio ligament were then assessed by angling the transducer from the coracoid process to the acromion. The transducer was orientated along the long axis of the clavicle, with the participants' arm in the neutral position.
- Imaging of the supraspinatus tendon (from its insertion in the greater tuberosity of the humerus) and rotator cuff interval followed, with internal rotation of the arm and the palm of the hand placed behind the participant's back. The long axis of the supraspinatus was done at the anterior and posterior levels of the superior facet of the greater tuberosity of the humerus.
- Dynamic assessment was done to evaluate sub acromial impingement. The probe was positioned obliquely at the lateral margin of the acromion, to view the greater tuberosity. The patient was thereafter asked to abduct and elevate the arm with internal rotation. During this manoeuvre, the supraspinatus and subacromial - subdeltoid bursa was observed sliding smoothly under the acromion.
- The Infraspinatus, teres minor tendons, posterior labrum and spino glenoid notch were finally imaged by placing the affected arm in front of the patient's chest, resting on the contralateral shoulder. The transducer was positioned in an axial position over the posterior shoulder, over the middle facet of the greater tuberosity using the spine of the scapula as an optimal landmark.

3.3.2 Research procedure of collection of Shear Wave Ultrasound Elastography data

Shear wave ultrasound elastography (SWUE) was performed following the collection of B- Mode data. Three standardised sites were scanned within each tendon, namely, the

proximal, mid and distal tendon in both the sagittal and axial planes. A total of six measurements were obtained on each tendon, and two measurements for the teres minor tendon, as this is a very short tendon. Using the 9 MHz linear transducer, the activation of the shear wave ultrasound elastogram mode on the ultrasound equipment was activated. The linear transducer, LE9, utilises the comb-push excitation method that concurrently transmits ARFI (Acoustic Radiation force impulse) pulses that produce shear waves. Thereafter, time-interleaved shear wave tracking estimated shear wave velocity. Young's modulus measurement in kilopascals was used.

During the examination, minimal contact pressure was applied by the transducer during data acquisition. The size of the SWUE window was selected to be examined in relationship to the size of the tendon of each rotator cuff and biceps tendon. During the examination, B-Mode and SWUE images were displayed side by side on the monitor (by use of a split screen), with SWUE superimposed on B-Mode image as a colour-coded, real-time picture. Colour scale, which represented the relative stiffness of the tissues, ranged from red (soft tissue), yellow/green (intermediate stiffness) to blue (hard tissue). A circle that delineated the region of interest (ROI) for the measurement of elastic modulus was placed in the centre of the tendon, within the acquisition box. Various diameter sizes of the ROI were placed within the examined tendon. The most representative SWUE image of at least three concordant cycles was chosen and recorded on a communication system for a further analysis. The visual indicator facilitated the acquisition process. Care was taken to hold the probe perpendicular to the target tissue to avoid anisotropy and tissue shifting when performing US and shear wave ultrasound elastography respectively.

The rotator cuff and biceps tendon as described in the B-Mode were examined in both the sagittal and axial planes (Singh 2012: 285 and Beggs 2011: 2) as follows:

- The region of interest (ROI) included the proximal, middle and distal part of each rotator cuff and biceps tendon. The diameter of each tendon width was recorded.
- After three signal rotations of the screen indicator, the quantitative estimates of the mean stiffness of each tendon of the rotator cuff and biceps tendon stiffness were measured from the propagation of the shear wave propagation velocity and recorded

in kilopascals (kPa). The parametric estimates were derived from the software implemented in the ultrasound equipment.

Verification of ultrasound data for both study groups were confirmed by a senior radiologist. Thereafter, each result was recorded on printed paper and stored on Picture Archiving and Communications System workstation (PACS).

3.4 DATA ANALYSIS

The data was analysed using IBM SPSS version 25. A p-value < 0.05 was considered as indicating a statistically significant result. Data was tested for normality and continuous data was summarised in terms of the mean, standard deviation, minimum and maximum. Categorical data was summarised as frequency tables. Independent Student t-tests were used to compare the means of elasticity of tendons regarding gender. A one-way analysis of variance (ANOVA) was used to test for equality of means for the elasticity of the tendons when there were more than two groups, for example age (three categories) and ethnicity (four categories). The Duncan's multiple range tests and Tukey's test were used to detect where there were differences in the means for the groups when the F-test was significant. Reference ranges for all the tendons are provided based on a 95% confidence interval for the mean.

CHAPTER 4: RESULTS

4.1 INTRODUCTION

Asymptomatic participants were investigated to establish normal reference values of the rotator cuff and biceps tendons, using shear wave ultrasound elastography. The elasticity of the tendons was measured in kilopascals (kPa).

4.2 DEMOGRAPHIC CHARACTERISTICS

The demographic profile of the study population is shown in Table 4.1. A total of 260 asymptomatic participants were recruited, of which 61.2% were females (n=159) and 38.8% were males (n=101). Of the total sample, 57.3% (n=149) were Indians, 35.4 % (n=92) Blacks, 3.8% (n=10) Coloureds and 3.5% (n=9) Whites. The participants were categorised based on the following age groups: 21-24 years, 25-34 years and 35-45 years respectively. The mean age of the study population was 34.52 ± 7.75 years, whilst the mean BMI was $26.70 \pm 5.10 \text{ kg/m}^2$. The mean weight was 71.76 ± 14.50 kg and the mean height, 1.64 ± 0.08 m. None of the participants reported the use of pain medication and all reported some level of physical activity. The level of activity was grouped into mild (n=11), moderate (n=194) and very active (n=55). The moderate level of activity category had the highest number of asymptomatic participants (74.6%), whilst the mild level of activity had the lowest number (4.2%).

Table 4.1: Demographic frequencies.

Gender (n/%)	
<i>Female</i>	159 (61.2)
<i>Male</i>	101 (38.8)
Race (n/%)	
<i>Indian</i>	149 (57.3)
<i>Black</i>	92 (35.4)
<i>Coloured</i>	10 (3.8)
<i>White</i>	9 (3.5)
BMI (kg/m²; n/%)	
<i>15-25</i>	118 (45.4)
<i>26-35</i>	128 (49.2)
<i>36-45</i>	14 (5.4)
Level of activity (n/%)	
<i>Mild</i>	11 (4.2)
<i>Moderate</i>	194 (74.6)
<i>Very Active</i>	55 (21.2)
Age (years/mean (SD))	34.52 ± 7.75

4.3 B-MODE AND SHEAR WAVE ULTRASOUND ANALYSIS

4.3.1 B-Mode Ultrasound Analysis

Selected sagittal and axial B-mode images of the proximal sites of the left biceps tendon, proximal, middle and distal sites of the left subscapularis and left infraspinatus tendons and middle and distal sites of the right supraspinatus tendon are shown in Figure 4.1. Only sagittal and axial planes of the right teres minor tendon were imaged at the humeral insertion (Figure 4.1). Ultrasound image analyses of the B-Mode images demonstrated a normal, homogenous, and fibrillary medium grey echo pattern in all tendons. Sagittal planes of B-Mode ultrasound images in normal tendons appeared as closely spaced echogenic parallel lines compared to the axial planes, which showed multiple echogenic dots (Figure 4.1).

4.3.2 Elastography Colour Map and Shear Wave Analysis

The qualitative analysis colour maps of all tendons investigated are shown in Figure 4.2. The elastograms (colour maps), superimposed over B-Mode ultrasound images of all tendons were evaluated based on their colour displayed. Dark blue denoted stiff elasticity (hard tendons) and dark to light blue depicted intermediate stiffness of elasticity, whilst a mixture of colours depicted soft elasticity (soft tendons).



Figure 4.1: B-Mode images of left biceps tendon (a-b), left subscapularis tendon (c-d), right supraspinatus tendon (e-f), left infraspinatus tendon (g-h) and right teres minor tendon (i-j) in both the sagittal and axial planes.

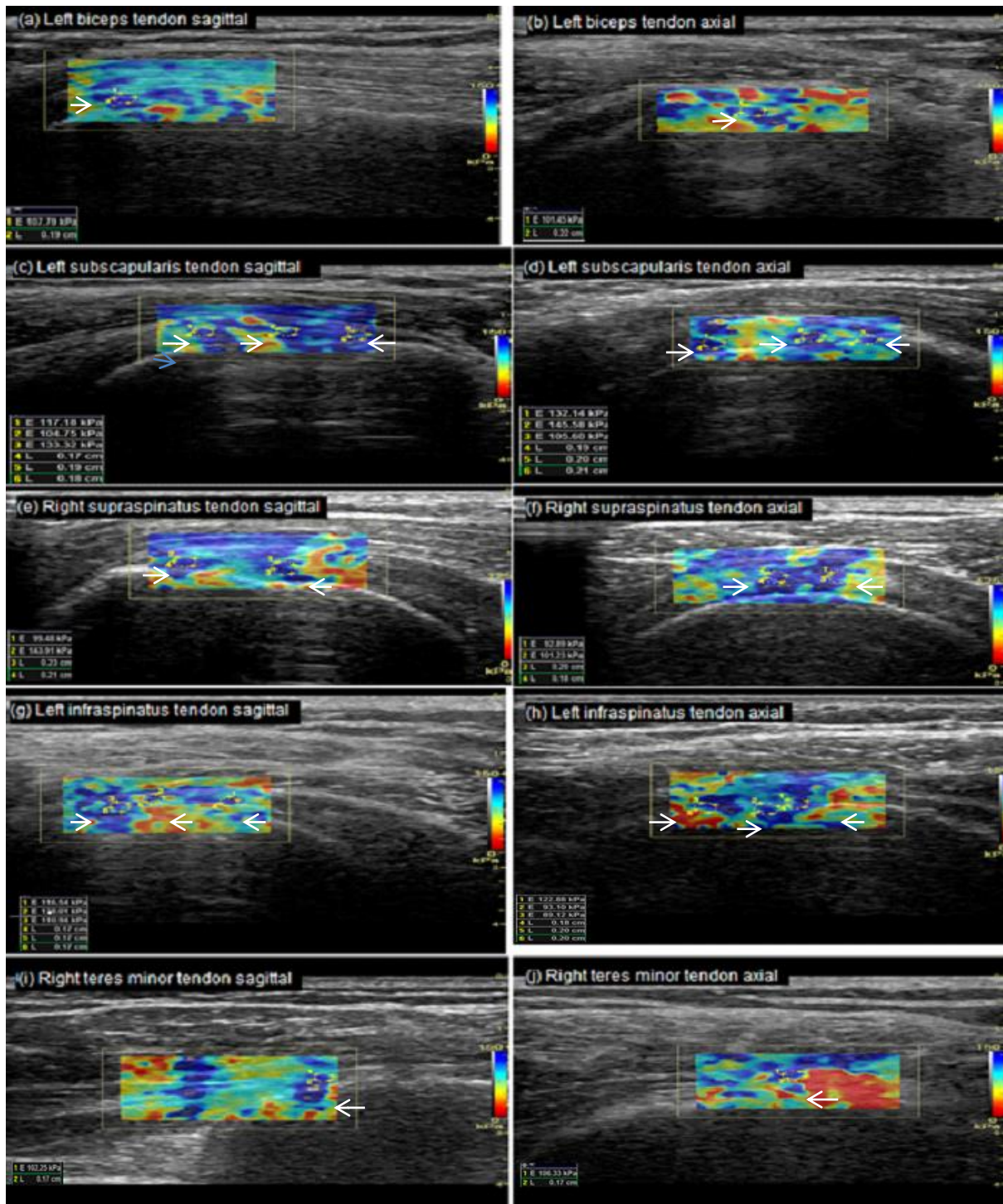


Figure 4.2: Shear wave colour mapping and kPa values of left biceps tendon (a-b), left subscapularis tendon (c-d), right supraspinatus tendon (e-f), left infraspinatus tendon (g-h) and right teres minor tendon (i-j) in both the sagittal and axial planes. The numbers to the left of images depict the shear wave velocity in kPa values, represented by 'E'. The yellow circles on the colour mapped tendon represent the region of interest (ROI) delineated by arrows (white). 'L' represents the width of the tendon examined.

The qualitative colour analyses of elasticity of all tendons at the humeral insertion are shown in Table 4.2. The colour maps depicted as ‘dark’ blue indicates harder elasticity in (74-86.15%) the number of tendons examined, confirming the strength of the tendons. Dark blue colour maps were highest (86.15%) at the distal supraspinatus tendon (n=224) in the sagittal plane, whereas the proximal biceps tendon (n=194) in the axial plane, and teres minor tendon (n=194) in the axial plane, demonstrated the lowest value (74.61%). Similarly, the colour map ‘dark to light blue’ demonstrated values between 12.69%-21.92% in the tendons whilst the colour map comprising a ‘mixture of colours’ demonstrated values between 0.76%-3.46%. The ‘mixture of colours,’ are indicative of tendon softening, present in asymptomatic participants.

Table 4.2: Colour maps (dark blue, dark to light blue and a mixture of colours) of rotator cuff and biceps tendons at humeral head insertion.

Tendon	Colour Map Categories (n: % participants)		
	Dark blue (n / %)	Dark to light blue (n / %)	Mixture of colours (n / %)
Biceps - sagittal <i>Prox</i>	211 (81.15%)	47 (18.07%)	2 (0.76%)
Biceps - axial <i>Prox</i>	194 (74.61%)	57(21.92)	9(3.46)
Subscapularis - sagittal <i>Dist</i>	219 (84.23%)	39 (15%)	2(0.76%)
Subscapularis - axial <i>Dist</i>	205 (74.84%)	45(17.30%)	7 (2.69)
Supraspinatus - sagittal <i>Dist</i>	224 (86.15%)	33 (12.69%)	3 (1.15%)
Supraspinatus - axial <i>Dist</i>	211 (81.15%)	35(13.46%)	13 (5%)
Infraspinatus - sagittal <i>Dist</i>	217 (83.46%)	35 (13.46%)	8 (3.07%)
Infraspinatus - axial <i>Dist</i>	207 (79.61%)	46 (17.69%)	7 (2.69%)
Teres minor - sagittal	204 (78.46%)	47 (18.07%)	9 (3.46%)
Teres minor – axial	194 (74.61%)	54 (20.76%)	12 (4.61%)

The quantitative shear wave ultrasound data for tendon elasticity, measured in kilopascals (kPa) are shown in Table 4.3. The middle supraspinatus tendon in the sagittal plane, demonstrated the highest mean value of 112.00 ± 20.76 kPa (range: 35.38-175.04), whilst the lowest mean of 98.32 ± 15.36 kPa (range: 56.49-144.65 kPa) was recorded in the distal biceps tendon in the axial plane. There was a statistically significant difference between the sagittal and axial planes ($p=0.001$) between the asymptomatic participant group for the proximal biceps, distal subscapularis, distal supraspinatus, distal infraspinatus and teres minor tendons.

Table 4.3: Shear wave elastography (kPa) of all evaluated tendons (n=260)

Tendon	Means \pm SD (kPa)	Min-Max range
Biceps - sagittal		
<i>Proximal</i>	104.83 \pm 18.89	53.25-164.90
<i>Middle</i>	105.43 \pm 18.32	43.01-174.35
<i>Distal</i>	106.16 \pm 17.91	58.25-170.22
Biceps - axial		
<i>Proximal</i>	98.91 \pm 17.70	47.93-155.25
<i>Middle</i>	99.04 \pm 16.14	47.87-149.32
<i>Distal</i>	98.32 \pm 15.36	56.49-144.65
Subscapularis - sagittal		
<i>Proximal</i>	105.33 \pm 20.42	34.79-163.07
<i>Middle</i>	108.05 \pm 20.86	55.04-190.18
<i>Distal</i>	105.06 \pm 18.02	42.17-161.78
Subscapularis - axial		
<i>Proximal</i>	105.67 \pm 19.20	38.88-167.81
<i>Middle</i>	104.68 \pm 19.90	29.83-169.61
<i>distal</i>	103.65 \pm 19.44	36.39-169.89
Supraspinatus- sagittal		
<i>Proximal</i>	109.78 \pm 22.50	23.65-173.05
<i>Middle</i>	112.00 \pm 20.76	35.38-175.04
<i>Distal</i>	109.10 \pm 18.57	41.91-162.11
Supraspinatus - axial		
<i>Proximal</i>	105.98 \pm 19.95	51.26-166.63
<i>Middle</i>	107.08 \pm 20.60	52.46-156.71
<i>Distal</i>	104.67 \pm 19.52	44.48-156.17
Infraspinatus - sagittal		
<i>Proximal</i>	106.80 \pm 19.55	27.01-178.22
<i>Middle</i>	109.52 \pm 19.26	48.93-170.16
<i>Distal</i>	104.79 \pm 19.64	31.51-175.21
Infraspinatus - axial		
<i>Proximal</i>	103.58 \pm 17.40	41.99-159.85
<i>Middle</i>	105.54 \pm 18.23	44.97-153.63
<i>Distal</i>	101.70 \pm 17.12	44.71-150.69
Teres minor - sagittal	99.05 \pm 17.62	39.12-152.63
Teres minor - axial	98.88 \pm 18.06	34.98-148.95

* $p<0.05$ was considered statistically significant

4.4 Bivariate Analysis of Tendons

The kPa values of all asymptomatic (n=260) participants were further analysed based on gender, age, ethnicity, BMI, 'level of activity' and tendon characteristics at humeral insertion (Tables 4.4-12).

4.4.1 Analysis of all evaluated tendons based on gender variations

The SWUE kPa values of both females and males were compared for all the tendons (Table 4.4). Males demonstrated the highest mean for the middle supraspinatus tendon in the sagittal plane (113.65 ± 20.51 kPa; $p=0.309$), whilst the females demonstrated a mean of (110.96 ± 20.92 kPa; $p=0.309$). In contrast, the lowest mean SWUE value observed for the males were in the proximal biceps tendon in the axial plane (101.21 ± 17.13 kPa; $p=0.096$), whilst in females, a lowest value of 96.71 ± 16.41 kPa was recorded for the teres minor tendon in the sagittal plane ($p=0.007$).

There was a statistically significant difference observed between males and females for the proximal ($p=0.002$), middle ($p=0.011$), and distal biceps tendon in the sagittal plane sag ($p=0.019$), middle biceps tendon in the axial ($p=0.030$), as well as the middle ($p=0.018$) subscapularis tendon in the sagittal plane. In addition, a statistically significant difference between males and females was observed for the distal supraspinatus tendon in the sagittal plane ($p=0.006$), middle supraspinatus in the axial plane ($p=0.007$), proximal infraspinatus tendon in the axial plane ($p=0.037$) teres minor tendon in the sagittal ($p=0.007$) and axial planes ($p=0.038$).

Table 4.4: Gender differences in Shear wave elastography, measured in kPa

Tendon	Females Means \pm SD	Males Means \pm SD	<i>p</i> values
Biceps - sagittal			
<i>Proximal</i>	101.93 \pm 18.84	109.40 \pm 18.15	0.002*
<i>Middle</i>	103.13 \pm 17.59	109.04 \pm 18.94	0.001*
<i>Distal</i>	104.09 \pm 16.86	109.41 \pm 19.07	0.019*
Biceps - axial			
<i>Proximal</i>	97.46 \pm 17.95	102.21 \pm 17.13	0.096
<i>Middle</i>	97.31 \pm 15.82	101.77 \pm 16.33	0.030*
<i>Distal</i>	97.41 \pm 14.84	99.75 \pm 16.11	0.232
Subscapularis - sagittal			
<i>Proximal</i>	103.68 \pm 20.02	107.93 \pm 20.87	0.102
<i>Middle</i>	105.48 \pm 18.44	112.11 \pm 23.73	0.018*
<i>Distal</i>	103.36 \pm 18.10	107.72 \pm 17.65	0.057
Subscapularis - axial			
<i>Proximal</i>	105.33 \pm 19.40	106.21 \pm 18.98	0.717
<i>Middle</i>	103.58 \pm 20.59	106.40 \pm 18.74	0.267
<i>Distal</i>	102.65 \pm 20.55	105.23 \pm 17.52	0.298
Supraspinatus - sagittal			
<i>Proximal</i>	110.41 \pm 23.59	106.21 \pm 18.98	0.717
<i>Middle</i>	110.96 \pm 20.92	113.65 \pm 20.51	0.309
<i>Distal</i>	106.60 \pm 18.23	113.04 \pm 18.52	0.006*
Supraspinatus -axial			
<i>Proximal</i>	104.44 \pm 20.59	108.40 \pm 18.73	0.118
<i>Middle</i>	104.32 \pm 20.38	111.42 \pm 20.29	0.007*
<i>Distal</i>	103.39 \pm 19.77	106.70 \pm 19.04	0.183
Infraspinatus - sagittal			
<i>Proximal</i>	105.16 \pm 18.77	109.38 \pm 20.55	0.090
<i>Middle</i>	109.32 \pm 18.92	109.84 \pm 19.87	0.832
<i>Distal</i>	104.85 \pm 19.66	104.69 \pm 19.72	0.949
Infraspinatus - axial			
<i>Proximal</i>	101.79 \pm 16.34	106.41 \pm 18.69	0.037*
<i>Middle</i>	105.35 \pm 16.81	105.84 \pm 20.35	0.834
<i>Distal</i>	100.64 \pm 16.07	103.37 \pm 18.61	0.201
Teres minor - sagittal	96.71 \pm 16.49	102.74 \pm 18.76	0.007*
Teres minor - axial	97.03 \pm 18.29	101.79 \pm 17.39	0.038*

* $p < 0.05$ was considered statistically significant

4.4.2 Analysis of all evaluated tendons based on age categorisation

The means between tendons were analysed by age categories of 21-24 years, 25-34 and 35-45 years respectively (Table 4.5). A statistically significant difference was noted in the middle infraspinatus tendon in the sagittal plane ($p=0.01$) for the age categories 35-45, and 21-24, respectively. The middle infraspinatus of the age category 35-45 years demonstrated a lower mean of 105.85 ± 17.82 kPa in comparison to a higher mean of 113.56 ± 20.22 kPa in the age category 21-24 years. A significant difference was also found between groups for the teres minor tendon in the axial plane ($p=0.025$) age categories 25-34 and 21-24 years. The highest mean of 99.94 ± 15.15 kPa was demonstrated in the age category 25-34, in comparison to a lower mean of 96.64 ± 20.44 kPa in the 21-24 age category.

4.4.3 Analysis of all evaluated tendons based on race

The differences between tendon characteristics based on race are shown in Table 4.6. A statistically significant difference was observed between the groups for the proximal supraspinatus in the sagittal plane ($p=0.018$), proximal supraspinatus in the axial plane ($p<0.001$), middle supraspinatus in the axial plane ($p=0.046$), middle infraspinatus in the sagittal plane ($p=0.033$), proximal infraspinatus in the axial plane ($p=0.028$) and teres minor in the axial plane ($p=0.001$). There was a lack of statistical significant difference between groups in the proximal subscapularis tendon in the sagittal plane. Despite the lack of statistical significance between tendons, there were notable kPa differences observed between the White (mean: 113.90 ± 20.32 kPa) and Coloured (mean: 98.46 ± 20.52 kPa) groups for the middle subscapularis tendon in the axial plane ($p=0.173$).

A statistical significant difference was observed for the proximal supraspinatus tendon with the highest mean of (123.85 ± 22.88 kPa; $p=0.000$) in the axial plane in the White group compared to the other three race groups. In addition, a statistical significant difference was noted in the middle infraspinatus tendon in the sagittal plane between the Whites compared to the Indian and Coloured groups (125.18 ± 18.75 ; $p=0.003$). Likewise, a lack of statistical significant difference was noted between the Indians, Blacks and Coloured groups. The proximal infraspinatus tendon for the Coloured group (93.24 ± 23.93 kPa; $p=0.028$) in the axial plane differed from the White and Black group as it demonstrated the lowest mean. A significant difference was also noted in the teres minor tendon in the axial plane between the

White and the other three groups, with the highest mean demonstrated in the White group (115 ± 7.93 kPa; $p=0.001$).

Table 4.5: Mean kPa values based on age categorisation

Tendon	Age (years): Means \pm SD			<i>p</i> value
	21-24	25-34	35-45	
Biceps - sagittal				
Proximal	107.54 \pm 22.18	104.19 \pm 17.19	103.40 \pm 20.92	0.186
Middle	114.55 \pm 21.29	104.58 \pm 17.43	102.57 \pm 16.93	0.295
Distal	110.99 \pm 21.13	104.70 \pm 16.48	105.67 \pm 17.75	0.570
Biceps - axial				
Proximal	102.67 \pm 21.16	99.69 \pm 16.92	96.44 \pm 16.68	0.329
Middle	102.78 \pm 18.59	98.16 \pm 15.16	97.44 \pm 17.92	0.523
Distal	99.48 \pm 17.62	98.49 \pm 14.01	97.79 \pm 15.79	0.082
Subscapularis - sagittal				
Proximal	110.15 \pm 22.13	105.29 \pm 19.19	103.18 \pm 20.63	0.204
Middle	114.91 \pm 24.00	106.58 \pm 19.83	106.69 \pm 20.23	0.839
Distal	105.36 \pm 21.15	104.66 \pm 15.05	105.10 \pm 19.35	0.294
Subscapularis - axial				
Proximal	108.07 \pm 23.41	106.64 \pm 17.33	103.00 \pm 21.16	0.075
Middle	104.95 \pm 20.82	107.42 \pm 20.10	102.02 \pm 19.19	0.283
Distal	105.01 \pm 15.96	104.17 \pm 18.99	102.49 \pm 21.33	0.188
Supraspinatus - sagittal				
Proximal	109.42 \pm 21.98	109.12 \pm 20.12	110.44 \pm 25.01	0.506
Middle	117.44 \pm 17.93	112.50 \pm 19.36	109.41 \pm 22.84	0.158
Distal	111.01 \pm 20.22	110.08 \pm 15.12	107.05 \pm 20.57	0.479
Supraspinatus - axial				
Proximal	105.76 \pm 24.56	107.05 \pm 20.46	104.09 \pm 19.31	0.586
Middle	107.87 \pm 22.82	109.77 \pm 18.84	103.32 \pm 22.95	0.059
Distal	104.86 \pm 20.23	106.12 \pm 17.00	103.06 \pm 21.52	0.848
Infraspinatus - sagittal				
Proximal	108.02 \pm 22.54	109.49 \pm 17.69	103.71 \pm 19.80	0.988
Middle	113.56 \pm 20.22	111.79 \pm 19.78	105.85 \pm 17.82	0.010*
Distal	109.35 \pm 22.91	106.00 \pm 18.33	101.79 \pm 19.25	0.830
Infraspinatus - axial				
Proximal	107.20 \pm 18.64	104.39 \pm 16.02	100.62 \pm 19.45	0.245
Middle	106.52 \pm 18.15	106.43 \pm 16.49	104.25 \pm 19.55	0.223
Distal	103.55 \pm 19.68	101.24 \pm 17.82	100.86 \pm 17.73	0.157
Teres minor - sagittal	95.67 \pm 19.38	101.50 \pm 16.67	99.08 \pm 17.69	0.074
Teres minor - axial	96.64 \pm 20.44	99.94 \pm 15.15	97.70 \pm 21.80	0.025*

* $p<0.05$ was considered statistically significant

Table 4.6: Means kPa values for the four race groups using ANOVA

Race Groups: Means±SD					
Tendons	Indian (n=149)	Black (n=92)	Coloured (n=10)	White (n=9)	p value
Biceps - sagittal					
<i>Proximal</i>	104.43±20.66	104.00±18.49	103.58±18.18	110.15±16.81	0.812
<i>Middle</i>	104.74±19.38	105.86±15.24	113.65±29.39	103.25±14.29	0.495
<i>Distal</i>	106.05±19.31	105.44±15.22	111.05±20.10	109.73±15.50	0.741
Biceps - axial					
<i>Proximal</i>	97.95±18.96	101.00±16.44	95.34±14.38	97.62±10.11	0.539
<i>Middle</i>	97.51±19.01	99.93±13.62	105.00±16.66	97.73±12.22	0.548
<i>Distal</i>	97.11±16.35	100.72±13.76	98.42±16.52	93.65±10.52	0.261
Subscapularis - sagittal					
<i>Proximal</i>	104.03±20.81	106.82±19.96	106.23±19.26	110.58±20.99	0.018*
<i>Middle</i>	106.32±20.64	110.99±20.48	110.23±31.65	104.30±11.73	0.046*
<i>Distal</i>	104.83±18.06	106.25±18.94	97.96±9.97	104.51±14.31	0.577
Subscapularis - axial					
<i>Proximal</i>	103.71±20.37	107.55±19.89	104.26±20.50	111.31±16.70	0.231
<i>Middle</i>	104.87±20.58	104.14±18.64	98.46±20.52	113.90±20.32	0.395
<i>Distal</i>	102.46±20.31	105.94±18.91	100.13±12.56	103.80±17.57	0.543
Supraspinatus - sagittal					
<i>Proximal</i>	106.04±20.45	115.13±25.03	111.05±26.28	115.45±10.80	0.594
<i>Middle</i>	110.54±19.82	113.56±22.40	112.19±22.81	120.21±16.01	0.449
<i>Distal</i>	108.72±18.24	109.45±19.71	104.92±16.49	116.59±14.23	0.562
Supraspinatus - axial					
<i>Proximal</i>	101.71±21.66	110.60±16.47	100.94±23.09	123.85±22.88	0.000*
<i>Middle</i>	103.79±20.57	110.99±22.61	102.09±20.92	115.93±15.70	0.189
<i>Distal</i>	104.07±20.28	104.39±18.91	107.01±17.60	115.01±13.24	0.421
Infraspinatus - sagittal					
<i>Proximal</i>	106.33±19.86	107.63±19.96	105.91±19.51	107.11±9.50	0.966
<i>Middle</i>	107.96±18.73	111.20±18.94	103.24±24.55	125.18±18.75	0.033*
<i>Distal</i>	104.46±19.59	104.62±20.06	101.64±18.63	115.42±16.89	0.403
Infraspinatus - axial					
<i>Proximal</i>	101.66±18.48	106.70±16.73	93.24±23.93	110.33±13.07	0.028*
<i>Middle</i>	104.71±18.78	106.36±16.63	102.52±22.81	116.51±13.59	0.248
<i>Distal</i>	100.24±18.69	103.40±17.99	95.78±12.39	107.29±8.35	0.314
Teres minor - sagittal	97.08±19.48	102.56±14.56	96.27±15.27	98.80±10.32	0.124
Teres minor - axial	95.74±19.04	101.83±19.17	93.97±13.34	115.31±7.93	0.001*

* $p < 0.05$ was considered statistically significant

4.4.4 Analysis of all evaluated tendons based on Body Mass Index (BMI)

One way analysis of variance revealed no statistically significant differences in kPa means across the different BMI categories (Table 4.7). However, notable mean kPa differences ($p=0.701$) were observed in the distal biceps tendon in the sagittal plane between BMI range 15-25 (106.50±19.13 kPa) and BMI range 36-45 (101.98±9.20 kPa), including in the middle supraspinatus tendon in the sagittal plane between BMI range 26-35 (113.14±22.13 kPa) and BMI range 36-45 (107.78±18.19 kPa) ($p=0.495$).

Table 4.7: Mean kPa values based on Body Mass Index

Tendon	BMI (kg/m ²): Means±SD			p value
	15-25 (n=118)	26-35 (n= 128)	36-45 (n= 14)	
Biceps - sagittal				
Proximal	105.61±18.69	103.47±19.38	109.65±15.51	0.333
Middle	103.96±16.44	106.63±20.18	105.80±15.67	0.503
Distal	106.50±19.13	106.27±17.52	101.98±9.20	0.701
Biceps - axial				
Proximal	100.27±17.76	97.24±17.63	102.33±18.12	0.285
Middle	99.41±16.10	98.48±16.58	101.24±13.19	0.807
Distal	97.79±15.07	98.48±15.74	101.99±15.30	0.713
Subscapularis - sagittal				
Proximal	104.62±21.12	105.67±19.98	107.59±19.99	0.792
Middle	107.00±20.33	108.36±21.69	112.67±17.39	0.476
Distal	104.28±19.59	105.46±17.16	106.19±14.17	0.729
Subscapularis - axial				
Proximal	105.48±18.55	105.09±20.10	112.00±16.02	0.369
Middle	105.14±19.85	104.80± 20.80	99.92±9.68	0.622
Distal	105.31±18.89	101.43±20.21	111.51±13.79	0.134
Supraspinatus - sagittal				
Proximal	108.94±21.48	110.59±23.45	108.03±23.85	0.846
Middle	111.40±19.54	113.14±22.13	107.78±18.19	0.495
Distal	109.59±18.61	108.93±18.87	106.85±17.03	0.841
Supraspinatus - axial				
Proximal	107.19±22.48	104.76±17.94	107.33±14.95	0.627
Middle	107.10±21.46	107.35±20.29	105.27±16.85	0.873
Distal	104.94±18.16	104.58±20.65	101.63±21.26	0.954
Infraspinatus - sagittal				
Proximal	106.82±20.05	106.56±18.87	108.04±23.53	0.923
Middle	112.08±19.85	107.46±18.99	106.67±15.13	0.148
Distal	105.80±20.38	103.86±19.57	103.20±13.18	0.743
Infraspinatus - axial				
Proximal	105.65±16.47	101.80±18.25	102.73±16.85	0.215
Middle	106.77±19.41	104.90±17.62	100.50±12.99	0.463
Distal	103.06±17.39	100.71±17.23	98.50±13.81	0.484
Teres minor - sagittal	98.96±18.45	98.79±16.92	101.15±18.01	0.800
Teres minor - axial	98.87±17.89	98.43±18.23	102.19±19.12	0.651

* $p<0.05$ was considered statistically significant

4.4.5 Analysis of all evaluated tendons based on ‘Level of Activity’

None of the participants recruited reported a lack of physical activity. Of the total participants, 11 were categorised into mildly active, 194 as moderately active and 55 as very active (Table 4.8). When categorised as ‘mild level of activity’, the lowest mean of 88.50 ± 20.28 kPa (range 62.87-126.20 kPa) was recorded in the proximal biceps tendon in the axial plane, whilst the highest mean of 108.14 ± 20.58 kPa (range 57.50-141.56 kPa) was recorded in the middle infraspinatus tendon in the axial plane. Similarly, for the ‘moderate level of activity’, the lowest mean was recorded in the distal biceps tendon in the axial plane 98.01 ± 15.25 kPa (range: 56.49-138.95 kPa) whilst the highest mean was recorded in the middle supraspinatus tendon in the sagittal plane 112.90 ± 19.62 kPa (range: 35.38-167.06 kPa).

In the category of ‘very active level of activity’, the lowest mean was recorded in the proximal biceps tendon in the axial plane 97.50 ± 17.14 kPa (range: 61.00-149.82 kPa) whilst the highest mean was recorded in the middle subscapularis tendon in the sagittal plane 111.04 ± 21.47 kPa (range: 66.04-163.35 kPa). A borderline statistical significant difference was noted for the middle subscapularis tendon in the sagittal plane ($p=0.049$) between the different levels of activity. There was no statistically significant difference in kPa means between the ‘very’ active category and the ‘mild’ activity category ($p>0.05$).

4.4.6 Tendon characteristics at humeral insertion

The insertion of the rotator cuff and biceps tendons into the head of the humerus were analysed, as these insertions are responsible for stability and range of movement of the shoulder joint. The Pearson's correlation and paired T test of the sagittal and axial planes of all tendons evaluated are shown in Table 4.9. There was a statistically significant difference between both planes in all tendons ($p<0.05$). The sagittal planes of the tendons demonstrated higher kPa values (harder elasticity) than the axial planes.

The means, standard deviations and p values are shown for age (Table 4.10), ethnicity (Table 4.11), BMI (Table 4.12) and ‘Level of Activity’ category (Table 4.13). The sagittal planes of the tendons were analysed by the age category (21-45 years) (Table 4.10). A statistically significant difference was noted in the tendons of age group 21-24 years, 25-34 years and 35-45 years ($p<0.05$). However, a lack of statistical significant difference in the kPa values in

both the sagittal and axial planes of the subscapularis tendon for the age category 21-24 years was noted ($p=0.061$).

Table 4.8: Mean kPa values based on Level of Activity

	Level of Activity: Means \pm SD			
Tendon	Mild (n=11)	Moderate(n=194)	Very Active(n=55)	p value
Biceps - sagittal				
<i>Proximal</i>	92.25 \pm 17.51	104.03 \pm 19.45	108.33 \pm 19.94	0.874
<i>Middle</i>	95.37 \pm 16.90	105.09 \pm 18.01	108.63 \pm 19.14	0.071
<i>Distal</i>	94.91 \pm 10.03	106.27 \pm 17.99	107.99 \pm 18.27	0.623
Biceps - axial				
<i>Proximal</i>	88.50 \pm 20.28	99.91 \pm 17.59	97.50 \pm 17.14	0.221
<i>Middle</i>	95.49 \pm 16.09	98.56 \pm 17.07	99.71 \pm 17.04	0.883
<i>Distal</i>	98.64 \pm 14.10	98.01 \pm 15.25	99.34 \pm 16.19	0.906
Subscapularis - sagittal				
<i>Proximal</i>	97.99 \pm 16.90	105.49 \pm 19.70	106.23 \pm 23.41	0.278
<i>Middle</i>	98.64 \pm 12.35	107.74 \pm 20.97	111.04 \pm 21.47	0.049*
<i>Distal</i>	92.80 \pm 10.48	106.03 \pm 17.92	104.09 \pm 18.82	0.326
Subscapularis - axial				
<i>Proximal</i>	95.58 \pm 18.27	106.05 \pm 20.01	104.86 \pm 20.56	0.741
<i>Middle</i>	92.51 \pm 13.24	105.57 \pm 18.93	103.95 \pm 23.44	0.938
<i>Distal</i>	94.02 \pm 21.35	104.09 \pm 18.13	104.05 \pm 23.21	0.466
Supraspinatus - sagittal				
<i>Proximal</i>	107.83 \pm 23.50	110.27 \pm 22.22	108.44 \pm 23.62	0.900
<i>Middle</i>	102.55 \pm 23.24	112.90 \pm 19.62	110.74 \pm 23.86	0.885
<i>Distal</i>	88.90 \pm 21.38	110.30 \pm 18.12	108.94 \pm 17.55	0.290
Supraspinatus - axial				
<i>Proximal</i>	106.05 \pm 16.05	105.43 \pm 20.16	106.08 \pm 23.41	0.754
<i>Middle</i>	100.23 \pm 23.05	106.75 \pm 21.55	107.78 \pm 20.44	0.167
<i>Distal</i>	90.47 \pm 19.39	105.17 \pm 19.21	105.76 \pm 19.87	0.258
Infraspinatus - sagittal				
<i>Proximal</i>	102.91 \pm 18.22	107.15 \pm 19.35	106.33 \pm 20.68	0.813
<i>Middle</i>	105.18 \pm 10.66	110.03 \pm 19.53	108.60 \pm 19.72	0.841
<i>Distal</i>	98.22 \pm 20.21	103.87 \pm 19.73	109.32 \pm 18.74	0.981
Infraspinatus - axial				
<i>Proximal</i>	94.83 \pm 17.18	103.85 \pm 18.73	103.56 \pm 16.13	0.395
<i>Middle</i>	108.14 \pm 20.58	104.64 \pm 17.21	108.58 \pm 20.58	0.909
<i>Distal</i>	94.28 \pm 13.50	101.51 \pm 17.60	102.58 \pm 20.20	0.329
Teres minor - sagittal	89.90 \pm 22.24	99.92 \pm 17.28	97.80 \pm 17.42	0.079
Teres minor - axial	92.27 \pm 17.76	98.62 \pm 19.22	99.31 \pm 18.86	0.090

* $p<0.05$ was considered statistically significant

Table 4.9: Tendon characteristics at humeral insertion of study population (n=260)

Tendon (n=260)	Means \pmSD	p value
Biceps - proximal		
<i>Sag</i>	104.83 \pm 18.89	0.000*
<i>Axial</i>	98.91 \pm 17.70	0.000*
Subscapularis - distal		
<i>Sag</i>	105.06 \pm 18.02	0.000*
<i>Axial</i>	103.65 \pm 19.44	0.000*
Supraspinatus - distal		
<i>Sag</i>	109.10 \pm 18.57	0.000*
<i>Axial</i>	104.67 \pm 19.52	0.000*
Infraspinatus - distal		
<i>Sagittal</i>	104.79 \pm 19.64	0.000*
<i>Axial</i>	101.70 \pm 17.12	0.000*
Teres Minor		
<i>Sag</i>	99.05 \pm 17.62	0.000*
<i>Axial</i>	98.88 \pm 18.06	0.000*

* $p < 0.05$ was considered statistically significant

Table 4.10 Tendon characteristics at humeral insertion based on age categorisation

Tendon	Age(years): Means\pmSD					
	21-24 (n=44)	p value	25-34 (n=106)	p value	35-45 (n=110)	p value
Biceps - proximal						
<i>Sag</i>	105.72 \pm 21.10	0.000*	107.01 \pm 18.51	0.000*	102.15 \pm 18.15	0.000*
<i>Axial</i>	102.51 \pm 19.87		98.43 \pm 16.09		97.84 \pm 18.30	
Subscapularis - distal						
<i>Sag</i>	104.20 \pm 21.46	0.061	107.14 \pm 15.64	0.003*	103.24 \pm 18.63	0.000*
<i>Axial</i>	107.19 \pm 20.34		104.63 \pm 18.24		101.26 \pm 18.15	
Supraspinatus - distal						
<i>Sag</i>	111.92 \pm 20.24	0.002*	109.19 \pm 17.38	0.000*	107.95 \pm 19.12	0.000*
<i>Axial</i>	105.22 \pm 21.66		105.29 \pm 15.95		103.81 \pm 21.86	
Infraspinatus - distal						
<i>Sagittal</i>	105.58 \pm 25.68	0.000*	105.36 \pm 17.60	0.000*	103.74 \pm 18.89	0.000*
<i>Axial</i>	103.87 \pm 16.90		103.27 \pm 17.00		99.19 \pm 17.21	
Teres Minor						
<i>Sag</i>	96.86 \pm 20.53	0.000*	102.05 \pm 16.73	0.000*	96.97 \pm 16.99	0.000*
<i>Axial</i>	99.33 \pm 20.72		102.17 \pm 15.78		95.25 \pm 18.40	

* $p < 0.05$ was considered statistically significant

With regards to race, the data showed a statistically significant difference between the sagittal and axial planes for both the Indian and Black groups ($p<0.05$) in all tendons (Table 4.11). There was no significant difference observed between the biceps ($p=0.642$) and subscapularis ($p=0.506$) tendons in both planes between the Coloured and White groups. However, statistically significant differences were noted in the supraspinatus, infraspinatus and teres minor tendons ($p<0.05$) between the White and other three race groups. Nevertheless, there were no significant differences observed between the sagittal and axial planes for the White group.

Table 4.11: Tendon characteristics at humeral insertion based on Race

Tendons	Race: Means \pm SD							
	Indian (n= 149)	<i>p</i> value	Black (n= 92)	<i>p</i> value	Coloured (n=10)	<i>p</i> value	White (n=9)	<i>p</i> value
Biceps - proximal								
Sag	105.10 \pm 19.38	0.000*	104.00 \pm 18.49	0.000*	103.58 \pm 18.80	0.642	110.15 \pm 16.81	0.310
Axial	97.95 \pm 18.96		101.00 \pm 16.44		95.34 \pm 14.38		97.62 \pm 10.11	
Subscapularis - distal								
Sag	104.83 \pm 18.06	0.000*	106.25 \pm 1.94	0.000*	97.96 \pm 9.97	0.506	104.51 \pm 14.13	0.511
Axial	102.47 \pm 20.24		105.94 \pm 18.91		100.13 \pm 12.56		103.80 \pm 17.57	
Supraspinatus - distal								
Sag	108.72 \pm 18.24	0.000*	109.45 \pm 19.71	0.000*	104.92 \pm 16.49	0.002*	116.59 \pm 14.23	0.379
Axial	104.07 \pm 20.28		104.39 \pm 18.91		107.01 \pm 17.60		115.01 \pm 13.24	
Infraspinatus - distal								0.192
Sagittal	104.46 \pm 19.59	0.000*	104.62 \pm 20.06	0.000*	101.64 \pm 18.63	0.038*	115.42 \pm 16.89	
Axial	100.71 \pm 17.14		103.40 \pm 17.99		95.78 \pm 12.39		107.25 \pm 8.39	
Teres Minor								
Sag	97.08 \pm 19.48	0.000*	102.56 \pm 14.56	0.000*	96.27 \pm 15.90	0.025*	98.80 \pm 10.32	0.061
Axial	95.74 \pm 19.04		102.90 \pm 15.92		93.97 \pm 13.34		115.31 \pm 10.93	

* $p<0.05$ was considered statistically significant

The sagittal and axial planes of the tendons based on BMI categories are illustrated in Table 4.12. Statistically significant differences were observed in all the tendons for the BMI categories ‘15-25 kg/m²’ and ‘26-35 kg/m²’ ($p<0.05$). It was noted that there was a lack of statistical significance between the sagittal and axial planes of the proximal biceps ($p=0.16$), subscapularis ($p=0.94$) and infraspinatus ($p=0.39$) tendons for the BMI category ‘36-45

kg/m²'. Significant differences were observed in the supraspinatus and teres minor tendon ($p<0.05$) for all BMI categories.

Table 4.12: Tendon characteristics at humeral insertion based on Body Mass Index

BMI (kg/m²): Means \pmSD						
Tendons	15-25 (kg/m²)	<i>p</i> value	26-35 (kg/m²)	<i>p</i> value	36-45 (kg/m²)	<i>p</i> value
Biceps - proximal						
<i>Sag</i>	105.61 \pm 18.61	0.000*	103.47 \pm 19.38	0.000*	109.65 \pm 15.51	0.162
<i>Axial</i>	100.27 \pm 17.76		97.24 \pm 17.63		102.33 \pm 18.12	
Subscapularis - distal						
<i>Sag</i>	104.28 \pm 19.29	0.000*	105.46 \pm 17.16	0.000*	106.19 \pm 14.17	0.941
<i>Axial</i>	105.31 \pm 18.89		101.43 \pm 20.21		111.51 \pm 13.79	
Supraspinatus - distal						
<i>Sag</i>	109.59 \pm 18.61	0.000*	108.93 \pm 18.97	0.000*	106.85 \pm 17.03	0.001*
<i>Axial</i>	104.94 \pm 18.16		104.58 \pm 20.65		101.63 \pm 21.06	
Infraspinatus - distal						
<i>Sagittal</i>	105.80 \pm 20.38	0.000*	103.86 \pm 19.57	0.000*	103.20 \pm 13.18	0.391
<i>Axial</i>	103.06 \pm 17.39		100.71 \pm 17.23		98.50 \pm 13.81	
Teres Minor						
<i>Sag</i>	98.96 \pm 18.45	0.000*	98.79 \pm 16.92	0.000	101.15 \pm 18.01	0.002*
<i>Axial</i>	98.87 \pm 17.89		98.43 \pm 18.23		102.19 \pm 19.12	

* $p<0.05$ was considered statistically significant

The sagittal planes of the tendons based on 'level of activity' are shown in Table 4.13. A statistically significant difference was noted in the proximal biceps and teres minor tendons ($p < 0.05$) for the 'mild level of activity' category. However, within this category, there were no significant differences observed between the sagittal and axial planes of the subscapularis ($p = 0.767$), supraspinatus ($p = 0.932$) and infraspinatus tendons ($p = 0.255$). In contrast, significant differences were noted in all the tendons for the 'moderate' and 'very active levels of activity' categories. Higher kPa values are indicative of the hard elasticity observed in the sagittal planes in all tendons at the humeral insertion.

Table 4.13: Tendon characteristics at humeral insertion based on “Level of Activity”

Level of activity: Means \pm SD						
Tendons	Mild	<i>p</i> value	Moderate	<i>p</i> value	Very Active	<i>p</i> value
Biceps – proximal						
<i>Sag</i>	103.48 \pm 23.27	0.009*	105.18 \pm 19.12	0.000*	103.85 \pm 17.41	0.000*
<i>Axial</i>	101.21 \pm 26.18		97.81 \pm 17.66		102.36 \pm 15.62	
Subscapularis - distal						
<i>Sag</i>	98.86 \pm 17.28	0.767	105.90 \pm 17.48	0.000*	103.31 \pm 19.89	0.000*
<i>Axial</i>	110.61 \pm 11.37		101.43 \pm 20.21		102.75 \pm 18.76	
Supraspinatus - distal						
<i>Sag</i>	117.45 \pm 15.96	0.932	108.48 \pm 18.58	0.000*	109.64 \pm 18.92	0.000*
<i>Axial</i>	110.66 \pm 21.86		103.57 \pm 19.45		107.38 \pm 19.18	
Infraspinatus - distal						
<i>Sagittal</i>	103.65 \pm 18.19	0.255	104.84 \pm 19.22	0.000*	104.84 \pm 21.67	0.000*
<i>Axial</i>	98.37 \pm 12.70		101.07 \pm 16.84		104.58 \pm 18.70	
Teres Minor						
<i>Sag</i>	99.49 \pm 21.95	0.003*	97.69 \pm 16.74	0.000*	103.75 \pm 19.20	0.000*
<i>Axial</i>	98.82 \pm 21.44		97.55 \pm 17.92		103.60 \pm 17.38	

* $p < 0.05$ was considered statistically significant

4.5 REFERENCE VALUES OF ALL TENDONS BASED ON THE 95% CONFIDENCE INTERVALS

The reference range of all tendons evaluated are shown in (Table 4.14), using confidence intervals. The upper and lower limits of the mean kPa provide data on shear wave ultrasound elastography with certainty that the true value of the elasticity lies within these limits. The point estimate of kPa values of each tendon evaluated in this study is reflected in the narrow confidence intervals. Using the proximal biceps tendon in the sagittal plane as an example, it can be stated with 95% confidence that the true average kPa within the population is between 102.52 kPa and 107.14 kPa (mean 104.83 kPa), with the standard error of the mean of 1.17 supporting the accuracy for use as reference values.

Table 4.14: Reference range of the rotator cuff and biceps tendons based on the Confidence interval

95 % Confidence Interval				
Tendons	Mean kPa	Lower limit	Upper limit	Standard error Difference
Biceps - sagittal				
<i>Proximal</i>	104.83	102.52	107.14	1.17
<i>Middle</i>	105.43	103.19	107.66	1.13
<i>Distal</i>	106.16	103.97	108.34	1.11
Biceps - axial				
<i>Proximal</i>	98.91	96.75	101.08	1.09
<i>Middle</i>	99.04	97.07	101.01	1.00
<i>Distal</i>	98.32	96.44	100.20	0.95
Subscapularis - sagittal				
<i>Proximal</i>	105.33	102.84	107.82	1.26
<i>Middle</i>	108.05	105.50	110.60	1.29
<i>Distal</i>	105.06	102.86	107.26	1.11
Subscapularis - axial				
<i>Proximal</i>	105.67	103.33	108.02	1.19
<i>Middle</i>	104.68	102.25	107.11	1.23
<i>Distal</i>	103.65	101.28	106.03	1.20
Supraspinatus - sagittal				
<i>Proximal</i>	109.78	107.03	112.52	1.39
<i>Middle</i>	112.00	109.47	114.54	1.28
<i>Distal</i>	109.10	106.83	111.37	1.15
Supraspinatus - axial				
<i>Proximal</i>	105.98	103.54	108.41	1.23
<i>Middle</i>	107.08	104.56	109.59	1.27
<i>Distal</i>	104.67	102.29	107.06	1.21
Infraspinatus - sagittal				
<i>Proximal</i>	106.80	104.41	109.19	1.21
<i>Middle</i>	109.52	107.17	111.87	1.19
<i>Distal</i>	104.79	102.39	107.19	1.21
Infraspinatus- axial				
<i>Proximal</i>	103.58	101.46	105.71	1.07
<i>Middle</i>	105.54	103.32	107.77	1.13
<i>Distal</i>	101.70	99.61	103.79	1.06
Teres Minor - sagittal	99.05	96.90	101.20	1.09
Teres Minor - axial	99.88	96.68	101.09	1.12

4.6 CONCLUSION

The reference ranges of the rotator cuff and biceps tendons have been evaluated by finding 95% confidence intervals for the mean elasticity for each of the tendons. A 95% confidence interval provides a lower and upper limit within which 95% of tendon measurements would be expected to fall. The reference ranges for the mean tendon elasticity for the tendons were as follows:

For the biceps tendon in sagittal and axial planes the reference ranges are 102.52-108.34 kPa and 96.44-101.08 kPa respectively. Similarly, for the subscapularis tendon in sagittal and axial planes, the reference ranges are 102.84-110.60 kPa and 110.60-108.02 kPa respectively. The supraspinatus tendon in the sagittal and axial planes has reference ranges of 106.83-114.54 kPa and 102.29-109.59 kPa, respectively. The infraspinatus tendon in the sagittal and axial planes has reference ranges of 102.39-111.87 kPa and 99.61-107.77 kPa respectively. The reference range for teres minor tendon in sagittal and axial planes are 96.90-101.20 kPa and 96.68-101.09 kPa respectively.

There was a statistically significant difference observed between males and females for the proximal, middle and distal biceps tendon in the sagittal plane ($p < 0.05$). The reference values ranged from 101.93 ± 18.84 - 109.41 ± 19.07 kPa. A statistically significant difference was also noted in the teres minor tendon in the sagittal and axial planes ($p < 0.05$). The reference values ranged from 96.71 ± 16.49 - 102.74 ± 18.76 kPa in the sagittal plane and 97.03 ± 18.29 - 101.79 ± 17.39 kPa.

CHAPTER 5: DISCUSSION

5.1 INTRODUCTION

Upper limb musculoskeletal abnormalities such as rotator cuff pathologies are made up largely of tendinopathies (Washburn, Onishi and Wang 2018: 9 and Ooi *et al* 2014: 1). Most tendinopathies are caused by tendon overuse with resultant biomechanical alteration of tissue fibres (Ooi *et al.* 2014: 1). Although Magnetic Resonance Imaging (MRI) is referred to as the gold standard in the diagnosis of shoulder pathologies (Tudisco *et al.* 2015: 394), this modality is extremely costly and less accessible to the average patient (Ooi *et al.* 2014: 2). B-mode ultrasound has been recognised as a viable alternative for soft tissue imaging owing to its affordability, real time imaging and lack of ionizing radiation (Li and Cao 2017: 3; Kaur 2013: 393). The B-Mode ultrasound, however, is limited in determining pathological and biomechanical properties (Fusini *et al.* 2017: 467; Ooi *et al.* 2014: 1).

New imaging modalities such as ultrasound elastography has made it possible for the imaging of tissue stiffness in order to provide a relevant diagnostic tool for diagnosis of organ pathology (Gennisson *et al.* 2013: 287). The two most frequently used elastography techniques in clinical practice are strain ultrasound and shear wave ultrasound elastography (Garra 2015: 683). Strain ultrasound elastography (SUE) relies on manual compression from a transducer in order to map tissue elastic properties (Ilhanli *et al.* 2015: 31). On the other hand, shear wave ultrasound elastography (SWUE) (on which this study is based) is related is a physical specification which allows for numerical calculation of tissue elasticity to be measured in kilopascals or metres/sec without manual compression (Shiina *et al.* 2015: 1139; Qiu *et al.* 2015:90). This new imaging modality has made it feasible to directly quantify tendon mechanical properties (Sikdar, Wei and Cortes. 2014: 126).

Based on the paucity of biomechanical data available on normal tendons, this study therefore aimed to establish a reference range of the rotator cuff and biceps tendons of 260 asymptomatic participants, by quantifying measurements in kPa, using shear wave ultrasound elastography (SWUE). Imaging modalities such as MRI are expensive or limited or in establishing pathological and biomechanical properties of tendinopathies. The proximal, middle and distal sites of the biceps, subscapularis, supraspinatus and infraspinatus tendons as well as the teres minor tendon in both the sagittal and axial planes were examined based on gender, race, age, BMI and level of activity. The study group was made up of 260 participants, of which 159 were females and 101 were males. The age category of participants ranged from 21-45 years (mean age 34.52 ± 7.75 years), whilst the distribution based on race

was 57.30% Indians (n=149), 35.38% Black (n=92), 3.84% Coloured (n=10) and 3.46% Whites (n=9). The mean BMI of the study population was 26.70 ± 5.10 kg/m². It is assumed that this is the first study to estimate a reference range value for all the rotator cuff and biceps tendons in a single examination of the shoulder joint. Despite the similarities observed in demographic data to the SWUE study conducted by Arda and co-workers (2011:533), 260 participants were evaluated in contrast to the 127 asymptomatic participants evaluated by Arda *et al.* (2011: 533). The aforementioned investigators did not report on racial variation in their study.

5.2 B-MODE ULTRASOUND AND ELASTOGRAPHY ANALYSIS

5.2.1 B-Mode Ultrasound Analysis

In this study, B-mode ultrasound of normal rotator cuff and biceps tendons displayed parallel echogenic lines in the sagittal planes and echogenic dots in axial planes, similar to that previously described (Hodgson, O'Connor and Grainger 2012: 1158). Rotator cuff pathology may present as tendinosis which is defined as a hypoechoic, poorly defined thickened tendon (Dong *et al.* 2015: 1485; Sahan *et al.* 2018: 196). In addition, calcium crystal deposition within the tendons, probably as a result of a degenerative or medical condition, could precipitate calcific tendinitis (Lee *et al.* 2016a: 1620). Calcifications exhibit hyperechoic echo pattern which may or may not cast posterior acoustic shadowing on B-Mode ultrasound (Lee *et al.* 2016a: 1621). Furthermore, partial thickness tears are located on either on the articular, bursal or the intratendinous surface of rotator cuff tendons (Matthewson *et al.* 2015:4) and may coexist with tendinosis (Singh 2012: 288). Partial thickness tears are visualised as a hypoechoic defect in the tendon, with resultant tendon thickness alteration (Gaitini 2012: 6), whilst full thickness tears appears anechoic or as low level echoes as a result of the presence of fluid (Beggs 2011: 113), extending from the articular surface to the bursal surface (Lee *et al.* 2016a: 1618).

Using B-Mode ultrasound analyses, eleven (4.23%) pathological changes in our cohort of asymptomatic participants were revealed. Of these eleven participants, nine were over the age of 40 years. Four (1.53%), out of the eleven demonstrated partial thickness tears of the supraspinatus tendon near the distal insertion into the humeral tuberosity. Calcifications were noted in four (1.53%) supraspinatus tendons and two (0.76%) subscapularis tendons near the humeral insertion. Fluid was also noted in the sub acromial sub deltoid bursa of two

participants (0.76%). It is possible that such intrinsic changes within the tendons could be attributed to the ageing process and decreased vascularity in tendons as previously described (Matthewson *et al.* 2015: 3). The anomalies demonstrated by the two asymptomatic participants aged younger than 40 years, could be due to extrinsic factors such as increased pressure between the rotator cuff tendons and coracoacromial ligament (Kijima *et al.* 2013: 1).

Studies report that the supraspinatus tendons are the most frequently affected tendon in pathologies associated with the rotator cuff (Escamilla, Hooks and Wilk 2014: 15; Lalitha, Reddy and Reddy 2011: 366). The data obtained for this study is similar to a B-Mode study conducted on the supraspinatus tendons reported by Hou *et al.* (2017). However, these investigators evaluated 55 asymptomatic participants, aged between 25-74 years old, and reported 14.5% tears at the distal insertion (footprint) of the supraspinatus tendon and 3.6% tears in the distal insertion to the mid tendon (Hou *et al.* 2017:101). The B-Mode ultrasound analyses of the normal supraspinatus tendons of this study also displayed similar fibrillary echo patterns as Hou and colleagues (Hou *et al.* 2017: 98). In contrast, Hackett and colleagues compared ten normal B-Mode ultrasound of supraspinatus tendon of asymptomatic participants aged between 21-69 years with ten tendinopathic tendons with focal areas of decreased echogenicity at their distal insertion (Hackett *et al.* 2019:3), whilst B-Mode of supraspinatus tendon was unreported by Arda and colleagues (Arda *et al.* 2011: 533).

The B-Mode ultrasound analysis revealed normal fibrillary echo patterns for the biceps tendons. Despite normal patterns observed in most tendons, minimal fluid was present in thirteen (5%) of this study population. However, minimal amounts of fluid around the biceps tendon are considered a normal variant (Messina *et al.* 2015: 6). Generally, there is little or no fluid observed around the biceps tendon (Sahan *et al.* 2018:195). Nonetheless, it is possible that this observation was due to the small sample number of 20 asymptomatic biceps tendons being evaluated, with a mean age of 47.55 ± 11.9 years (Sahan *et al.* 2018:195). Similarly, in the findings of this study, normal fibrillary echo patterns were also noted in the subscapularis, infraspinatus and teres minor tendons.

5.2.2 Elastography Analysis

We also analysed the qualitative colour mapping of the rotator cuff and biceps tendons, as well as the quantitative shear wave elastic values in kPa, were also analysed. Albeit, due to the paucity of data, comparisons linked to the subscapularis and teres minor tendons could not be drawn. Both SUE and SWUE contribute to the analysis of tissue stiffness, measured by Young's modulus (elaborated on in Chapter 2) (Washburn, Onishi and Wang 2018:10). Consequently, differences in tissue displacements or elasticity are analysed and displayed as colour maps or elastograms (Zaleska-Dorobisza *et al* 2013: 645).

5.2.2.1 Colour Map Analysis

Tissue stiffness is shown as a grey or colour coded map on the shear wave ultrasound monitor (Nowicki and Dobruch-Sobczak 2016: 117). Variations of colour coded mapping, however, do exist during soft and hard tissue analysis, as a result of pre-sets prescribed by the vendor or operator's preference (Ooi *et al.* 2014: 11). This results in inconsistencies when using colour map analysis. The GE Logiq E9 ultrasound equipment was utilised during this study, as opposed to the Siemens ultrasound equipment S3000 (Virtual Touch Image Quantification) employed by Hou and colleagues (Hou *et al* 2017: 97). Furthermore, 74.61%-86.15% of all tendons at the humeral insertion were recorded as 'dark blue' colour maps based on vendor specifics. The 'dark blue' colour maps are indicative of harder elasticity and therefore higher kPa values. Collected data also supports the SWUE study, conducted by Hou and colleagues who chose red (pre-set on equipment) indicative of stiffer areas and blue as softer areas (Hou *et al.* 2017: 98). The findings of this research also corroborate a SUE study, which also reported a predominant blue colour map (with the GE E8 ultrasound equipment), of the evaluated supraspinatus and Achilles tendons in asymptomatic young participants (Lalitha *et al.* 2011: 370). In contrast Ohuegbe (2014) who evaluated 284 asymptomatic participants in a SUE ratio study, reported a 85.9% predominance of blue/green colour maps in the supraspinatus tendons, thus grading them as hard tendons (Ohuegbe 2014: 70). The study by Ohuegbe (2014: 55) omitted the name of the ultrasound equipment.

Pathological changes of the supraspinatus tendons at the distal insertion were also observed in four (1.53%) asymptomatic participants in our study, representative of a mixture of colours as a colour map in the sagittal plane. This observation was analogous to that reported by Lalitha, Reddy and Reddy (2011: 370), who demonstrated tendinosis as a mixture of green

and red colour maps, indicative of fluctuations in soft elasticity. Added to this, tears of the supraspinatus tendon displayed colour maps of blue and green, with traces of red at site of tears (Lalitha, Reddy and Reddy 2011: 370). In contrast, Hou and colleagues reported blue colour maps in regions of tendinosis or tears (Hou *et al.* 2017: 99), whilst Ohuegbe (2014: 70) reported a 14.1% tendinopathy in 40 asymptomatic tendons, as yellow colour maps, indicative of intermediate tissue stiffness.

‘Dark blue’ colour maps for the biceps tendon were noted in this investigation, indicative of hard and normal tendon structure. Similarly, Sahan and colleagues evaluated 20 asymptomatic participants (47.95 ± 11.19 years), and reported a 10% blue green colour maps, indicative of hard tissue, based on their vendor specifics (G.E. Logiq E 9 ultrasound equipment) (Sahan *et al.* 2018:197). Although the ultrasound equipment utilised was identical to that of the aforementioned investigators, the researchers of this study reported 81.15% of normal tendons as ‘dark blue’ in contrast to the predominant ‘blue’ colour map study by Sahan and colleagues (0%) (Sahan *et al.* 2017: 195). In addition, 55% of the normal biceps tendons were characterised as green, indicative of intermediate stiffness, with 35% as green and yellow, indicative of soft elasticity (Sahan *et al.* 2018:195). The differences between these two studies could be attributed to the pre-sets on the ultrasound equipment.

5.2.2.2 Shear Wave analysis

This study reports the elasticity of the rotator cuff and biceps tendon in Young’s modulus (E), measured in kilopascals (kPa), as previously reported by Ryu and Jeong (2017: 2) in contrast to measurements of the supraspinatus tendon elasticity done in m/sec. Elasticity values in kPas, were reported, although slight discrepancies exist between this study and previously reported studies, which could be due to arm positioning and scan planes. Much effort was used to establish the most appropriate method for aligning the transducer parallel to the tendon in the sagittal plane. Transducer orientation is essential to achieve optimum skeletal muscle recording, since shear waves propagate poorly at transducer orientations of 45° and 90° to the long axis of muscle fibres (Eby *et al.* 2013: 2381).

A statistically significant difference was noted in this study between the sagittal and axial planes at the humeral insertion of the rotator cuff and biceps tendons of the entire group ($p = 0.001$), indicative that higher elasticity values in the sagittal plane in comparison to the axial

planes of the tendons. It is possible that the lower elasticity values acquired in the axial plane could be due to orientation of the muscular skeletal fibres in the axial plane (Davis *et al.* 2019: 5).

Higher elasticity values were identified in the sagittal plane of the proximal biceps tendon, as 104.83 ± 18.89 kPa, the middle as 105.43 ± 18.32 kPa and the distal as 106.16 ± 17.91 kPa, in contrast to the lower elastic values reported by Sahan *et al.* (2018). Likewise, higher elasticity values were also observed in the axial plane in the proximal biceps tendon as 98.91 ± 17.70 kPa, middle 99.04 ± 16.14 kPa, and distal biceps tendon 98.32 ± 15.36 kPa. Twenty biceps tendons from asymptomatic participants (mean age 47.55 ± 11.9 years) were evaluated by Sahan and colleagues, in which elasticity values of 39.42 ± 7.4 kPa were noted in the sagittal plane (1-4 cm below proximal insertion) and 18.6 ± 3.4 kPa in the axial plane at the site where the tendon was prominent (Sahan *et al.* 2018: 195). Variations in the reported elasticity values could be due to the degree of transducer pressure and transducer orientation in relation to the examined structures, as previously reported by Taljanovic *et al.* (2017: 862). Nevertheless, both our findings and that reported by Sahan's group were similar in that no significant differences in the elastic values between the fluid and non-fluid portions of the biceps tendon sheath were noted. As reported, shear wave does not exist in pure fluids and may therefore be ineffective in the examination of cystic structures (Winn, Lalam and Cassar-Pullicino 2016: 869).

An extensive evaluation of the proximal, middle and distal sites of the supraspinatus tendon in both the sagittal and axial plane was conducted by the investigators of this study, whilst others assessed the supraspinatus tendon in the sagittal plane only (Hackett *et al.* 2019:5; Baumer *et al.* 2018:287). Results of the distal insertion of the normal supraspinatus tendon in the sagittal plane yielded a mean elastic value of 108.72 ± 18.74 kPa. In contrast, Hackett *et al.* (2019: 8) reported a much higher mean value of 297 kPa (9.96 ± 0.02 m/sec) in ten asymptomatic participants, with a mean age of 37 years, ranging between 21-69 years (Hackett *et al.* 2019: 8). Similarly, Arda and co-workers also reported lower mean elastic values in the supraspinatus tendons of 127 asymptomatic participants (Arda *et al.* 2011: 535). These investigators reported a mean elastic value of 36.0 ± 13 kPa (range 11-77) in males and 29.1 ± 12.4 kPa (range 6-90 kPa) in females. Likewise, Dischler's group reported lower elasticity values (2.2 ± 0.3 m/sec) in a study of the supraspinatus tendons of 19 swimmers, with

a mean age 19.4 ± 1.1 years (Dischler *et al.* 2018:114). Such discrepancies may be due to the use of different laboratory ultrasound equipment and algorithm programs acquired from different vendors, as well as patient positioning, the number of measurements conducted and the acquisition depth (Shin *et al.* 2016: 3366). Notably, we ensured the use of the lightest transducer pressure and minimal acquisition time for each examination, and employed the scanning protocol according to previously published techniques (Oliveira *et al.* 2016:3; Singh, 2012: 285; Beggs, 2011: 2).

Elasticity values of 109.78 ± 22.50 kPa (range 51.26-166.63 kPa) were reported at the proximal site of the supraspinatus tendon in the sagittal plane. In contrast, Baumer and co-workers assessed the proximal tendon at its intramuscular site in sagittal plane only, in order to avoid artefacts precipitated by the humerus head (Baumer *et al.* 2018: 287). Elasticity values reported in m/sec, showed that the mean of the intramuscular portion of the proximal supraspinatus tendon in the sagittal plane (6.1 ± 1.5 m/s; range 4.2 ± 7.7 m/sec; $p=0.011$) increased significantly with age under both active and passive (2.9 ± 0.4 m/sec; range 2.5-3.9 m/s; $p=0.005$) conditions. Higher shear wave velocity means were recorded in active conditions in comparison to passive conditions (Baumer *et al.* 2018: 287). A limitation identified by these investigators is the lack of axial measurements at the proximal supraspinatus tendon (Baumer *et al.* 2018: 287). Furthermore, additional limitations to both Hackett's and Baumer's groups included the lack of various evaluation sites and elastography of axial planes of the supraspinatus tendons, in order to reach a conclusive reference value.

A minimal degree of tension in positioning techniques was employed so that each participant was made comfortable. It has been established that increased tension used in musculoskeletal elastography has been associated with increased stiffness, therefore higher kPa values of structures (Eby *et al.* 2013: 2382). The speed of shear wave is reported to be more rapid through stiff contracted tissue due to tendon anisotropy, including along the long axis of tendons and muscle, when compared to the axial plane (Aubrey *et al.* 2014: 827). Aubrey's group evaluated Achilles tendons in 105 asymptomatic (aged between 31-60 years) and 30, symptomatic (aged between 43-63 years). They established that tension or stretching of tendons resulted in higher stiffness in asymptomatic participants whilst tendon positioning under passive and active conditions did not influence SWUE in confirming tendon softening in the mid portion of the pathologic Achilles tendon (Aubrey *et al.* 201: 826). Aubrey's data opposes that stated by Baumer and colleagues, who reported lower mean elasticity values on

application of tension in the symptomatic tendon ($p < 0.024$), in comparison to the relaxed symptomatic supraspinatus tendon ($p > 0.783$) (Baumer *et al.* 2017: 282). It is possible that this may be due to underlying rotator cuff pathologies or changes in the neuromuscular firing patterns linked to pathology (Baumer *et al.* 2017: 286).

In this study, a statistically significant difference was also noted in the teres minor tendon in the sagittal and axial planes ($p < 0.05$). The reference values ranged from 96.71 ± 16.49 - 102.74 ± 18.76 kPa in the sagittal plane and 97.03 ± 18.29 kPa in the axial plane. Due to the paucity of data on SWUE studies of the infraspinatus tendon the current study was compared to a SUE study that employed a force measuring device onto the region of the infraspinatus tendons of 20 asymptomatic baseball players (age 20: range 15-25 years). No significant difference ($p > 0.05$) was found between the strain groups when $> 15\%$ stress was applied during their positioning technique but a statistically significant difference ($p = 0.001$) was revealed when the applied stress was $< 15\%$ (Trent 2013: 34). By computing the elastic modulus the mean elasticity was 96.1 kPa, which indicated that elastic modulus is different between individuals (Trent 2013:35). Apart from a small population, inconsistencies with transducer pressure were a limitation in their study (Trent 2013:38).

5.3 GENDER ANALYSIS

A statistically significant difference between males and females for biceps, supraspinatus infraspinatus and teres minor tendons ($p < 0.05$) was observed. Higher elastic values were shown in males compared to female tendons. Statistically significant differences were noted for the proximal, middle and distal biceps tendon in the sagittal plane ($p = 0.019$), middle biceps tendon in the axial plane ($p = 0.030$), and middle subscapularis tendon in the sagittal plane ($p = 0.018$). Significant differences were also observed for the distal supraspinatus tendon in the sagittal plane ($p = 0.006$) and the middle supraspinatus in the axial plane ($p = 0.007$).

Despite the results corroborating a study by Arda *et al.* (2011: 533), in that males had higher elasticity values than females, the actual elasticity values of the supraspinatus tendons reported for both males (36.0 ± 13.0 kPa) and females (29.1 ± 12.4 kPa) were lower compared to our values (Arda *et al.* 2011: 533). It is possible that higher elasticity (kPa) values observed in males in the current study may be due to our procedure of locating the region of

interest (ROI) by location and size and by matching the ROI values in all tendons under study. These measured ROI values were assessed and captured by two independent observers and thereafter all acquisition imaging planes were verified. In contrast, Arda's group did not conduct the ROI within the supraspinatus tendon (Arda *et al.* 2011: 533).

This study reported slightly higher elasticity values of the supraspinatus tendon in males, ranging from 106.21 ± 18.9 kPa to 113.65 ± 20.51 kPa in the sagittal plane, in comparison to the females which ranged from 106.60 ± 18.23 kPa to 110.96 ± 20.92 kPa and elasticity values in the axial plane of 106.70 ± 19.04 kPa to 111.42 ± 20.29 kPa in comparison to females which ranged from 103.39 ± 19.97 kPa to 104.44 ± 20.59 kPa. However, there was no statistical difference between the proximal and middle supraspinatus tendons elastic values in the sagittal plane and proximal and distal plane in the axial planes ($p > 0.05$) between males and females. Males demonstrated the highest mean for the middle supraspinatus tendon in the sagittal plane (113.65 ± 20.51 kPa; $p = 0.309$), whilst the females demonstrated a mean of (110.96 ± 20.92 kPa; $p = 0.309$).

In contrast, Baumer *et al.* (2017: 284) was unable to report gender elasticities for both males and females as well as demonstrate significant differences for the supraspinatus tendon based on gender. This was probably due to the disproportionate distribution of females ($n=17$) vs males ($n=2$) ($p > 0.317$). It is possible that the study of Baumer and co-researchers focussed mainly on the effects of age on normal and pathological rotator cuff tendons. Hou and colleagues in 2017 also investigated the supraspinatus tendons of 12 males and 10 asymptomatic females (mean age 42.1 years), were unable to report gender elasticity differences regardless of their mean SWUE of 8-9 m/sec in asymptomatic participants (Hou *et al.* 2017: 102). Moreover, this discrepancy was also observed in symptomatic and asymptomatic supraspinatus tendons in females ($n=14$) and males ($n=6$) (Hackett *et al.* 2019: 4). It is possible that the focus of these studies was linked to structural differences between normal and pathological supraspinatus tendons.

The current study also demonstrates a significant difference in the data for the proximal infraspinatus tendon in the axial plane ($p = 0.037$), whilst the teres minor tendon showed notable differences in the sagittal ($p = 0.007$) and axial planes ($p = 0.038$), indicative that males had higher elastic values in comparison to female tendons. Due to the paucity and lack of

data, it was impossible to compare the SWUE findings of gender of these tendons recognised in this study, with the findings of other investigators.

Elasticity values of the biceps tendon based on gender differences in the current study could not be compared with those submitted by Sahan and co-workers, since they reported one mean elasticity value for both males and females. The reference range of 20.62 ± 4.6 kPa (range 13.3-30) was acquired in the sagittal plane and 18.6 ± 3.4 (range 14.3-28.8) in the axial plane by the aforementioned investigators (Sahan *et al.* 2018: 195). Elasticity values acquired in the sagittal plane in this study were lower in the proximal biceps tendon for females (101.93 ± 18.94 kPa), in comparison to the males (109.40 ± 18.15 kPa), whilst the elasticity values for the axial plane was 97.46 ± 17.95 kPa for females in contrast to 102.21 ± 17.13 kPa in males. A principal reason for the differences in between this study and the study by Sahan and colleagues (2018) could be due to anisotropic changes as a result of transducer angulation between operators. As described by Guo *et al.* (2016: 62) this common pitfall occurs as a failure to align the tendon perpendicular to the ultrasound beam. In addition, a comparative study on elasticity values of the infraspinatus tendon at the musculotendinous junction (proximal site) for the males were 109.38 ± 20.55 kPa in this study, whilst a SUE report by (Trent 2013: 37) demonstrated a lower mean elasticity value of 96.1 kPa. However, this SUE study was specifically performed on a smaller population of twenty males (Trent 2013: 8).

5.4 AGE ANALYSIS

Data was further categorised by age in order to determine if age influenced elasticity values. The results revealed a statistically significant difference for the middle infraspinatus tendon in the sagittal plane ($p=0.01$) and the teres minor tendon in the axial plane ($p=0.025$) for both the 35-45 and 21-24 age categories respectively. The Duncan's multiple range test detected a difference in mean kPa for the age categories 35-45 years (mean=95.53 kPa) and the category 25-34 years (mean=102.18 kPa). Interestingly, the age category 21-24 years had higher kPa values, compared to the other age categories. Lower kPa values in the older age categories is probably due to the increase in tendinosis incidence observed in patients over 35 years as a result of collagen breakdown, and the subsequent tendon softening (Yoon *et al.* 2014:111). Comparably, a SUE study conducted by Lalitha and co-workers, reported hardness, indicated by predominantly blue colour mapping, in supraspinatus tendons of younger asymptomatic

individuals (Lalitha, Reddy and Reddy 2011: 370). These investigators albeit, did not report the age category of younger individuals.

Arda and co-workers, in contrast, report no significant correlation between tendon stiffness and age, in their study population of 127 participants, ranging from 17 to 63 years of age (Arda *et al.* 2011). This was confirmed on a SUE (strain index) study by Tudisco and colleagues on 50 (mean age 58 ± 12 years) asymptomatic supraspinatus tendons which showed a slight difference in gender strain index (males: 1.05 versus females: 1.04), thereby concluding that age had a limited role in clinical practice (Tudisco *et al.* 2015: 396). These investigators emphasised that other factors such as working activities, dominant arm and lifestyle were contributory factors in influencing elasticity changes in individuals (Tudisco *et al.* 2015: 96). Notwithstanding, this study was based on an older population and was not categorised into age groups, as this study.

On the contrary, a SUE ratio study conducted on the supraspinatus tendon ($n=30$, age range 25-84 years), suggests that age is directly proportional to tendon hardness ($p<0.05$), predisposing tendons to partial thickness tears (Ilhanli *et al.* 2015: 033). Similarly, Baumer's group found a significant increase in tendon stiffness with increasing age during both active and passive conditions in asymptomatic participants (Baumer *et al.*, 2018: 287). It is possible though, that the small sample number ($n=19$) combined with the mean age grouping of 42.4 ± 18.9 years, may have influenced these recordings (Baumer *et al.* 2018: 282). Sahan and co-workers also reported lower elasticity values in their study group ($n=20$ biceps tendons), in comparison to our study. The variations are probably age related, since rotator cuff pathologies increases with increasing age and this study group was 34.52 ± 7.7 years versus 47.55 ± 11.9 years. Additionally, the lack of routine shoulder positioning protocols, as well as the orientation of transducers could be contributing factors in the variations between the studies reported.

5.5 RACE ANALYSIS

The data in the current study could not be compared to other studies due to the paucity of ultrasound elastography data based on race. This study revealed statistical significant differences in the proximal supraspinatus tendon in the axial plane ($p=0.000$) and the middle infraspinatus tendon in the sagittal plane ($p=0.003$), among the Whites, Blacks, Indians and

Coloured groups. These findings indicate the predominance of harder elasticity amongst the Whites in comparison to other race groups. However, the small sample numbers of asymptomatic participants (Coloured: n=10 vs White: n=9) may have significantly added to these variations.

A significant difference was also noted for the proximal infraspinatus tendon in the axial plane, between the Coloureds versus the White and Black groups ($p=0.028$). The lowest elasticity values were observed amongst the Coloureds. Significant differences were also noted in the teres minor tendon in the axial plane ($p=0.001$) between the Whites and the other three race groups, again demonstrating higher elastic values in the White group. It is possible that these variations could be attributed to the differences in social and economic status of the White group in comparison to the other Black and Coloured groups, taking into consideration the large health inequality of Black South Africans and poor people was 88% (Obuaku- Igwe 2015: 125). It was observed in this study that the highest percentage differences occurred between the 'very active' participants amongst the Indian group (n=37; 24.83%), compared to the Black (n=9; 9.78%), Coloured (n=2; 20%) and White groups (n=2; 22.2%). The 'moderate level of activity' in the Indian group was 71.81%, (n=107); 86.95% for the Black group (n=80), 70% amongst the Coloured group (n=7) and 66% for the White group (n=6). Previous reports suggest that health inequalities were more prevalent among Black and Coloured groups, compared to White and Indian groups (Obuaku-Igwe 2015: 125). It is possible that such inequalities may lead to poor health outcomes. It is surmised that these differences between the White and other race groups could be a possible contributory factor to the disparity in elastic values.

5.6 BODY MASS INDEX AND LEVEL OF ACTIVITY

The non-significant variations in BMI kPas observed in the current study were similar to that reported by Sahan *et al.* (2018: 195). Likewise, a study of the biceps brachii muscle also failed to demonstrate significant differences in BMI (Eby *et al.* 2015:26). Similarly, despite the evaluation of various organs by SWUE, Arda and colleagues also failed to demonstrate significant differences with tendon studies and BMI (Arda *et al.* 2011: 536). It is possible that these non-significant data could be attributed to the broad range of anatomical regions evaluated. Moreover, since BMI is based on the height and weight of a person, factors such

as analysis of body composition, waist circumference and skin fold thickness are not included in a BMI profile (Chandrasekaran 2018: 1).

In the study, a borderline statistical significant difference for the middle subscapularis tendon in the sagittal plane ($p=0.049$) between the different levels of activity was demonstrated. This was corroborated by a study in asymptomatic biceps brachii muscle ($n=133$, aged between 21-94 years). The investigators failed to demonstrate any statistical significance between the level of activity and the tendons under study (Eby *et al.* 2015:26). The present study also reported the highest elasticity value of $111.04\pm21.47\text{kPa}$ in the 'very active' category, $107.94\pm29.97\text{kPa}$ in the 'moderate' level of activity and $98.64\pm12.35\text{kPa}$ in the 'mild' level of activity. It is possible that the study lacked the relevant data on mode, frequency and duration of exercise. Data in the present study nonetheless, differs from that conducted by Takenaga *et al.* (2016:2935), who demonstrated a significant difference in the posterior capsule of the shoulder joint in a population of baseball players ($n=45$) amongst the 'very active throwing shoulders' (elasticity values $=40\text{kPa}$) compared to 'mild non-throwing shoulders' (elasticity values $=32\text{kPa}$; $p<0.001$). The higher kPa values observed in 'very active' asymptomatic participants is indicative of an increase in stiffness, whilst a reduction in stiffness was noted in the 'mildly active' participant. It is possible that the 'very active' asymptomatic participants of this study were involved in less strenuous sports than the baseball and basketball players with almost ten years experienced evaluated by Takenaga *et al.* (2016).

Moreover, variations in elasticity in 'very active' participants were reported by Dischler and colleagues, who suggested that supraspinatus tendon stiffness (mean $2.2\pm3\text{m/sec}$; $p=0.01$) decreases during long-term swimming, whilst the thickness increased with increased years of participation in a group of 18 female swimmers, aged between 18-22 years (Dischler *et al.* 2018: 113). Prolonged swimming careers are known to precipitate changes in biomechanical properties in the supraspinatus muscle and tendon, thus giving rise to rotator cuff pathology (Dischler *et al.* 2018: 116). Although the study by Dischler *et al.* (2018: 116) established that supraspinatus tendon thickness $> 6.2\text{mm}$ in width were predisposed to tendinosis, their study sample population was small and limited to female swimmers only. Thus, based on these documented differences in elasticity values, it is possible those different codes of sport and thus the varying level of activities influences elasticity kPa values.

5.7 CONCLUSION

The elastographic measurements within the various categories have been analysed in detail in this study. The disproportionate ethnic distribution of the study population may be attributed to the geographical location of the radiology practice in proximity to the race groups. It is also possible that the research site could have been the preferential health practice of certain ethnic groups in contrast to others. Some people did not want to take part in the study due to the length of the study (30minutes). We tried our utmost in recruiting an equal number of categorized participants but the researcher had to meet the deadline of target of 260 during the time frame of the research. All shear wave ultrasound elastographic studies were performed in both the sagittal and axial planes and the difference between the planes has been reported. A 95% confidence interval for the rotator cuff and biceps tendons has been reported. There was a statistically significant difference observed between males and females for the proximal, middle and distal biceps tendon in the sagittal plane ($p<0.05$). A statistical difference was also noted in the sagittal and axial planes of the teres minor tendons ($p<0.05$). Even though the transducer was maintained perpendicular to the tissue in order to avoid anisotropy, artefacts were still observed

According to Kot *et al* (2012:2) transducer pressure can be classified as light, moderate or hard. Minimal or excessive transducer pressure may impact on elastic properties of tissues (Paluch *et al* 2016: 244; Shiina *et al* 2015: 1138), therefore minimal transducer pressure was used in this study. Artefacts presented as colour variation on certain colour maps and some discrepancies of shear wave kPa values on certain tendon images. These artefacts may be attributed to the orientation of the transducer relative to obliquity of tendons during positioning, including structural interfaces. The size of the ROI impacts on the elastograms in order to estimate the mean elasticity as larger areas may cause a tendon to appear harder than smaller areas (Wu *et al* 2012: 83). In this study ROI of tendon sites ranged from 1.8-4mm. The study by Kot *et al* (2012: 1) established that there was no difference in the mean elasticity modulus with different sizes of ROI (8-12mm for the rectus femoris muscle and 2-4mm for the patellar tendon). Similarly, the study by Kot and colleagues found no difference on acquisition times in the study of the rectus femoris muscle and patellar tendon. The acquisition time refers to the time the transducer is kept stationary (5, 10, 15 and 20 seconds) while accessing the SWUE images (Kot *et al* 2012: 2). This study kept the acquisition time between 10 and 15 seconds per tendon site. Of note, different transducer types and ultrasound equipment from different vendors may influence the measurements of the evaluated tendons.

CHAPTER 6: CONCLUSION

This study assessed the biomechanics of the rotator cuff and biceps tendons of the shoulder joint in asymptomatic participants, in order to establish a reference range for use in clinical practice. The objectives were: to measure the rotator cuff and biceps tendons and report in kilopascals, using shear wave ultrasound elastography, as well as to establish a shear wave ultrasound elastographic reference range of the rotator cuff and biceps tendons for use in clinical practice. Imaging analysis on shear wave ultrasound elastography included the utilisation of a sensitive; quantitative technique with the aid of a built in algorithm within an ultrasound machine, for measurements of the rotator cuff and biceps tendons *in vivo*.

Shear wave ultrasound elastography in asymptomatic participants was investigated and correlated, based on various demographic factors in an attempt to provide a reference range of the rotator cuff and biceps tendons. Normal B-Mode imaging was noted in 95.76% of asymptomatic participants. Normal colour maps of dark blue were noted in 74.61%-86.15% of tendons at the humeral insertion. Although slight discrepancies were noted in patient positioning, higher elastic values in the sagittal in comparison to the axial plane ($p=0.001$) were established. Higher shear wave elasticity measurements were noted in stiff or hard tendons. Additionally, statistically significant differences of certain rotator cuff and biceps tendons between the male and female tendons ($p<0.05$) were observed. Higher elastic modulus in the younger age category 21-24 years was determined. Although the Coloured and White groups had small samples, a significant difference between the White and other race groups ($p=0.000$) was noted. With regards to the White and Coloured race group, this study was limited by factors such as uneven number of these participants in the various categories such as age, 'level of activity' and gender difference. There was no statistically significant difference in the BMI category. A borderline statistical significant difference was evident for the middle subscapularis tendon in the sagittal plane ($p=0.049$) between the different levels of activity. However, significant differences were observed between this and other studies. The present study could only compare the SWUE of the supraspinatus and biceps tendons to other studies and have found both similarities as well as disparities. This study also endeavoured to compare the elasticity value of the proximal infraspinatus tendon to a SUE study with a small population of twenty athletic asymptomatic participants.

Factors such as transducer type, size of ROI and acquisition time were consistent during all measurement. A standardised examination protocol was employed for the B-Mode ultrasound and SWUE of the shoulder joint, including the specific sites of the tendons under

examination. The protocol employed in the study guarantees reproducibility as well as the applicability of ultrasound elastography. This study confirms several previously reported, though limited, studies on the rotator cuff and biceps tendons. Imaging procedures contribute an important role in the diagnosis and management of rotator cuff and biceps tendon pathology. The value is greatest when B-Mode findings are indeterminate. Although B- Mode ultrasound and Doppler studies may provide additional qualitative assessment, the above methods are hindered by the lack of quantitative assessment of tendon stiffness. Therefore, the contribution of SWUE as a complementary examination to B-mode ultrasound is of paramount importance.

A major limitation in the present study was the scarcity of White and Coloured participants at the private radiology practice. Therefore, future recommendations should include studies of these race groups in order to maintain a proportionate assessment of the population. In addition, the study population was small. It is recommended that a larger population could contribute to a stronger database. Furthermore, artefacts were encountered as a result of positioning techniques, as well as technical limitations of the ultrasound equipment. Further studies should include standardisation of shear wave ultrasound positioning techniques of the rotator cuff and biceps tendons. Technical parameters differ between vendors, resulting in variable results between investigators. Therefore, it is recommended that these parameters such as frame rate, and dynamic range within the software of the ultrasound equipment be standardised amongst various vendors. Future studies should aim at integrating shear wave ultrasound elastography with other imaging modalities such as CT and MRI in order to strengthen their diagnostic performance in surgical planning. In addition, the use of SWUE in real time will make provision for the development of 3D elastography imaging for diagnosis, planning treatment and monitoring of treatment in clinical practice. Moreover, ultrasound tissue characterisation which looks at transverse images over the length of the entire tendon and compiles images into 3D blocks, should be proposed as an adjunct to elastography in the assessment of tendons.

Shear wave ultrasound elastography has gained much attention as an excellent imaging tool, capable of non-invasive quantification of tissue stiffness. This cost effective technique does not utilise ionising radiation and is therefore regarded as a safe modality to characterise elasticity. The results of our study demonstrate the diagnostic potential of SWUE for assessment of the rotator cuff and biceps tendons, based on its excellent 95% confidence

intervals for reference ranges. The reference ranges of the rotator cuff and biceps tendons have been evaluated by finding 95% confidence intervals for the mean elasticity for each of the tendons. The point estimate of kPa values of each tendon evaluated in this study is reflected in the narrow confidence intervals. The reference values presented here can be used as a baseline for future studies, as well as to influence practice in the diagnosis, treatment and follow up of rotator cuff and biceps tendon pathology. In addition, the use of reference values could be an excellent screening tool for athletes in order to follow up progress of any possible biomechanical alterations during sporting events. Further, multi-centre studies would benefit in the formation of a database in order to ascertain elasticity values of normal and pathological rotator cuff and biceps tendons.

REFERENCES

- Arda, K., Ciledag, N., Aktas, E., Aribas, B.K. and Köse, K. 2011. Quantitative assessment of Normal Soft- Tissue elasticity Using Shear- Wave Ultrasound Elastography. *American Journal of Roentgenology*, 197: 532-536. Available: www.ajronline.org/105.186.78.42 (Accessed 28 February 2016).
- Aubry, S., Nueffer, J.P., Tanter, M., Becce, F., Vidal, C. and Michel, F. 2014. Viscoelasticity in Achilles tendonopathy: quantitative assessment by using real-time shear-wave elastography. *Radiology*, 274 (3): 821-829. Available: <https://pubs.rsna.org/doi/pdf/10.1148/radiol.14140434> (Accessed 3 November 2016).
- Bamber, J., Cosgrove, D., Dietrich, C., Fromageau, J., Bojunga, J., Calliada, F., Cantisani, V., Correas, J.M., D'onofrio, M. and Drakonaki, E. 2013. EFSUMB guidelines and recommendations on the clinical use of ultrasound elastography. Part 1: Basic principles and technology. *Ultraschall in der Medizin-European Journal of Ultrasound*, 34 (02): 169-184. Available: <https://www.thieme-connect.com/products/ejournals/pdf/10.1055/s-0033-1335205.pdf> (Accessed 20 February 2016).
- Bamidele, J.O., Debbage, P., Taljanovic, M., Jaschke, W. and Klauser, A.S., 2015. Future of musculoskeletal ultrasound. *Current Radiology Reports*, 3 (6): 21. Available: <https://link.springer.com/article/10.1007/s40134-015-0101-4> (Accessed 15 January 2016).
- Baumer, T. G., Dischler, J., Davis, L., Labyed, Y., Siegal, D. S., van Holsbeeck, M., Moutzouros, V. and Bey, M. J. 2018. Effects of age and pathology on shear wave speed of the human rotator cuff. *Journal of Orthopaedic Research®*, 36 (1): 282-288. Available: <http://dx.doi.org/10.1016/j.jbiomech.2017.01.008> (Accessed 15 May 2017).
- Beggs, I. 2011. Shoulder ultrasound. In: *Proceedings of Seminars in Ultrasound, CT and MRI*. Elsevier, 101-113. Available: DOI: <http://dx.doi.org/10.1053/j.sult.2010.10.003> (Accessed 10 March 2016).
- Bhargava, S., Bhargava, S. K., Sharma, S. and Prakash, M. 2013. Elastography: a new imaging technique and its application. *JIMSA*, 26: 25-30. Available: <http://medind.nic.in/jav/t13/i1/javt13i1p25.pdf> (Accessed 20 February 2016).
- Bosson, A., Ward, K. and Horsley, I., 2015. The shoulder region: anatomy, assessment and injuries. In: Ward, K. ed., 2015. *Routledge handbook of sports therapy, injury assessment and rehabilitation*. London.saxon graphics. 382-457. Available: <https://books.google.co.za>. (Accessed 10 March 2016).

Botar Jid, C., Vasilescu, D., Damian, L., Dumitriu, D., Ciurea, A. and Dudea, S. M. 2012. Musculoskeletal sonoelastography. Pictorial essay. *Med Ultrason*, 14 (3): 239-245. Available: <http://hdl.handle.net/2078.1/158472> (Accessed 10 July 2015).

Brandenburg, J. E., Eby, S. F., Song, P., Zhao, H., Brault, J. S., Chen, S. and An, K.-N. 2014. Ultrasound elastography: the new frontier in direct measurement of muscle stiffness. *Archives of physical medicine and rehabilitation*, 95 (11): 2207-2219. Available: <http://dx.doi.org/10.1016/j.apmr.2014.07.007> (Accessed 10 September 2016).

Carlsen, J. F., Pedersen, M. R., Ewertsen, C., Săftoiu, A., Lönn, L., Rafaelsen, S. R. and Nielsen, M. B. 2015. A comparative study of strain and shear-wave elastography in an elasticity phantom. *American Journal of Roentgenology*, 204 (3): W236-W242. Available: <http://www.ajronline.org/doi/abs/10.2214/AJR.14.13076> (Accessed 15 April 2016).

Chandrasekaran, A. 2018. Body Mass Index-Is it Reliable Indicator of Obesity. *J Nutr Weight Loss*, 2 (111): 1-3. Available: <https://www.longdom.org/open-access/body-ms-indexis-it-reliable-indicator-of-obesity.pdf> (Accessed 13 May 2019).

Chaudhury, S., Holland, C., Vollrath, F. and Carr, A. 2011. Comparing normal and torn rotator cuff tendons using dynamic shear analysis. *The Journal of bone and joint surgery. British volume*, 93 (7): 942-948. Available: <http://www.bjj.boneandjoint.org.uk/content/jbjsbr/93-B/7/942.full.pdf> (Accessed 17 February 2017).

Chen, X.-M., Cui, L.-G., He, P., Shen, W.-W., Qian, Y.-J. and Wang, J.-R. 2013. Shear wave elastographic characterization of normal and torn achilles tendons: a pilot study. *Journal of Ultrasound in Medicine*, 32 (3): 449-455. Available: <http://onlinelibrary.wiley.com/doi/10.7863/jum.2013.32.3.449/epdf> (Accessed 16 August 2016).

Chepeha, J. C., Bouliane, M. J. and Sheps, D. M. 2015. Rotator Cuff Pathology. *Pathology and Intervention in Musculoskeletal Rehabilitation-E-Book*: 240. Available: <http://www.elsevier.com> (Accessed 25 February 2016).

Chernak, L. A. and Thelen, D. G. 2012. Tendon motion and strain patterns evaluated with two-dimensional ultrasound elastography. *Journal of biomechanics*, 45 (15): 2618-2623. Available: <http://dx.doi.org/10.1016/j.biomec.2012.08.000> (Accessed 11 March 2016).

Corazza, A. 2015. Real-time Shear Wave and Strain Sonoelastography in muscles and tendons. In: Proceedings of. European Congress of Radiology 2015. Available: https://posterkey.netkey.at/esr/viewing/index.php?module=viewing_poster&doi=10.1594/ecr2015/C-2384 (Accessed: 28 February 2016).

Cosgrove, D., Piscaglia, F., Bamber, J., Bojunga, J., Correias, J.-M., Gilja, O., Klauser, A., Sporea, I., Calliada, F. and Cantisani, V. 2013. EFSUMB guidelines and recommendations on the clinical use of ultrasound elastography. Part 2: Clinical applications. *Ultraschall in der Medizin-European Journal of Ultrasound*, 34 (03): 238-253.

Available: <https://www.thieme-connect.com/products/ejournals/pdf/10.1055/s-0033-1335375.pdf> (Accessed 17 March 2016).

Cowling, P., Gamble, A. and Rangan, A. 2011. The use of shoulder ultrasound in a one-stop clinic: diagnostic accuracy for rotator cuff tear and biceps tendon pathology. *Shoulder & Elbow*, 3 (1): 13-16. Available: [www.http://dx.doi.org/10.1111/j.1758-5740.2010.00092.x](http://dx.doi.org/10.1111/j.1758-5740.2010.00092.x) (Accessed 4 April 2016).

Davis, L. C., Baumer, T. G., Bey, M. J. and Van Holsbeeck, M. 2019. Clinical utilization of shear wave elastography in the musculoskeletal system. *Ultrasonography*, 38 (1): 2-12. Available: <https://www.ncbi.nlm.nih.gov/pmc/articles/PMC6323314/pdf/usg-18039.pdf> (Accessed 6 April 2019).

De Carli, A., Fabbri, M., Lanzetti, R. M., Ciompi, A., Gaj, E., Beccarini, G., Vetrano, M. and Ferretti, A. 2017. Functional treatment in rotator cuff tears: is it safe and effective? A retrospective comparison with surgical treatment. *Muscles, ligaments and tendons journal*, 7 (1): 40-45. Available: <https://www.ncbi.nlm.nih.gov/pmc/articles/PMC5505594/pdf/40-45.pdf> (Accessed 26 March 2018).

DeWall, R. J. 2013. Ultrasound elastography: principles, techniques, and clinical applications. *Crit Rev Biomed Eng*, 41 (1): 1-19. Available: <https://www.researchgate.net/publication/236062404> (Accessed April 2016).

De Zordo, T., Lill, S. R., Fink, C., Feuchtner, G. M., Jaschke, W., Bellmann-Weiler, R. and Klauser, A. S. 2009. Real-time sonoelastography of lateral epicondylitis: comparison of findings between patients and healthy volunteers. *American Journal of Roentgenology*, 193 (1): 180-185. Available: <http://www.ajronline.org/doi/pdf/10.2214/AJR.08.2020> (Accessed 10 July 2016).

De Zordo, T., Chhem, R., Smekal, V., Feuchtner, G., Reindl, M., Fink, C., Faschingbauer, R., Jaschke, W. and Klauser, A. 2010. Real-time sonoelastography: findings in patients with symptomatic achilles tendons and comparison to healthy volunteers. *Ultraschall in der Medizin-European Journal of Ultrasound*, 31 (04): 394-400. Available: <http://dx.doi.org/10.1055/s-0028-1109809> (Accessed 10 July 2016).

Dirrichs, T., Quack, V., Gatz, M., Tingart, M., Kuhl, C. K. and Schradin, S. 2016. Shear wave elastography (SWE) for the evaluation of patients with tendinopathies. *Academic radiology*, 23 (10): 1204-1213. Available: <http://www.sciencedirect.com/science/article/pii/S1076633216300915> (Accessed 21 September 2016).

Dischler, J. D., Baumer, T. G., Finkelstein, E., Siegal, D. S. and Bey, M. J. 2018. Association between years of competition and shoulder function in collegiate swimmers. *Sports health*, 10 (2): 113-118. Available: <https://journals.sagepub.com/doi/abs/10.1177/194173811772677> (Accessed 8 March 2019).

Dong, Q., Jacobson, J. A., Jamadar, D. A., Girish, G., Morag, Y., Brandon, C. J. and Fessell, D. P. 2015. Sonographic evaluation of subscapularis tendon tears with surgical correlation. *British Journal of Medicine and Medical Research*, 5 (12): 1484-1490. Available: http://www.journalrepository.org/media/journals/BJMMR_12/2014/Nov/Dong5122014BJMMR14500_1.pdf (Accessed 20 July 2017).

Drakonaki, E., Allen, G. and Wilson, D. 2009. Real-time ultrasound elastography of the normal Achilles tendon: reproducibility and pattern description. *Clinical radiology*, 64 (12): 1196-1202. Available: <https://doi.org/10.1016/j.crad.2009.08.06> (Accessed 24 March 2015).

Drakonaki, E., Allen, G. and Wilson, D. 2012. Ultrasound elastography for musculoskeletal applications. *The British journal of radiology*, 85 (1019): Available: <https://www.birpublications.org/doi/pdf/10.1259/bjr/93042867> (Accessed 14 March 2016).

Dresner, M. A., Rose, G. H., Rossman, P. J., Muthupillai, R., Manduca, A. and Ehman, R. L. 2001. Magnetic resonance elastography of skeletal muscle. *Journal of Magnetic Resonance Imaging: An Official Journal of the International Society for Magnetic Resonance in Medicine*, 13 (2): 269-276. Available: <https://onlinelibrary.wiley.com/doi/epdf/10.1002/1522-2586%28200102%2913%3A2%3C269%3A%3AAID-JMRI1039%3E3.0.CO%3B2-1> (Accessed 22 August 2018).

Eby, S. F., Song, P., Chen, S., Chen, Q., Greenleaf, J. F. and An, K.-N. 2013. Validation of shear wave elastography in skeletal muscle. *Journal of biomechanics*, 46 (14): 2381-2387. Available: <http://dx.doi.org/10.1016/j.jbiomech.2013.07.033> (Accessed 29 April 2016).

Edwards, P., Ebert, J., Joss, B., Bhabra, G., Ackland, T. and Wang, A. 2016. Exercise rehabilitation in the non-operative management of rotator cuff tears: a review of the literature. *International journal of sports physical therapy*, 11 (2): 279-301. Available: <https://www.ncbi.nlm.nih.gov/pmc/articles/PMC4827371/pdf/ijsp-11-279.pdf> (Available 26 March 2018).

Ehrenfest, D. M. D., Andia, I., Zumstein, M. A., Zhang, C.-Q., Pinto, N. R. and Bielecki, T. 2014. Classification of platelet concentrates (Platelet-Rich Plasma-PRP, Platelet-Rich Fibrin-PRF) for topical and infiltrative use in orthopedic and sports medicine: current consensus, clinical implications and perspectives. *Muscles, ligaments and tendons journal*, 4 (1):

Available: <https://www.ncbi.nlm.nih.gov/pmc/articles/PMC4049647/pdf/3-9.pdf> (Accessed 14 May 2018).

Encyclopaedia Britannica. Young's modulus 2016. Available: <https://www.britannica.com/science/Youngs-modulus> (Accessed 20 October 2017).

Escamilla, R. F., Hooks, T. R. and Wilk, K. E. 2014. Optimal management of shoulder impingement syndrome. *Open access journal of sports medicine*, 5: 13. Available: <https://www.ncbi.nlm.nih.gov/pmc/articles/PMC3945046/pdf/oajsm-5-013.pdf> (Accessed 20 August 2016).

Filippucci, E., Salaffi, F., Carotti, M. and Grassi, W. 2013. Doppler ultrasound imaging techniques for assessment of synovial inflammation. *RMI*, 2013 (6): 83-91. Available: <http://citeseerx.ist.psu.edu/viewdoc/download?doi=10.1.1.458.9415&rep=rep1&type=pdf> (Accessed (3 February 2016).

Fischer, T., Sack, I. and Thomas, A. 2013. Characterization of focal breast lesions by means of elastography. In: *Proceedings of RöFo-Fortschritte auf dem Gebiet der Röntgenstrahlen und der bildgebenden Verfahren*. © Georg Thieme Verlag KG, 816-82. Available: <https://www.thieme-connect.com/products/ejournals/pdf/10.1055/s-0033-1335939.pdf> (Accessed 15 August 2018).

Franchi-Abella, S., Elie, C. and Correias, J.-M. 2013. Ultrasound elastography: advantages, limitations and artefacts of the different techniques from a study on a phantom. *Diagnostic and interventional imaging*, 94 (5): 497-501. Available: <http://dx.doi.org/10.1016/j.diii.2013.01.024> (Accessed 15 March 2017).

Frisch, C. K. V. 2011. Measuring regional changes in damaged tendon (Order No. 3488583). Available from ProQuest Dissertations & Theses Global. (911044684). Available: <http://search.proquest.com/docview/911044684?accountid=10612> (Accessed 8 July 2016).

Fusini, F., Langella, F., Busilacchi, A., Tudisco, C., Gigante, A., Masse, A. and Bisicchia, S. 2017. Real-time sonoelastography: principles and clinical applications in tendon disorders. A systematic review. *Muscles, ligaments and tendons journal*, 7 (3): 467. Available: <https://www.ncbi.nlm.nih.gov/pmc/articles/PMC5774920/pdf/467-477.pdf>. (Accessed 30 June 2018).

Gaitini, D. 2012. Shoulder ultrasonography: performance and common findings. *Journal of clinical imaging science*, 2. Available: <https://www.ncbi.nlm.nih.gov/pmc/articles/PMC3424700/> (Accessed 8 July 2016).

Galletti, S., Oliva, F., Masiero, S., Frizziero, A., Galletti, R., Schiavone, C., Salini, V. and Abate, M. 2015. Sonoelastography in the diagnosis of tendinopathies: an added value. *Muscles, ligaments and tendons journal*, 5 (4): 325.

Available: <https://www.ncbi.nlm.nih.gov/pmc/articles/PMC4762647/> (Accessed 15 January 2016).

Garra, B. S. 2015. Elastography: history, principles, and technique comparison. *Abdominal imaging*, 40 (4): 680-697. Available: <https://doi.org/10.1007/s00261-014-0305-8> (Accessed 24 June 2017).

Gennisson, J.L., Deffieux, T., Fink, M. and Tanter, M. 2013. Ultrasound elastography: principles and techniques. *Diagnostic and interventional imaging*, 94 (5): 487-495. Available: <https://www.sciencedirect.com/science/article/pii/S2211568413000302> (Accessed 19 January 2016).

Gennisson, J.L. 2016. New parameters in shear wave elastography in vivo. Available: <http://www.mecamat.asso.fr/Aussois/2016/document/TexteGenisson.pdf> (Accessed 1 June 2017).

Greenleaf, J. F. and Urban, M. W. 2016. Shear Wave Elastography Applied for the Investigation of Tendon Material Properties. *Academic radiology*, 23 (10): 1201. Available: <https://doi.org/10.1016/j.acra.2016.07.001> (Accessed 20 June 2017).

Guerini, H., Femand, M., Godefroy, D., Feydy, A., Chevrot, A., Morvan, G., Gault, N. and Drapé, J. 2012. US appearance of partial-thickness supraspinatus tendon tears: Application of the string theory. Pictorial essay. *Journal of ultrasound*, 15 (1): 7-15. Available: <https://doi.org/10.1016/j.jus.2011.12.001> (Accessed 9 July 2016).

Guo, L.P., Wang, W.M., Wang, Y.H., Liu, Y.P., Yu, X.B. and Ma, X.J. 2016. Ultrasound in assessment of supraspinatus tendon injury: correlation with Arthroscopy. *Chinese medical journal*, 129 (3): 361. Available:

<https://www.ncbi.nlm.nih.gov/pmc/articles/PMC4799583/pdf/CMJ-129-361.pdf> (Accessed 18 April 2017).

Gupta, H. and Robinson, P. 2015. Normal shoulder ultrasound: anatomy and technique. In: *Proceedings of Seminars in musculoskeletal radiology*. Thieme Medical Publishers, 203-211. Available: <https://www.thieme-connect.com/products/ejournals/html/10.1055/s-0035-1549315> (Accessed 7 October 2018).

Hackett, L., Aveledo, R., Lam, P. H. and Murrell, G. A. 2019. Reliability of shear wave elastography ultrasound to assess the supraspinatus tendon: An intra and inter-rater in vivo study. *Shoulder & Elbow*: 1758573218819828. Available:

<https://journals.sagepub.com/doi/10.1177/1758573218819828> (Accessed 12 April 2019).

Hatta, T., Giambini, H., Uehara, K., Okamoto, S., Chen, S., Sperling, J. W., Itoi, E. and An, K.-N. 2015. Quantitative assessment of rotator cuff muscle elasticity: reliability and feasibility of shear wave elastography. *Journal of biomechanics*, 48 (14): 3853-3858. Available: <https://onlinelibrary.wiley.com/doi/pdf/10.1002/ca.22498> (Accessed 15 January 2016).

Hawkins, C., Agbaji, O., Placid, U., Thio, C.L., Auwal, M.M., Ani, C., Okafo, C., Wallender, E. and Murphy, R. 2013. Assessment of liver fibrosis by transient elastography in patients with HIV and hepatitis B virus coinfection in Nigeria. *Clinical Infectious Disease*. 57(12):189-192. Available: <https://doi.org/10.1093/cid/cit564> (Accessed 14 August 2016).

Henning, P., Truter, R., Boeyens, M., Andronikou, S. and Suleman, F. E. 2015. Intra-osseous calcifying tendinitis of the infraspinatus tendon with erosion into the greater tuberosity. *SA Orthopaedic Journal*, 14 (3): 43-46. Available: <http://www.scielo.org.za/pdf/saoj/v14n3/05.pdf> (Accessed 4 April 2017).

Hodgson, R.J., O'Connor, P.J. and Grainger, A.J., 2012. Tendon and ligament imaging. *The British journal of radiology* 85(1016): 1157-1172. Available: <http://www.birpublications.org/doi/pdf/10.1259/bjr/34786470> (Accessed 12 March 2016).

Hong, Y., Liu, X., Li, Z., Zhang, X., Chen, M. and Luo, Z. 2009. Real-time ultrasound elastography in the differential diagnosis of benign and malignant thyroid nodules. *Journal of Ultrasound in Medicine*, 28 (7): 861-867. Available: <https://onlinelibrary.wiley.com/doi/epdf/10.7863/jum.2009.28.7.861> (Accessed 3 September 2018).

Hou, S.W., Merkle, A.N., Babb, J.S., McCabe, R., Gyftopoulos, S. and Adler, R.S., 2017. Shear Wave Ultrasound Elastographic Evaluation of the Rotator Cuff Tendon. *Journal of Ultrasound in Medicine*, 36(1):95-106. Available: <http://onlinelibrary.wiley.com/enhanced/exportCitation/doi/10.7863/ultra.15.07041> (Accessed 25 March 2017).

Hoyt, K., Parker, K. J. and Rubens, D. J. 2007. Real-time shear velocity imaging using sonoelastographic techniques. *Ultrasound in medicine & biology*, 33 (7): 1086-1097. Available: [http://www.umbjournal.org/article/S0301-5629\(07\)00044-0/pdf](http://www.umbjournal.org/article/S0301-5629(07)00044-0/pdf) (Accessed 20 October 2016).

Iagnocco, A., Giulio, C., Leone, A. and Guido, V. 2003. Sonographic study of painful shoulder. *Clinical and experimental rheumatology*, 21(3): 355-358. Available: <https://iris.unito.it/retrieve/handle/2318/1613149/268324/184.pdf> (Accessed 20 June 2016).

Ilhanli, I., Tosun, A., Guder, N. and Gul, M. 2015. Savant Journals 2052-1480,1(3)30-34. Available:https://www.researchgate.net/profile/Ilker_Ilhanli/publication/280829978_Predictivity_of_Elastography_for_Supraspinatus_Tears/links/55c850cc08aeb9756746fcdf/Predictivity-of-Elastography-for-Supraspinatus-Tears.pdf (Accessed 4 July 2016).

Inami, T. and Kawakami, Y. 2016. Assessment of individual muscle hardness and stiffness using ultrasound elastography. *The Journal of Physical Fitness and Sports Medicine*, 5 (4): 313-317. Available: https://www.jstage.jst.go.jp/article/jpfsm/5/4/5_313/pdf (Accessed 11 March 2017).

Jacobson, J. A. 2011. Shoulder US: anatomy, technique, and scanning pitfalls. *Radiology*, 260 (1): 6-16. Available: <https://pubs.rsna.org/doi/pdf/10.1148/radiol.11101082> (Accessed May 2016).

Kang, T., Horton, L., Emery, P. and Wakefield, R. J. 2013. Value of ultrasound in rheumatologic diseases. *Journal of Korean medical science*, 28 (4): 497-507. Available: <https://synapse.koreamed.org/Synapse/Data/PDFData/0063JKMS/jkms-28-497.pdf> (Accessed 16 December 2016).

Kaur, K. 2013. Digital image processing in ultrasound images. *International Journal on Recent and Innovation Trends in Computing and Communication*, 1 (4): 388-393. Available: <https://pdfs.semanticscholar.org/f923/56bc1e3b936708fe43a938e75eac8b19a430.pdf> (Accessed 15 March 2017).

Kehl, A. S., Corr, M. and Weisman, M. H. 2016. Enthesitis: new insights into pathogenesis, diagnostic modalities, and treatment. *Arthritis & rheumatology (Hoboken, NJ)*, 68 (2): 312. Available: <https://www.ncbi.nlm.nih.gov/pmc/articles/PMC5195265/pdf/nihms835582.pdf> (Accessed 20 March 2017).

Kijima, H., Minagawa, H., Tomioka, T., Yamada, S., Nozaka, K., Saito, H. and Shimada, Y. 2013. Elasticity of the Coracoacromial Ligament in Shoulders with Rotator Cuff Tears: Measurement with Ultrasound Elastography. *Surgical Science*, 4 (09): 1. Available: http://file.scirp.org/pdf/SS_2013080217055615.pdf (Accessed 28 November 2015).

Klauser, A. S., Miyamoto, H., Tamegger, M., Faschingbauer, R., Moriggl, B., Klima, G., Feuchtner, G. M., Kastlunger, M. and Jaschke, W. R. 2013. Achilles tendon assessed with sonoelastography: histologic agreement. *Radiology*, 267 (3): 837-842. Available: <https://pubs.rsna.org/doi/pdf/10.1148/radiol.13121936> (Accessed 12 April 2016).

Klauser, A.S., Miyamoto, H., Bellmann-Weiler, R., Feuchtner, G.M., Wick, M.C. and Jaschke, W.R., 2014. Sonoelastography: musculoskeletal applications. *Radiology*, 272(3): 622-633. Available: <https://pubs.rsna.org/doi/pdf/10.1148/radiol.14121765> (Accessed 5 April 2016).

Lalitha, P., Reddy, M. C. and Reddy, K. J. 2011. Musculoskeletal applications of elastography: a pictorial essay of our initial experience. *Korean journal of radiology*, 12 (3): 365-375. Available: <https://synapse.koreamed.org/Synapse/Data/PDFData/0068KJR/kjr-12-365.pdf> (Accessed 24th January 2015).

Lavagnino, M., Wall, M. E., Little, D., Banes, A. J., Guilak, F. and Arnoczky, S. P. 2015. Tendon mechanobiology: Current knowledge and future research opportunities. *Journal of Orthopaedic Research*, 33 (6): 813-822. Available: <http://onlinelibrary.wiley.com/doi/10.1002/jor.22871/epdf> (Accessed 20 May 2016).

Lee, M. H., Sheehan, S. E., Orwin, J. F. and Lee, K. S. 2016a. Comprehensive shoulder US examination: a standardized approach with multimodality correlation for common shoulder disease. *Radiographics*, 36 (6): 1606-1627. Available: <https://pubs.rsna.org/doi/pdf/10.1148/rg.2016160030> (Accessed 7 September 2016).

Lee, S.U., Joo, S. Y., Kim, S. K., Lee, S.H., Park, S.R. and Jeong, C. 2016b. Real-time sonoelastography in the diagnosis of rotator cuff tendinopathy. *Journal of shoulder and elbow surgery*, 25 (5): 723-729. Available: <https://doi.org/10.1016/j.jse.2015.10.019> (Accessed 4 November 2016)

Li, G.Y. and Cao, Y. 2017. Mechanics of ultrasound elastography. *Proceedings of the Royal Society A: Mathematical, Physical and Engineering Sciences*, 473 (2199): 20160841. Available: <http://rspa.royalsocietypublishing.org/content/royprsa/473/2199/20160841.full.pdf> (Accessed 20 November 2015).

Lin, Y.-H., Chiou, H.-J., Wang, H.-K., Lai, Y.-C., Chou, Y.-H. and Chang, C.-Y. 2015. Management of rotator cuff calcific tendinosis guided by ultrasound elastography. *Journal of the Chinese Medical Association*, 78 (10): 603-609. Available: <http://dx.doi.org/10.1016/j.jcma.2015.05.006> (Accessed 25 June 2016).

Maganaris, C. N., Chatzistergos, P., Reeves, N. D. and Narici, M. V. 2017. Quantification of internal stress-strain fields in human tendon: unraveling the mechanisms that underlie regional tendon adaptations and mal-adaptations to mechanical loading and the effectiveness of therapeutic eccentric exercise. *Frontiers in physiology*, 8: 91. Available: <https://www.frontiersin.org/articles/10.3389/fphys.2017.00091> (Accessed 2 February 2018).

Marcy, P.Y., Thariat, J. and Lacout, A. 2012. Should we catch the train of shear-wave elastography? *American Journal of Roentgenology*, 198 (6): W624-W625. Available: <https://www.ajronline.org/doi/pdf/10.2214/AJR.11.8078> (Accessed 18 November 2016).

Matthewson, G., Beach, C. J., Nelson, A. A., Woodmass, J. M., Ono, Y., Boorman, R. S., Lo, I. K. and Thornton, G. M. 2015. Partial thickness rotator cuff tears: current concepts. *Advances in orthopedics*, 2015 .Available: Available: <http://dx.doi.org/10.1155/2015/458786> (Accessed 12 August 2016).

Messina, C., Banfi, G., Orlandi, D., Lacelli, F., Serafini, G., Mauri, G., Secchi, F., Silvestri, E. and Sconfienza, L. M. 2015. Ultrasound-guided interventional procedures around the shoulder. *The British journal of radiology*, 89 (1057): 20150372. Available: <https://www.birpublications.org/doi/pdf/10.1259/bjr.20150372> (Accessed 8 April 2018).

Minagawa, H., Yamamoto, N., Abe, H., Fukuda, M., Seki, N., Kikuchi, K., Kijima, H. and Itoi, E. 2013. Prevalence of symptomatic and asymptomatic rotator cuff tears in the general population: from mass-screening in one village. *Journal of orthopaedics*, 10 (1): 8-12. Available: <https://www.sciencedirect.com/science/article/pii/S0972978X13000093> (Accessed 18 June 2016).

Muraki, T., Ishikawa, H., Morise, S., Yamamoto, N., Sano, H., Itoi, E. and Izumi, S.-i. 2015. Ultrasound elastography–based assessment of the elasticity of the supraspinatus muscle and tendon during muscle contraction. *Journal of shoulder and elbow surgery*, 24 (1): 120-126. Available: <http://dx.doi.org/10.1016/j.jse.2014.04.012> (Accessed 10 February 2016).

Mutala, T. M., Ndaiga, P. and Aywak, A. 2016. Comparison of qualitative and semiquantitative strain elastography in breast lesions for diagnostic accuracy. *Cancer Imaging*, 16 (1): 12. Available: <https://cancerimagingjournal.biomedcentral.com/track/pdf/10.1186/s40644-016-0070-8> (Accessed 5 August 2016).

Nader, A., John, G. and Kendall, M. C. 2016. Basics of Ultrasound. *Multimodality Imaging Guidance in Interventional Pain Management*: 25. Available: <https://books.google.co.za/books?hl=en&lr=&id=OWT0DAAQBAJ&oi=fnd&pg=PA25&dq=Nader,+A.,+John,+G.+and+Kendall,+M.+C.+2016.+Basics+of+Ultrasound.+Multimodality+Imaging+Guidance+in+Interventional+Pain+Management&ots=pQWKwNuxyo&sig=OMRW39AHooUYi24Rxej0d65zfJc#v=onepage&q&f=false> (Accessed 4 June 2017).

Naidoo, N., Lazarus, L., Satyapal, K.S., 2016. The Rotator Cuff Footprint: A Cadaveric Study of the Morphometry and Morphology. *Int. J. Morphol*, 34(3): 975-985. Available: <https://www.researchgate.net/publication/309689983> (Accessed 20 April 2017).

Nazarian, L. N., Jacobson, J. A., Benson, C. B., Bancroft, L. W., Bedi, A., McShane, J. M., Miller, T. T., Parker, L., Smith, J. and Steinbach, L. S. 2013. Imaging algorithms for evaluating suspected rotator cuff disease: Society of Radiologists in Ultrasound consensus conference statement. *Radiology*, 267 (2): 589-595.

Available: <https://pubs.rsna.org/doi/pdf/10.1148/radiol.13121947> (Accessed 8 July 2017).

Nordenfur, T. 2013. *Comparison of pushing sequences for shear wave elastography*.). Master of Science Thesis in Medical engineering). KTH technology and Health. Available: <http://www.diva-portal.org/smash/get/diva2:633046/fulltext01.pdf> (Accessed 20 May 2017).

Nowicki, A. and Dobruch-Sobczak, K. 2016. Introduction to ultrasound elastography. *Journal of ultrasonography*, 16 (65): 113. Available: <https://www.ncbi.nlm.nih.gov/pmc/articles/PMC4954857/pdf/JoU-2016-0013.pdf> (Accessed 13 October 2018).

Nwawka, O. K. 2016. Update in musculoskeletal ultrasound research. *Sports health*, 8 (5): 429-437. Available: <http://journals.sagepub.com/doi/abs/10.1177/1941738116664326> (Accessed 24 February 2016)

Nyakoe, D. D. K. 2011. Ultrasound elastography in the evaluation of solid thyroid nodules. University of Nairobi. Available: <https://pdfs.semanticscholar.org/5a4c/fb8ff4ffdb6e63a8e27415e3a74a146863ea.pdf> (Accessed 13 September 2015).

Obuaku Igwe, C. C. (2015). Health inequality in South Africa: a Systematic Review. *African Sociological Review*, 19(2). Available: <https://www.ajol.info/index.php/asr/article/view/132917/122544> (Accessed 2 May 2019).

Ohuegbe, C. I. 2014. Measurement of supraspinatus tendon strain ratio with sonoelastography: an exploratory study. University of Portsmouth. Available: <http://eprints.port.ac.uk/id/eprint/19081> (Accessed 10 May 2016).

Oliveira, P.G., Cruz, M., Ferreira, C., Ruivo, C. and Alves, F.C., 2017. Shoulder ultrasonography: A comprehensive review of scanning technique and normal findings (poster). *European Society of Radiology*. Available: <http://clinicauniversitariaradiologia.pt/epos/ECR2017> (Accessed 7 October 2018).

Ooi, C.C., Malliaras, P., Schneider, M.E., and Connel, D.A. 2014. "Soft, hard or just right?" Applications and limitations of axial – strain sonoelastography and shear wave elastography in the assessment of tendon injuries. *Skeletal Radiol*, (43): 1-12. Available: www.ncbi.nlm.nih.gov/pubmed/23925561 (Accessed 23 February 2016).

Ophir, J., Céspedes, I., Ponnekanti, H., Yazdi, Y. and Li, X. 1991. Elastography: a quantitative method for imaging the elasticity of biological tissues. *Ultrasonic imaging*, 13 (2): 111-134. Available: <http://www.sciencedirect.com/science/article/pii/016173469190079W> (Accessed 20 June 2015).

Palmeri, M. L. and Nightingale, K. R. 2011. What challenges must be overcome before ultrasound elasticity imaging is ready for the clinic? *Imaging in medicine*, 3 (4): 433. Available: <https://www.ncbi.nlm.nih.gov/pmc/articles/PMC3235674/pdf/nihms-341135.pdf> (Accessed 20 November 2015).

Paluch, Ł., Nawrocka-Laskus, E., Wieczorek, J., Mruk, B., Frel, M. and Walecki, J. 2016. Use of ultrasound elastography in the assessment of the musculoskeletal system. *Polish journal of radiology*, 81: 240. Available: <https://www.ncbi.nlm.nih.gov/pmc/articles/PMC4880311/pdf/poljradiol-81-240.pdf> (Accessed 28 June 2016).

Park, S.I., Choi, Y.K., Lee, J.H. and Kim, Y.-M. 2013. Effects of shoulder stabilization exercise on pain and functional recovery of shoulder impingement syndrome patients. *Journal of physical therapy science*, 25 (11): 1359-1362. Available: https://www.jstage.jst.go.jp/article/jpts/25/11/25_jpts-2013-108/_pdf/-char/ja (Accessed 7 October 2016).

Peltz, C., Haladik, J., Divine, G., Siegal, D., Van Holsbeeck, M. and Bey, M. 2013. ShearWave elastography: repeatability for measurement of tendon stiffness. *Skeletal radiology*, 42 (8): 1151-1156. Available: <https://link.springer.com/article/10.1007/s00256-013-1629-0> (Accessed 14 April 2016).

Qiu, W., Wang, C., Li, Y., Zhou, J., Yang, G., Xiao, Y., Feng, G., Jin, Q., Mu, P., Qian, M. and Zheng, H., 2015. A scanning-mode 2D shear wave imaging (s2D-SWI) system for ultrasound elastography. *Ultrasonics*, 62:89-96.

Available: <http://dx.doi.org/10.1016/j.ultras.2015.05.005> (Accessed 25 November 2016).

Rahman, M. M., Islam, M., Nargis, M., Sarker, S. C., Hasan, M. J., Quddush, A. R. and Sen, S. 2013. Ultrasound elastography applications. *Community Based Medical Journal*, 2 (1): 76-85. Available: <http://dx.doi.org/10.3329/cbmj.v2i1.14191> (Accessed 25 May 2015).

Rajabally, N. 2017. New non-invasive scan for liver disease. Mediclinic. The future of healthcare (blog). Available: <https://www.thefutureofhealthcare.co.za/liverscan/> (Accessed 4 June 2018).

Redondo-Alonso, L., Chamorro-Moriana, G., Jiménez-Rejano, J. J., López-Tarrida, P. and Ridao-Fernández, C. 2014. Relationship between chronic pathologies of the supraspinatus tendon and the long head of the biceps tendon: systematic review. *BMC musculoskeletal disorders*, 15 (1): 377. Available: <https://bmcmusculoskeletdisord.biomedcentral.com/track/pdf/10.1186/1471-2474-15-377> (Accessed 13 October 2016).

Riente, L., Delle Sedie, A., Filippucci, E., Iagnocco, A., Sakellariou, G., Talarico, R., Carli, L., Di Geso, L., Fulvia, C. and Bombardieri, S. 2013. Ultrasound imaging for the rheumatologist XLV. Ultrasound of the shoulder in psoriatic arthritis. *Clin Exp Rheumatol*, 31 (3): 329-333.

Available: <https://aperto.unito.it/retrieve/handle/2318/1613271/266963/52.pdf> (Accessed 21 September 2017).

Roskopf, A. B., Ehrmann, C., Buck, F. M., Gerber, C., Flück, M. and Pfirrmann, C. W. 2015. Quantitative shear-wave US elastography of the supraspinatus muscle: reliability of the method and relation to tendon integrity and muscle quality. *Radiology*, 278 (2): 465-474. Available: <http://pubs.rsna.org/doi/pdf/10.1148/radiol.201515090> (Accessed 11 September 2016).

Ryu, J. and Jeong, W. K. 2017. Current status of musculoskeletal application of shear wave elastography. *Ultrasonography*, 36 (3): 185-187.

Available: <https://www.ncbi.nlm.nih.gov/pmc/articles/PMC5494870/pdf/usg-16053.pdf> (Accessed 24 May 2017).

Sahan, M. H., Inal, M., Burulday, V. and Kultur, T. 2018. Evaluation of tendinosis of the long head of the biceps tendon by strain and shear wave elastography. *Medical ultrasonography*, 20 (2): 192-198. Available:

<https://www.medultrason.ro/medultrason/index.php/medultrason/article/view/1323/1235> (Accessed 27 January 2019).

Saltykova, V. 2013. Shear Wave Elastography in diagnostics of supraspinatus tendon. In: Proceedings of European Congress of Radiology (poster) 2013.

Available: <http://dx.doi.org/10.1594/ecr2013/C-2168> (Accessed 10 October 2016).

Sarvazyan, A. P., Urban, M. W. and Greenleaf, J. F. 2013. Acoustic waves in medical imaging and diagnostics. *Ultrasound in medicine & biology*, 39 (7): 1133-1146. Available: <http://dx.doi.org/10.1016/j.ultrasmedbio.2013.02.006> (Accessed 30 June 2015).

Sconfienza, L. M., Silvestri, E. and Cimmino, M. A. 2010. Sonoelastography in the evaluation of painful Achilles tendon in amateur athletes. *Clin Exp Rheumatol*, 28 (3): 373-378. Available: <https://www.clinexprheumatol.org/article.asp?a=639> (Accessed 11 August 2016).

Screen, H.R., Berk, D.E., Kadler, K.E., Ramirez, F. and Young, M.F., 2015. Tendon functional extracellular matrix. *Journal of Orthopaedic Research*, 33(6): 793-799. Available: <http://onlinelibrary.wiley.com/doi/10.1002/jor.22818/epdf> (Accessed 25 July 2017).

Seo, J.B., Yoo, J.S. and Ryu, J.W. 2014. Sonoelastography findings of biceps tendinitis and tendinosis. *Journal of ultrasound*, 17 (4): 271-277.

Available: <https://doi.org/10.1007/s40477-014-0075-8> (Accessed 16 April 2017).

Sessions, W. C., Lawrence, R. L., Steubs, J. T., Ludewig, P. M. and Braman, J. P. 2017. Thickness of the Rotator Cuff Tendons at the Articular Margin: An Anatomic Cadaveric Study. *The Iowa orthopaedic journal*, 37: 85.

Available: https://www.ncbi.nlm.nih.gov/pmc/articles/PMC5508269/pdf/IOJ_2017_85.pdf (Accessed 6 November 2018).

Sheng, J.-M. 2013. Rotator cuff tendons of the shoulder joint: anatomy and investigation of strain profile. Doctor of Philosophy. Nanyang Technological University. Available: <https://dr.ntu.edu.sg/handle/10356/53504> (Accessed 12 October 2016).

Shiina, T., Nightingale, K. R., Palmeri, M. L., Hall, T. J., Bamber, J. C., Barr, R. G., Castera, L., Choi, B. I., Chou, Y.-H. and Cosgrove, D. 2015. WFUMB guidelines and recommendations for clinical use of ultrasound elastography: Part 1: basic principles and terminology. *Ultrasound in medicine & biology*, 41 (5): 1126-1147. Available: <http://dx.doi.org/10.1016/j.ultrasmedbio.2015.03.009> (Accessed 15 September 2016).

Shin, H. J., Kim, M.-J., Kim, H. Y., Roh, Y. H. and Lee, M.-J. 2016. Comparison of shear wave velocities on ultrasound elastography between different machines, transducers, and acquisition depths: a phantom study. *European radiology*, 26 (10): 3361-3367. Available: <https://doi.org/10.1007/s00330-016-4212-y> (Accessed 14 January 2017).

Sikdar, S., Wei, Q. and Cortes, N. 2014. Dynamic ultrasound imaging applications to quantify musculoskeletal function. *Exercise and sport sciences reviews*, 42 (3): 126.-135 Available: <https://www.ncbi.nlm.nih.gov/pmc/articles/PMC4066199/pdf/nihms-572889.pdf> (Accessed 20 April 2016).

Simic, M. 2012. Shear wave ultrasound elastography: from physics to future. In: Proceedings of. European Congress of Radiology 2012. Available: <http://dx.doi.org/10.1594/ecr2012/C-1868> (Accessed 13 April 2017).

Singh, J. P. 2012. Shoulder ultrasound: what you need to know. *The Indian journal of radiology & imaging*, 22 (4): 284. Available: <https://www.ncbi.nlm.nih.gov/pmc/articles/PMC3698891/> (Accessed 3 April 2016).

Song, P.F. 2014. Innovations in Ultrasound Shear Wave Elastography. Doctor of philosophy in Biomedical Sciences. Mayo Clinic College of Medicine.

Available: <https://www.researchgate.net/publication/27503323> (Accessed 4 March 2016).

Srinivasan, S. and Dubey, N. 2011. Re: Musculoskeletal applications of elastography: a pictorial essay of our initial experience. *Korean journal of radiology*, 12 (5): 646-647. Available: <https://synapse.koreamed.org/pdf/10.3348/kjr.2011.12.5.646> (Accessed 17 April 2015).

Strode, A., Slack, C. and Essack, Z. 2010. Child consent in South African law: Implications for researchers, service providers and policy-makers. *South African Medical Journal*, 100 (4): 247-249. Available: <http://dx.doi.org/10.7196/SAMJ.3609> (Accessed 15 July 2016).

Tagg, C. E., Campbell, A. S. and McNally, E. G. 2013. Shoulder impingement. In: *Proceedings of Seminars in musculoskeletal radiology*. Thieme Medical Publishers, 003-011. Available: <https://www.thieme-connect.com/products/ejournals/pdf/10.1055/s-0033-1333908.pdf> (Accessed 2 May 2017).

Takenaga, T., Sugimoto, K., Goto, H., Nozaki, M., Fukuyoshi, M., Tsuchiya, A., Murase, A., Ono, T. and Otsuka, T. 2015. Posterior shoulder capsules are thicker and stiffer in the throwing shoulders of healthy college baseball players: a quantitative assessment using shear-wave ultrasound elastography. *The American journal of sports medicine*, 43 (12): 2935-2942. Available: <http://ajs.sagepub.com/content/43/12/2935> (Accessed 15 May 2017)

Taljanovic, M. S., Gimber, L. H., Becker, G. W., Latt, L. D., Klauser, A. S., Melville, D. M., Gao, L. and Witte, R. S. 2017. Shear-wave elastography: basic physics and musculoskeletal applications. *Radiographics*, 37 (3): 855-870. Available: <https://pubs.rsna.org/doi/pdf/10.1148/rg.2017160116> (Accessed 5 October 2018).

Tamborrini, G., Möller, I., Bong, D., Miguel, M., Marx, C., Müller, A. M. and Müller-Gerbl, M. 2017. The rotator interval—A link between anatomy and ultrasound. *Ultrasound international open*, 3 (03): E107-E116. Available: <https://www.thieme-connect.com/products/ejournals/pdf/10.1055/s-0043-110473.pdf> (Accessed 15 September 2018).

Thomas, A., Fischer, T., Frey, H., Ohlinger, R., Grunwald, S., Blohmer, J. U., Winzer, K. J., Weber, S., Kristiansen, G. and Ebert, B. 2006. Real-time elastography-an advanced method of ultrasound: first results in 108 patients with breast lesions. *Ultrasound in Obstetrics and Gynecology: The Official Journal of the International Society of Ultrasound in Obstetrics and Gynecology*, 28 (3): 335-34. Available: <https://obgyn.onlinelibrary.wiley.com/doi/epdf/10.1002/uog.2823> (Accessed 15 August 2018).

Trent, E. 2013. Assessment and characterization of insitu rotator cuff biomechanics. Masters of science Bioengineering. Clemson University. Available: http://tigerprints.clemson.edu/all_theses (Accessed 8 February 2016). Available: <https://obgyn.onlinelibrary.wiley.com/doi/epdf/10.1002/uog.2823> (Avaliable: 15 August 2018).

Tudisco, C., Bisicchia, S., Stefanini, M., Antonicoli, M., Masala, S. and Simonetti, G., 2015. Tendon quality in small unilateral supraspinatus tendon tears. Real-time sonoelastography correlates with clinical findings. *Knee Surgery, Sports Traumatology, Arthroscopy*,

23(2):393-398. Available: <http://link.springer.com/article/10.1007/s00167-013-2551-7> (Accessed 11 January 2016).

Van Zuydam, J., van Rensburg, D. J., Grant, C. C., van Rensburg, A. J. and Patricios, J. 2015. Shouldering the blame for impingement: the rotator cuff continuum. *South African Family Practice*, 57 (1): 34-38.

Available: <https://www.ajol.info/index.php/safp/article/view/114679/10434> (Accessed 28 March 2017).

Wang, L., Chen, S., An, K.N., Yang, H.L. and Luo, Z.P., 2013. Theoretical prediction of ultrasound elastography for detection of early osteoarthritis. *The Scientific World Journal*, 2013: 106. Article ID 5657151-6. Available:

<http://dx.doi.org/10.1155/2013/565717> (Accessed 14 April 2017).

Washburn, N., Onishi, K. and Wang, J. H. 2018. Ultrasound elastography and ultrasound tissue characterisation for tendon evaluation. *Journal of orthopaedic translation*, 15: 9-20.

Available: <https://www.sciencedirect.com/science/article/pii/S2214031X18300238> (Accessed 20 January 2019).

Weinreb, J. H., Sheth, C., Apostolakos, J., McCarthy, M.B., Barden, B., Cote, M. P. and Mazzocca, A. D. 2014. Tendon structure, disease, and imaging. *Muscles, ligaments and tendons journal*, 4 (1): 66-73.

Available: <http://www.ncbi.nlm.nih.gov/pmc/articles/PMC4049653/> (Accessed 12 April 2015).

Winn, N., Lalam, R. and Cassar-Pullicino, V. 2016. Sonoelastography in the musculoskeletal system: Current role and future directions. *World journal of radiology*, 8 (11): 868.

Available: <https://www.ncbi.nlm.nih.gov/pmc/articles/PMC5120246/> (Accessed 7 May 2017).

Wright, R. 2016. How long does it take for ibuprofen to leave ones system? 3 December.

Available: <https://www.healthtap.com/topics/how-long-does-ibuprofen-take-to-leave-your-system>. (Accessed 3 December 2016).

Wu, C.H., Chen, W.S., Park, G.Y., Wang, T.G. and Lew, H. L. 2012. Musculoskeletal sonoelastography: a focused review of its diagnostic applications for evaluating tendons and fascia. *Journal of Medical Ultrasound*, 20 (2): 79-86. Available:

<https://www.sciencedirect.com/science/article/pii/S0929644112000318> (Accessed 29 December 2018).

Yoon, S., Seo, J.-B., Yoo, J.-S. and Ryu, J.-W. 2014. Diagnostic Consistency between Sonoelastography and Conventional Sonography of Long Head of the Biceps.

대한건축관절학회지, 17 (3): 107-113. Available:

<http://dx.doi.org/10.5397/cise.2014.17.3.107> (Accessed 24 March 2017).

Zaleska-Dorobisza, U., KaczorowskiB, K., PawluśB, A., PuchalskaB, A. and InglotB, M. 2013. Ultrasound elastography–review of techniques and its clinical applications. *brain*, 6: 10-14. Available: <http://www.advances.umed.wroc.pl/pdf/2014/23/4/645.pdf> (Accessed 27 August 2016).

APPENDICES

APPENDIX 1A: PERMISSION FROM DIRECTOR OF RADIOLOGY

Dr P.V.Moodley
Radiology Director
Mount Edgecombe Hospital
163 Redbury Rd
Phoenix
4068

Dear Dr P.V.Moodley

REQUEST FOR PERMISSION TO CONDUCT STUDY

I am currently registered as a Masters student at the Durban University of Technology in the Department of Radiography. I would like to embark on a research project towards a Master's degree in Ultrasound. I have already obtained a National Diploma in Radiography (Diagnostic), a Higher Education Diploma and a B. Tech in Radiography (Ultrasound).

The proposed title of my project is: **Shear wave ultrasound elastography of the shoulder joint tendons**. The aim of this study is to therefore assess the biomechanics of the rotator cuff and biceps tendons of the shoulder joint in asymptomatic participants, in order to establish a reference range for use in clinical practice. The study will include 260 asymptomatic participants aged between 21-45 years. Identities of the participants will remain confidential. I plan to commence the data collection in July 2017 and complete the process by January 2018. This study will be conducted in collaboration with a senior radiologist. I strongly believe that this study will benefit both ultrasonographers and radiologists in terms of new techniques used to achieve optimal sonographic imaging. The early detection of rotator cuff disease may improve patient management.

I am currently employed as a senior sonographer in the radiology practice and would therefore like to utilize the site for the proposed study. The ultrasound unit is equipped with a shear wave modality. The radiology practice is accredited by the Health Professions Council of South Africa. I intend selecting 260 participants from the Northwest region of KwaZulu Natal for this study. This study is not structured to alter the course of protocol or procedure in any way and will not incur any additional cost to the patient or hospital.

I hereby apply for permission to undertake this study in the radiography practice of this hospital following the approval of the director of the radiology department and the unit manager. Permission is also required to place advertisements or flyers on the notice boards of the hospital, including community centres and shopping centres in the Northwest region of KwaZulu Natal. The current proposal has been reviewed and approved by the Department of Radiography, Research and Higher Degrees committee of the Faculty of Health Sciences, at the Durban University of Technology. Ethical approval has been obtained from the Institutional Research Ethics Committee (IREC 73/11).

My research proposal is attached for your perusal. Your support and permission (in writing) to perform this study at Mount Edgecombe Hospital, radiology practice, will be greatly appreciated.

Yours sincerely

Harashalata Ramdev

Senior sonographer

Radiology Department

Jackpersad and Partners Inc

1. Student name: Harashalata Ramdev email:lataramdev@hotmail.com. Phone no: 0834616575

2. Supervisor: Dr Nalini Govender on 031 373 2796.

APPENDIX 1B: PERMISSION GRANTED FROM DIRECTOR OF RADIOLOGY



**JACKPERSAD
& PARTNERS INC.**
SPECIALIST DIAGNOSTIC
RADIOLOGISTS

3rd Floor Maxwell Centre
71/73 Ismail C Meer St (Lorne St), Durban
Tel : 031-365 2100
Fax : 031-365 2199
E-mail: info@jrp.co.za
www.jackpersad.co.za

17 March 2016

The Research Committee
Faculty of Health Sciences
DUT
Durban
4000

Dear Sir/ Madam

Re: Permission to conduct Study at Jackpersad and Partners Inc

Permission is hereby granted to Ms Harashalata Ramdev to conduct her research at our premises in support of her research project. All efforts will be made to ensure that she has access to all the necessary resources which will benefit her research.

Harashalata will have the full support of the practice during her term of study.

Should you have any queries please do not hesitate to contact me on, hr@jrp.co.za

Yours Faithfully

Jenny Bux
Human Resources Manager

DR RS Ballaram
MBCHB. (Natal) FFRAD (D)
SA

DR KD Daji
MBCHB. (Natal) FFRAD (D)
SA

DR VV Moodley
MBCHB. (Medunsa) FCRAD
(D) SA

DR I Hansrod
BSC (UCT), MBChB (WITS),
FCRAD (D) (SA)

DR RC Hurribunce
MBCHB. (Natal) FFRAD (D) SA

DR I Govender
MBCHB. (Medunsa) FCRAD (D)
SA

DR A Vanmali
MBCHB. (Natal) FCRAD (D) SA

DR BK Kassim
MBCHB. (Natal) FFRAD (D) SA

DR F Lockhat
MBCHB. (Natal) FCRAD (D) SA

DR IG Moodley
MBCHB. (Medunsa) FCRAD (D)
SA
FINR(SWITZERLAND)

DR PV Moodley
MBCHB. (Natal) FCRAD(D) SA

DR K Pillay
MBCHB. (Medunsa) FCRAD (D)
SA

DR M Naidoo
MBCHB. (Natal) FFRAD (D) SA
MSL (UNISA)

DR S Panday
MBCHB. (Natal) DCH (SA)
FCRAD (D) SA

DR HJ Ramjee
MBCHB. (Natal) FCRAD (D) SA

DR M Singh
MBChB. (Natal) FFRAD (D)
SA

DR ME Vayej
DMT (Clin. Path) (SA)
MBChB. (Natal) DCH (SA)
FFRAD (D) SA

DR M Pillay
MBCHB. (Medunsa) FCRAD
(D) SA

Practice No. 3804917 Co.Reg 2007/027164/21

APPENDIX 1C: PERMISSION GRANTED FROM DIRECTOR OF RADIOLOGY AT COMMENCEMENT OF RESEARCH



**JACKPERSAD
& PARTNERS INC.**
SPECIALIST DIAGNOSTIC
RADIOLOGISTS

3rd Floor Maxwell Centre
71/73 Ismail C Meer St (Lorne St), Durban
Tel : 031-365 2100
Fax : 031-365 2199
E-mail: info@jrp.co.za
www.jackpersad.co.za

16 October 2017

The Research Committee
Faculty of Health Sciences
DUT
Durban
4000

Dear Sir/Madam

Re. Permission to conduct research project at Jackpersad & Partners Inc.

This letter is to confirm that permission was granted to Ms Harashalata Ramdev, employee number 302, to conduct her research at Jackpersad & Partners premises in order to fulfill requirements for her Masters degree in Ultrasound. The original letter granting permission is attached for reference.

We can once again confirm that Harashalata will have the full support of the practice during her term of study, including for her research project which will be conducted on site in the Mount Edgecombe hospital radiography department.

Please contact me if you require any further confirmation.

Yours Sincerely


Gemma Ryan
Human Resources Manager

DR RS Ballaram
MBChB. (Natal) FFRAD (D) SA

DR RC Hurribunce
MBChB. (Natal) FFRAD (D) SA

DR F Lockhat
MBChB. (Natal) FCRAD (D) SA

DR M Naidoo
MBChB. (Natal) FFRAD (D) SA
MBL (UNISA)

DR M Singh
MBChB. (Natal) FFRAD (D) SA

DR KD Daji
MBChB. (Natal) FFRAD (D) SA

DR I Govender
MBChB. (Medunsa) FCRAD (D) SA

DR IG Moodley
MBChB. (Medunsa) FCRAD (D) SA
FINR(SWITZERLAND)

DR S Panday
MBChB. (Natal) DCH (SA)
FCRAD (D) SA

DR ME Vayej
DMT (Clin. Path) (SA)
MBChB. (Natal) DCH (SA)
FFRAD (D) SA

DR VV Moodley
MBChB. (Medunsa) FCRAD (D) SA

DR A Vanmali
MBChB. (Natal) FCRAD (D) SA

DR PV Moodley
MBChB. (Natal) FCRAD(D) SA

DR HJ Ramjee
MBChB. (Natal) FCRAD (D) SA

DR M Pillay
MBChB. (Medunsa) FCRAD (D) SA

DR I Hansrod
BSC (UCT), MBChB (WITS),
FCRAD (D) (SA)

DR BK Kassim
MBChB. (Natal) FFRAD (D) SA

DR K Pillay
MBChB. (Medunsa) FCRAD (D) SA

Practice No. 3804917 Co.Reg 2007/027164/21

APPENDIX 2: PERMISSION GRANTED FROM INSTITUTIONAL RESEARCH ETHICS COMMITTEE (IREC)

		<p>Institutional Research Ethics Committee Research and Postgraduate Support Directorate 2nd Floor, Berwyn Court Gate 1, Steve Biko Campus Durban University of Technology</p> <p>P O Box 1334, Durban, South Africa, 4001</p> <p>Tel: 031 373 2375 Email: lavishad@dut.ac.za http://www.dut.ac.za/research/institutional_research_ethics www.dut.ac.za</p>
<p>30 October 2017</p>		
<p>IREC Reference Number: REC 73/17</p>		
<p>Ms H Ramdev 11 Gildcroft Close Unit 8 Phoenix Durban 4001</p>		
<p>Dear Ms Ramdev</p>		
<p>Shear wave ultrasound elastography of the shoulder joint tendons</p>		
<p>The Institutional Research Ethics Committee acknowledges receipt of your gatekeeper permission letters.</p>		
<p>Please note that Full Approval is granted to your research proposal. You may proceed with data collection.</p>		
<p>Any adverse events [serious or minor] which occur in connection with this study and/or which may alter its ethical consideration must be reported to the IREC according to the IREC SOP's.</p>		
<p>Please note that any deviations from the approved proposal require the approval of the IREC as outlined in the IREC SOP's.</p>		
<p>Yours Sincerely,</p>		
<p>Professor J K Adam Chairperson: IREC</p>		
 <p>2017-10-30</p> <p>INSTITUTIONAL RESEARCH ETHICS COMMITTEE P O BOX 1334 DURBAN 4000 SOUTH AFRICA</p>		

APPENDIX 3A: REQUEST FOR PERMISSION FROM HOSPITAL MANAGER

Mrs Bhavishka Maharaj
Hospital Manager
Mount Edgecombe Hospital
163 Redberry Rd, Phoenix
4068

Dear Mrs Maharaj

REQUEST FOR PERMISSION TO CONDUCT STUDY

I hereby wish to request permission to advertise flyers on the hospital notice boards for recruitment of asymptomatic participants into my study. I am currently registered for a Master's degree in Ultrasound in the Department of Radiography, Durban University of Technology. My current qualifications include a National Diploma in Radiography (Diagnostic), a Higher Education Diploma and a B. Tech in Radiography (Ultrasound).

The proposed title of my project is: **Shear wave ultrasound elastography of the shoulder joint tendons**. The aim of this study is to therefore assess the biomechanics of the rotator cuff and biceps tendons of the shoulder joint in asymptomatic participants, in order to establish a reference range for use in clinical practice. The study will include 260 asymptomatic participants aged 21-45 years. Identities of the participants will remain confidential. I plan to commence the data collection in July 2017 and complete the process by January 2018. This study will be conducted in collaboration with a senior radiologist. I strongly believe that this study will benefit both ultrasonographers and radiologists in terms of new techniques used to achieve optimal sonographic imaging. The early detection of rotator cuff disease may improve patient management.

I am currently employed as a senior sonographer in the radiology practice and therefore would like to utilize the radiology site for the proposed study. The ultrasound unit is equipped with a shear wave modality. The radiology practice is accredited by the Health Professions Council of South Africa. I intend selecting 260 participants from the Northwest region of KwaZulu Natal for this study. This study is not structured to alter the course of protocol or procedure in any way and will not incur any additional cost to the patient or hospital. Only asymptomatic participants will be allowed to participate in this study.

My research proposal together with information letters to the participants and consent forms (see attached appendices) are attached for your perusal. Permission is therefore required to place advertisements or flyers on the notice boards of Mount Edgecombe Hospital, Durban, Kwazulu Natal. Prior permission was requested from the radiology practice (Appendix 1B) before the commencement of my research proposal. The current proposal has been reviewed and approved by the Department of Radiography, Research and Higher Degrees committee of the Faculty of Health Sciences, and the Institutional Research Ethics Committee (IREC), Durban University of Technology. Provisional IREC approval has been obtained from the Institutional Research Ethics Committee (IREC 73/17; Appendix 2). However, full approval will only be granted once gatekeepers' permission is obtained from the hospital, in order to commence the study.

I would therefore be most grateful if permission is granted to place flyers on the notice board of Mount Edgecombe hospital.

Thanking you in advance for your support and co-operation.

Yours sincerely

Harashalata Ramdev

Supervisor: Dr Nalini Govender on 031-373 2796/0842582795; Co-supervisor: Mrs Zombuso Cynthia Dlodla on 0765995836.

APPENDIX 3B: PERMISSION GRANTED FROM HOSPITAL MANAGER

Maharaj,Bhaviksha <Bhaviksha.Maharaj@lifehealthcare.co.za>



Reply

Today, 09:37 AM

You;

Fatima Farouk (vmmte@jrp.co.za);

Beckerling,Sandra (Sandra.Beckerling@lifehealthcare.co.za)

You replied on 2017-10-20 09:53 AM.

Great thanks

Lata please proceed with the flyers – please engage with Sandra Beckerling in terms of the placement

Kind regards

Bhaviksha Maharaj

Hospital Manager

Life Mount Edgemcombe Hospital

Life Mount Edgemcombe Hospital, 163 - 179 Redberry Road, Rockford, Phoenix, 4068

PO Box 204, Mount Edgemcombe, 4300

Tel: 031 537 4200

Cell: 083 776 6484

Fax: 031 502 1204

Email: bhaviksha.maharaj@lifehealthcare.co.za

Website: www.lifehealthcare.co.za

From: Fatima Farouk [mailto:vmmte@jrp.co.za]

Sent: Friday, 20 October 2017 9:36 AM

To: Maharaj,Bhaviksha

Cc: Lataramdev@hotmail.com

Subject: Re: Permission to place flyers on noticeboard of hospital

Hi

Thank you so much for the feedback. Lata really appreciates this approval.

We accept the flyer. There are no concerns as it has been approved by the DUT Research Ethics Committee and our Company is also aware of this research.

Kind Regards

Bhaviksha Maharaj

Hospital Manager

Life Mount Edgemcombe Hospital

APPENDIX 4A: LETTER OF INFORMATION IN ENGLISH



LETTER OF INFORMATION

Dear participant

I wish you a warm welcome and would like to thank you for taking the time to take part in this ultrasound study of the shoulder.

Title of Research study: Shear wave ultrasound elastography of the shoulder joint tendons.

Principal Researcher: Harashalata Ramdev (BTech Ultrasound)

Supervisor: Dr Nalini Govender (PhD). **Co- supervisor:** Ms. Zombuso Cynthia Dlodla -MEd (HE).

Brief Introduction and Purpose of the Study: The aim of this study is to establish a set of values of the specific tendons (rotator cuff and biceps tendon) found in your shoulder using an ultrasound technique called shear wave ultrasound elastography. This study will be done on participants who do not have shoulder pain. Normally, the shoulder is examined using B-mode ultrasound. However, in this study, we will use an additional ultrasound technique called shear wave ultrasound elastography in order to assist in identifying problems related to the shoulder joint.

Outline of the Procedures: This study will take place in the private radiology department. You will only be included in the study if you are aged between 21-45 years and you are not on any steroids or anti-inflammatory medication within the last 24 hours. Your acceptance in the study will occur once you have read and understood this letter of information and signed the Informed Consent. Once you are accepted, a participant code will be given to you to maintain confidentiality and prevent disclosure of any of your personal details. During your first meeting you will have to provide general details such as gender (male or female), age, weight, height, race, how active you are and your medical history. Once this information is gathered, you will be asked to come into the examination room to do the scan. A water based gel will be applied to the shoulder and ultrasound pictures will be taken using a probe which will be gently moved over the shoulder. Shear wave ultrasound elastography will be used to measure how soft or hard the tendons are. The study will take about 30 minutes to finish once you give permission.

Risks or discomforts to the Participant: You will not experience any discomfort during the ultrasound examination. You may be asked to limit movement of your arm if you experience any pain.

Benefits: This study aims to help people who have shoulder problems and may help the referring health care professionals to treat shoulder problems earlier to any major problems occurring.

Reason/s why the Participant May Be Withdrawn from the Study: As a voluntary participant in this study, you are free to withdraw from this study at any time, without giving a reason. You may also be withdrawn from the study if you do not meet your appointment times.

Remuneration: There is no remuneration for taking part in this study.

Costs of the Study: There is no cost for taking part in this study. All scans will be done free of charge.

Confidentiality: Your confidentiality will be maintained throughout the research process through the use of participant codes that will not reveal your personal details. The results of this study will be used for research purpose only. All information collected will be destroyed after a period of five years.

Research - related Injury: There are no risks involved in this study.

Please contact the following people if you have any concerns or queries:

Researcher: Harashalata Ramdev (0834616575)

Supervisor: Dr Nalini Govender (031 373 2796)

Co-Supervisor: Ms. Zombuso Cynthia Dlodla (0765995836) or

the Institutional Research Ethics administrator on 031 373 2900.

Complaints can be reported to the DVC: TIP, Prof F. Otieno on 031 373 2382 or dvctip@dut.ac.za

APPENDIX 4B: LETTER OF INFORMATION IN ISIZULU



INCWADI SA IMININGWANE

Mhlanganyeli othandekayo

Ngifisa ukukwemukela ngezandla ezifudumele futhi ngithanda nokukubonga ngokuthatha isikhathi ngokubamba iqhaza kulolu cwaningo lwe ultrasound yehlombe.

Isihloko Socwaningo: Ukuhlolwa kwemisipha yehlombe (rotator cuff and biceps) usebenzisa uhlobo lwe ultrasound ebizwa nge-elastography.

Umcwaningi Omkhulu: Harashalata Ramdev((BTech Ultrasound)

Umphathi : Dr Nalini Govender (PhD).

Umphathi ngokubambisana:Ms. Zombuso Cynthia Dlodla -MEd (HE).

Isingeniso esifushane Nenjongo yocwaningo: Inhloso yalolu cwaningo ukubona kahle iqoqo lemisipha ethize (rotator cuff and biceps) etholakala ehlobo lakho usebenzisa uhlobo lwe ultrasound ebizwa nge elastography. Lolu cwaningo luzokwenziwa kubantu kwabangenabo ubuhlungu behlombe. Ngokuvamile ucwaningo lwehlobo lwenziwa ngokusebenzisa i B-mode ultrasound. Nokho, kulolu cwaningo, sizosebenzisa enye indlela eyengeziwe yokucwaninag nge ultrasound elastography ukusiza ekuboneni izinkinga ezihlobene nehlombe.

Uhlaka lwezinqubo: Lolu cwaningo luzokwenzeka kuMnyango yangasese ye Radiology. Uzothola ukubandakanywa kulolucwaningo uma uneminyaka ephakathi kwengu 21 kuya ku45 futhi ungeyena usebenzisa noma iluphi uhlobo lwezikhuthazi (steroids) noma imithi ethile eqeda ukuvuvukala ngaphakathi esikhathini esingamahora angu 24. Ukwamukelwa kulolu cwaningo kuzokwenzeka uma usufundile waqonda le ncwadi yolwazi futhi wasayina nemvume yokuthi unolwazi. Uma sewemukelwe kulolucwaningo, uzonikezwa ikhodi njengomhlanganyeli ukuze kugcineke imfihlo futhi kuvimbele ukuvezwa noma iyiphi imininingwane yakho siqu. Emhlanganweni wenu wokuqala kuzodingeka ukuba unikeze imininingwane jikelele efana nobulili (owesilisa noma owesifazane), ubudala, isisindo, ubude, uhlanga, indlela esebenzisa umzimba ngayo kanye nomlando wakho wezokwelashwa. Uma lolu lwazi seluthathiwawe, uzocelwa ukuba ungene endlini yokucwaninga nge scan. Kuzosetshenziswa i gel engamanzi ehlobo bese kuthathwa izithombe ze ultrasound sisebenzisa uphenyo oluzokwenziwa ngobumnene phezu kwe ehlobo. I ultrasound elastography izosetshenziswa ukukala ukuthamba noma ukuqina kwemisipha esehlombe.Lolu cwaningo luzothatha cishe imizuzu engu-30 ukuqeda ucwaningo uma usunikezile imvume.

Izingozi noma ukungaphatheki kahle okubangelwa ukumba iqhaza kulolucwaningo: Ngeke uhlangabezane nokungakhululeki ngesikhathi socwaningo lwe ultrasound. Ungacelwa ukuthi ubeke umkhawulo wokunyakaza ingalo yakho uma uhlangabezana nobuhlungu.

Izinzuzo: Lolu cwaningo luhlose ukusiza abantu abanezinkinga ehlobo, kungasiza oqondene nokunakekelwa kwezempilo ukwelapha izinkinga ehlobo ngaphambi kokuba izinkinga ezinkulu zenzeke.

Izizathu ezingadala ukuthi umbambiqhaza akhishwe kulolu cwaningo: Njengomhlanganyeli ozithandele ukungena kulolu cwaningo, ukhululekile ukuba ungaphuma kule cwaningo nganoma isiphi isikhathi, ngaphandle kokunikeza izizathu. Ungahoxiswa kulolucwaningo uma wehluleka ukuzigcina izikhathi obekelwe zona.

Amaholo: Akukho mholo otholakalayo ngokubamba iqhaza kulolu cwaningo.

Izindleko zalolucwaningo: Akukho zindleko ongahlangabezana nazo ngokubamba iqhaza kulolu cwaningo. Wonke ama ultrasound scan azokwenziwa mahhala.

Imfihlo yocwaningo: izimfihlo zakho zizogcinwa kuyo yonke inqubo yocwaningo ngokusebenzisa amakhodi okuhlanganyela ukuze kungadalulwa imininingwane yakho. Imiphumela yalolu cwaningo izosetshenziselwa inhloso yocwaningo kuphela. Yonke imininingwane eqoqwe kulolucwaningo izolahlwa emva isikhathi esiyiminyaka emihlanu.

Ukulimala okuhlobene nocwaningo: Azikho izingozi ezilindelekile kulolu cwaningo.

Sicela uxhumane nabantu abalandelayo uma unanoma iluphi uhlobo lokukhathazeka noma imibuzo:

Umcwaningi: Harashalata Ramdev (0834616575)

Umphathi: Dr Nalini Govender (031 373 2796)

Umphathi ngokubambisana: Ms Zombuso Cynthia Dlodla (0765995836) noma

Umlawuli ngokuziphatha ngesikhathi socwaningo wendawo yokufundela 031 373 2900.

Izikhazazo zingabikwa kwi DVC: ISU, uSolwazi F. Otieno ku 031 373 2382 noma dvctip@dut.ac.za

APPENDIX 5A: CONSENT FORM IN ENGLISH



CONSENT

Statement of Agreement to Participate in the Research Study:

- I hereby confirm that I have been informed by the researcher, Miss Harashalata Ramdev, about the nature, conduct, benefits and risks of this study - Research Ethics Clearance Number: 73/17,
- I have also received, read and understood the above written information (Participant Letter of Information) regarding the study.
- I am aware that the results of the study, including personal details regarding my sex, age, date of birth, initials and diagnosis will be anonymously processed into a study report.
- In view of the requirements of research, I agree that the data collected during this study can be processed in a computerised system by the researcher.
- I may, at any stage, without prejudice, withdraw my consent and participation in the study.
- I have had sufficient opportunity to ask questions and (of my own free will) declare myself prepared to participate in the study.
- I understand that significant new findings developed during the course of this research which may relate to my participation will be made available to me.

_____	_____	_____	_____
Full Name of Participant	Date	Time	Signature/Right Thumbprint

I, _____ (name of researcher) herewith confirm that the above participant has been fully informed about the nature, conduct and risks of the above study.

_____	_____	_____
Full Name of Researcher	Date	Signature

_____	_____	_____
Full Name of Witness (If applicable)	Date	Signature

_____	_____	_____
Full Name of Legal Guardian (If applicable)	Date	Signature

Please note the following:

Research details must be provided in a clear, simple and culturally appropriate manner and prospective participants should be helped to arrive at an informed decision by use of appropriate language (grade 10 level - use Flesch Reading Ease Scores on Microsoft Word), selecting of a non-threatening environment for interaction and the availability of peer counseling (Department of Health, 2004)

If the potential participant is unable to read/illiterate, then a right thumb print is required and an impartial witness, who is literate and knows the participant e.g. parent, sibling, friend, pastor, etc. should verify in writing, duly signed that informed verbal consent was obtained (Department of Health, 2004).

If anyone makes a mistake completing this document e.g. wrong date or spelling mistake a new document has to be completed. The incomplete original document has to be kept in the participant file and not thrown away and copies thereof must be issued to the participant.

References:

Department of Health: 2004. *Ethics in Health Research: Principles, Structures and Processes* <http://www.doh.gov.za/docs/factsheets/guidelines/ethnics/>

Department of Health. 2006. *South African Good Clinical Practice Guidelines*. 2nd Ed. Available at: http://www.nhrec.org.za/?page_id=14

APPENDIX 5B: CONSENT FORM IN ISIZULU



Isitatimende Sesivumelwano sokubamba iqhaza esifundweni socwaningo:

- Mina ngalamazwi ngiyaqinisekisa ukuthi ngazisiwe ngumcwaningi, Miss Harashalata Ramdev, mayelana nobunjalo, ukuziphatha, izinzu nezingozi zalolu cwaningo - Inombolo ye Clearance yemigomo Yokuziphatha kulolucwaningo: 73/17.
- ngiye ngathola, ngafunda futhi ngaqonda ngolwazi olubhalwe ngaphezulu (Incwadi yemininingwane mayelana cwaningo yombambiqhaza) .
- ngiyazi ukuthi imiphumela yocwaningo, kuhlenganise neminingwane siqu ngokuqondene nobulili, ubudala, usuku lokuzalwa, isiqalo samagama kanye nemiphumela kuzokhishwa ngokungaziwa kwesifundo sami.
- Uma kucatshangelwa izidingo zocwaningo, ngiyavuma ukuthi ukubhalwa kwemininingwane eqoqwe ngenkathi yalolu cwaningo zingahlukaniswa ngendlela yohlelo lwekhompuyutha ngumcwaningi.
- Kunoma yisiphi isigaba socwaningo, ngaphandle kokubandlululwa, ngingahoxisa imvume yami yokubamba iqhaza ocwaningweni.
- ngiye ngaba nethuba elanele ukuba ngibuze imibuzo futhi ngenkululeko yami nangokuzikhethela) ngiyavuma ngokwami ukuthi ngikulungele ukubamba iqhaza ocwaningweni.
- Ngayaqonda ukuthi okubalulekile okusha okutholakele phakathi lolu cwaningo nokuqondene nokuhlanganyela kwami kulolucwaningo nginganikezwa khona.

Igama lomhlanganyeli

usuku

Isikhathi

Isignesha / gingqa isithupha sesandla sokudla

Mina, _____ (Igama lomcwaningi), lapha ngiyaqinisekisa ukuthi umhlanganyeli ongenhla wazisiwe ngokugcwele mayelana nobunjalo, ukuziphatha nezingozi zesifundo esingenhla.

Igama lomcwaningi.

Usuku

Isignesha

Igama likafakazi (Uma kudingeka)

Usuku

Isignesha

Igama lomnakekeli osemthethweni (Uma kudingeka)

Usuku

Isignesha

Sicela uqaphele okulandelayo:

Imininingwane yocwaningo kumele ihlinzekwe ngendlela ecacile, elula futhi ngokuhambisana namasiko futhi abahlanganyeli kufanele basizwe futhi baziswe ngokufinyelela esinqumweni ngokusebenzisa kolwimi lolufanele (grade 10 level - zisebenzisa Flesch Reading Scores ku-Microsoft Word), ngokukhetha indawo engasabisi yokuxhumana kanye nokutholakala ukwelulekwa kontanga (umnyango Wezempilo, 2004).

Uma umhlanganyeli engakwazi ukufunda / engafundile, kudingeka ushicilelo lwesithupha sangakwesokudla kanye nofakazi ongakhethi, ofundile nowazi umhlanganyeli, isbonelo, kungaba umzali, umfowenu noma udadewenu, umngane, umfundisi, njll kufanele uqinisekise ngokubhala usayine imvume nokuthi umvume itholakele (Umnyango Wezempilo, 2004).

Uma kunomuntu owenza iphutha ngokugcwalisa le dokhumenti, isbonelo, usuku oluphambene noma isipelingi okungesona, idokhumenti entsha kufanele ligcwaliswe. Idokhumenti yokuqala engagcwele kufanele igcinwe kwifayela yomhlanganyeli, futhi amakhophi angahlwa, kufanele ikhishwe noma inikezwe umhlanganyeli.

Izinkomba :

Umnyango Wezempilo: 2004. Iziko lezimilo kweZempilo: Izimiso, izinhloko kanjalo nezindlela zokwenza

<http://www.doh.gov.za/docs/factsheets/guidelines/ethnics/>

Umnyango Wezempilo. 2006. Good Clinical Practice: Izinkombandlela zaseNingizimu Afrika. 2nd Ed. Uyatholakala: http://www.nhrec.org.za/?page_id=14

ULTRASOUND SHOULDER USING ELASTOGRAPHY

VOLUNTEERS REQUIRED

**ADULTS BETWEEN 21-45
YEARS WITHOUT
SHOULDER PAIN**

WHERE : Radiology
Dept (Mount
Edgecombe Hospital)

WHY : To improve
shoulder diagnosis
using advanced
ultrasound techniques

Participation will
be voluntary.
No compensation
for participants.
Confidentiality will
be maintained .

PARTICIPANTS WILL :

- COMPLETE A
DEMOGRAPHIC
QUESTIONNAIRE
- HAVE ULTRASOUND
OF SHOULDER
INCLUDING
ELASTOGRAPHY
- EXAM TIME : +/- 30
MINS

For more details ,please
contact: Lata Ramdev
Email :
lataramdev@hotmail.com
Phone : 0834616575

APPENDIX 6 B: ADVERTISEMENT IN ISIZULU

Ucwaningo lwehlombe kusebenziswa uhlobo lwe ultrasound ebizwa nge elastography!

Abantu abadala abaphakathi
kweminyaka engu 21 kuya ku
45 abangenabo ubuhlungu

Indawo: Emnyangweni
wokuthatha izithombe,
esibhedlela sase Mount
Edgecombe

indlela yokuxilonga ihlombe
ngokusebenzisa amasu
asezingeni eliphezulu lwe
ultrasound

Kungani: Ukwenza ngcono
indlela yokuxilonga ihlombe
ngokusebenzisa amasu
asezingeni eliphezulu lwe
ultrasound

Abahlanganyeli kucwaningo:

Bogcwalisa uhlu lwemibuzo yokubala ubuningi babantu

Bokwenziwa ukuxolongwa kwehlombe kusetshenziswa i
ultrasound (amafutha) kuhlangele nokuhlolwa ngohlobo
olwaziwa nge elastography, okuwuhlobo lokuxilonga
ngamafutha olusebenza ukuqina nokunwebeka kwezicubu.

Isikhathi socwaningo kungaba imizuzu engamashumi amathathu

Ukubamba iqhaza kuzoba ngokuzithandela

Asikho esinxephezelo kubabambiqhaza

Ucwaningo luzogcinwa luyimfihlo

Uma udinga eminye imininingwane xhumana no : Lata Ramdev

Imeyili : Lataramdev@hotmail.com

Inombolo yocingo: 0834616575

APPENDIX 7: CONSULT WITH BIOSTATISTICIAN

From: lata ramdev <lataramdev@hotmail.com>
Sent: Wednesday, 01 August 2018 6:24 PM
To: Glenda Beverley Matthews <GlendaM@dut.ac.za>
Cc: Nalini Govender <nalinip@dut.ac.za>; Zombuso Cynthia Dlodla <zombusod@dut.ac.za>
Subject: Sample query

Dear Professor Matthews
I trust you are well.

Firstly, thank you for assisting me with my sample number for my study.

Initially, I had asked you for a sample for the North Central eThekwini population. The population number was 476,727. The sample given by you was 380. This has been quite a challenge as each study is approximately 30 minutes. To date the number of participants scanned total up to 253.

Is it possible to amend my sample population as my target population is based on my research site which services Kwamashu, Phoenix and MountEdgecombe? The specific region will be the northwest regions of Kwazulu Natal. Almost all my participants are from these areas. The total population from these three regions add up to 359,975.

I would be grateful for your kind assistance
Thank you
Kind Regards

Harashalata Ramdev (Lata)
Student number: (19002285)

Glenda Beverley Matthews <GlendaM@dut.ac.za>

Reply

Wed 08/15, 2:09 PM

You

Inbox

You replied on 2018/08/15 2:30 PM.

Hi Lata,

Could you please send me your PG2a proposal so that I can just refresh my memory on the aims of the study? Dr Govender has sent me a paper that she says is similar to the work you are doing. What tendons are you observing and what is the type of measurement that you will make?

Kind regards
Glenda

From: lata ramdev <lataramdev@hotmail.com>
Sent: Monday, 06 August 2018 6:03 PM
To: Glenda Beverley Matthews <GlendaM@dut.ac.za>
Cc: Nalini Govender <nalinip@dut.ac.za>; Zombuso Cynthia Dlodla <zombusod@dut.ac.za>
Subject: Re: Sample query

Dear Professor Matthews

Thank you so much for your acknowledgement with regards to my sample amendment.

Since the previous email my sample has risen to 259.I can possibly round up to 260 this week.

Could you please send me an email to confirm that my sample number is sufficient for the study which can be used for statistical inferences? This will be sent with my application for approval of amendment to ETHICS.

Thank you once again
Kind Regards

Miss Harashalata Ramdev (Lata).

From: Glenda Beverley Matthews <GlendaM@dut.ac.za>
Sent: Wednesday, 15 August 2018 5:35 PM
To: lata ramdev
Cc: Nalini Govender; Zombuso Cynthia Dlodla
Subject: RE: Apologies

Hi Lata,

Thanks for this info.

What I need to know is what measurements you are taking and what are the typical values expected. See below for an example: so for supraspinatus muscle the mean obtained was 51.5 and the standard deviation was 25.1.

Have you some idea of the values you will obtain for the variables you will be measuring?

RESULTS. The mean elasticity values were determined to be 10.97 ± 3.1 kPa for the thyroid, 10.92 ± 3.1 kPa for the submandibular glands, 10.38 ± 3.5 kPa for the parotid glands, 10.4 ± 3.7 kPa for the masseter muscle, 11.1 ± 4.1 kPa for the gastrocnemius muscle, 31.2 ± 13 kPa for the supraspinatus muscle, 51.5 ± 25.1 kPa for the Achilles tendons, 5.0 ± 2.9 kPa for the renal cortex, 23.6 ± 5.4 kPa for the renal pelvis, 4.8 ± 3 kPa for the pancreas, and 2.9 ± 1.8 kPa for the spleen.

Hi Professor Matthews

Since each tendon, except the teres minor tendon is divided in three parts, the proximal (upper third), mid, and distal (lower third), I thought of doing a detailed measurement of the elasticity (stiffness value in kilopascals (kPa).

Arda *et al* has chosen one point of measurement of the asymptomatic tendon and only one tendon, and according to the article the mean value of the supraspinatus tendon is approximately 36 ± 12.4 in males and 29.1 ± 12.4 in females with a max value of 11 -77 in males and 6 - 90 kPa in females. Please see page 535.

Their ultrasound machine is the Supersonic imaging system, different to the G.E Logiq E 9, which I am currently using.

We may have to find and average for each tendon by using all three values in the longitudinal scan and three values in the transverse plane

I will send you an example of Appendix 6. Possibly mean and maximum values

Most of the higher shear wave measurements range from above 85 kPa to 150 kPa and the lower range noted was below 80 kPa. This is a rough estimate. Hope this information helps.

Thank you
Kind Regards

Lata

On 20 Aug 2018, at 15:57, Glenda Beverley Matthews <GlendaM@dut.ac.za> wrote:

Hi Lata and Nalini,

I have used G power with a 1 sample test approach. I have taken level of significance = 0.05, power = 0.80 and what is called the effect size as 0.2 and the sample size is about 200. You have more than this.

My original estimate was based on your large population size.

I think this will be fine.

Regards
Glenda

APPENDIX 8: DATA COLLECTION TOOL
SECTION A: DEMOGRAPHIC DATA

Participant code: --

Age (years)	21 – 24	25 – 34	35 – 45
Gender	Male		Female
Level of activity/lifestyle(Rate from 0 – 10)	Not active (0)	Mildly active (1 – 3)	Moderately active (4 – 6)
			Very active (7 – 10)

Weight (kg): _____ Height (m : _____) BMI (kg/m²) _____

Race: _____

Are you on any medication ? Yes No

If Yes, Please specify the name of medications used.

SECTION B ULTRASOUND DATA**B- MODE ULTRASOUND REPORT:**

B- MODE ULTRASOUND				
	INTACT	TEAR	ECHO PATTERN	OTHER (EG. CALCIUM DEPOSIT)
Biceps tendon				
Subscapularis tendon				
Supraspinatus tendon				
Infraspinatus tendon				
Teres minor tendon				

General observation on B-mode shoulder ultrasound

SHEAR WAVE ULTRASOUND ELASTOGRAPHY REPORT:

	SHEAR WAVE ULTRASOUND ELASTOGRAPHY							
	LONGITUDINAL SAGITTAL				TRANSVERSE/AXIAL			
	Proximal	Middle	Distal	Site of pathology if any	Proximal	Middle	Distal	Site of pathology if any
	Color map/ref value	Color map/ref value	Color map/ref value		Color map/ref value	Color map/ref value	Color map/ref value	
Biceps tendon								
Subscapularis tendon								
Supraspinatus tendon								
Infraspinatus tendon								
Teres minor tendon								

General observation on shear wave ultrasound elastography of the shoulder

Date:

Signature of Doctor/ Sonographer: